# Tumors of Lymphoid and Hematopoietic Tissues

5

Vasiliki Leventaki, Joseph D. Khoury, and Stephan D. Voss

## Introduction

### Normal Anatomy and Development

Lymph nodes are an integral component of the adaptive immune system. Normally, they are encapsulated ovoid structures with a rubbery consistency and a homogeneous light tan cut surface. On a microanatomic level, the lymph node is divided into four compartments: cortex, paracortex, hilum, and sinusoids (Fig. 5.1a). The cortex contains lymphoid follicles comprised primarily of B-cells. Stimulated lymphoid follicles consist of a germinal center immediately surrounded by a mantle zone and an outer marginal zone. The cells of the germinal center exhibit morphologic and functional zonation (Fig. 5.1b). The paracortex, also referred to as the interfollicular area, is generally rich in T-cells that are associated with histiocytes, interdigitating reticulum cells, and high endothelial venules. Histologic prominence of the lymph node hilar area varies by anatomic location and is most evident in nodes of the inguinal and pelvic areas. The hilum contains variable amounts of lymphoplasmacytoid cells and fibroconnective tissue. Lymph node sinusoids are vascular structures that channel lymphatic flow from the capsule towards efferent hilar lymphatics. They contain varying numbers of histiocytes.

V. Leventaki, M.D.
St. Jude Children's Research Hospital, Memphis, TN, USA

J.D. Khoury, M.D.
The University of Texas M.D. Anderson Cancer Center, Houston, TX, USA

S.D. Voss, M.D., Ph.D. (✉)
Department of Radiology, Boston Children's Hospital, 300 Longwood Avenue, Boston, MA 02115, USA
e-mail: stephan.voss@childrens.harvard.edu

### Lymph Node Sampling and Tissue Handling

Excisional and core biopsies are generally most suitable for de novo evaluation of an enlarged lymph node. Fine needle aspiration cytology is often fraught with sampling limitations and does not permit evaluation of the lymph node architecture. In most clinical practices, lymph node samples are submitted either without fixative or in a nutrient-rich medium. Ideally, triage of tissue material from a patient with unexplained lymphadenopathy should be based on evaluation of a touch preparation. If neoplasia is a consideration, lymph node tissue should be handled in the following priority order: (1) formalin fixation for histologic evaluation (paraffin-embedded tissue may be also used for immunohistochemistry, fluorescence or colorimetric in situ hybridization, and molecular testing); (2) unfixed tissue in nutrient-rich media for immunophenotyping by flow cytometry; and (3) unfixed tissue in nutrient-rich media for cytogenetic analysis.

## Overview of Diagnostic Imaging Approaches

### Conventional Radiography/Fluoroscopy

Conventional radiographs (x-rays) are still commonly obtained as the initial imaging study in patients with disorders of the lymphoid system. Despite the emergence of sophisticated cross-sectional and functional imaging techniques, radiographs remain attractive for the initial evaluation, and they are inexpensive, rapid, and relatively easy to perform. They can be done without sedation and can be accomplished at far lower radiation doses than computed tomography (CT). Although many disorders will not be evident radiographically, the presence of primary intrathoracic tumors, mediastinal and/or paraspinal masses, intra-abdominal masses and destructive bone lesions can all be detected radiographically. The presence of calcifications in lymphoid masses may be helpful in establishing a differential diagnosis. For the evaluation of children with suspected

D.M. Parham et al. (eds.), *Pediatric Malignancies: Pathology and Imaging*,
DOI 10.1007/978-1-4939-1729-7_5, © Springer Science+Business Media New York 2015

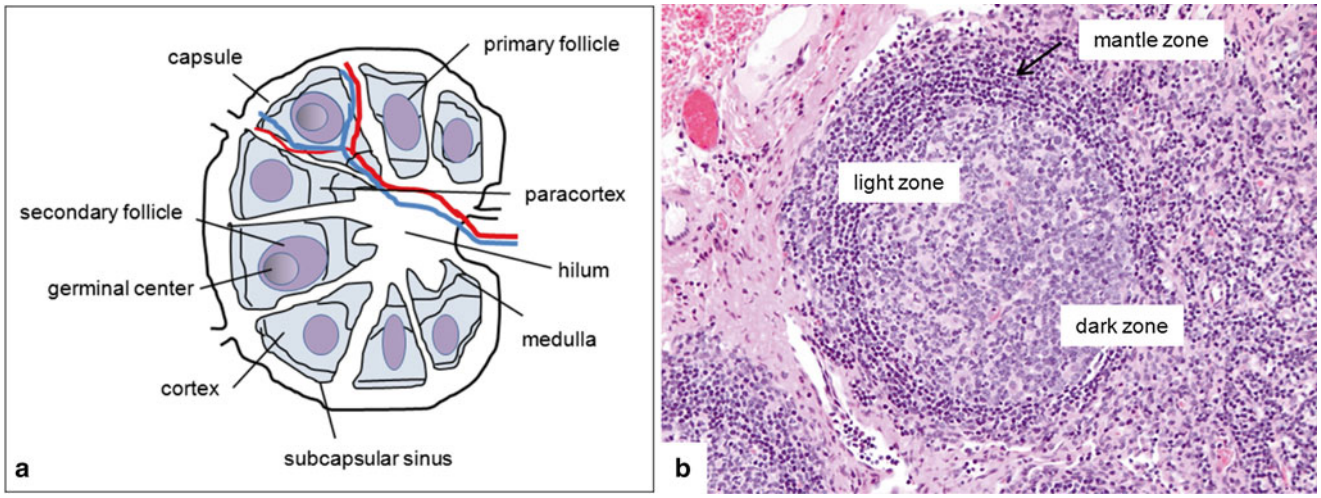


**Fig. 5.1** Basic structure of normal lymph node. (**a**) Schematic representation of the anatomy of a lymph node with the cortical, paracortical, and medullary regions. The cortex contains multiple follicles including primary follicles and secondary follicles with germinal centers. (**b**) A secondary follicle with germinal center (GC) and well-defined mantle zone. In the GC, a loosely associated network of follicular dendritic cells, follicular helper T-cells, and centrocytes forms the light zone, whereas a dense area of dividing centroblasts can be recognized as a dark zone

abdominal conditions, radiographs of the abdomen should be the initial examination of choice to assess for acute obstruction or bowel perforation.

Historically, fluoroscopy was the primary modality used to evaluate the gastrointestinal tract and the upper airway. With the emergence of cross-sectional imaging, fluoroscopy is now rarely used for the primary evaluation of suspected lymphoid lesions. However, children with poorly characterized symptoms and physical exam findings may undergo fluoroscopic evaluation to assess the intestinal tract, and the radiologist should be aware of the imaging findings associated with lymphoid lesions involving the GI tract. Mucosa-based processes such as esophagitis, gastritis, or duodenitis are diagnosed almost exclusively by endoscopy nowadays. However, esophageal and intestinal strictures may benefit from further delineation by fluoroscopy, which can be performed safely and effectively. Current fluoroscopic techniques generally employ very low radiation doses due to advances in pulsed fluoroscopy, image intensifier sensitivity, and improved automatic dose rate controls [1]. Both water-soluble contrast or barium enteric contrast agents used in conjunction with fluoroscopy are considered safe even in immunocompromised children. While there are few contraindications to fluoroscopic evaluation of the intestinal tract, contrast enemas are generally avoided in neutropenic patients and barium enteric contrast should be avoided when bowel stricture or perforation are suspected.

## Ultrasound

Ultrasound is an excellent technique for evaluating the child with a lymphoid system disease. With the availability of an array of high and low frequency transducers, ultrasound can be used to evaluate both superficial and deeper structures and is particularly useful in evaluating lymph nodes in the neck and axilla as well as the abdominal visceral organs [2]. Diagnostic ultrasound is relatively quick, inexpensive, and does not utilize ionizing radiation. In the hands of a skilled operator, ultrasound can also be used to evaluate even the most anxious child and does not usually require sedation. In contrast to adults, ultrasound images in children are usually of very high quality due to the relative paucity of intra-abdominal fat and other attenuating soft tissues seen in older patients and adults.

Color and pulse wave Doppler as well as the increasing availability of three-dimensional imaging techniques allow dynamic flow and vascularity to be assessed. This can be helpful in distinguishing between hyperemic/inflamed lymphoid tissue and normal tissue. The use of microbubble ultrasound contrast agents is still experimental and not routinely available for use in children [3]. The use of sonoelastography to measure the compressibility and elasticity of tissues—initially used in the evaluation of the liver—is presently under evaluation to determine tissue characteristics of superficial lymphoid structures in an effort to discriminate benign from neoplastic nodal enlargement [4].

## Computed Tomography

Since its emergence in the 1970s, the use of CT has become routine in the evaluation of patients with suspected abnormalities of the lymphoid system. With the development of multiple detector row and ultrafast CT imaging techniques,

examinations of the entire body can now be performed in under one minute and, depending on the area of interest, even young children may be evaluated without the need for sedation.

CT scanning is routinely performed in transaxial cross-sections with multiplanar reconstructions being rapidly generated from the axial image data. With the use of multidetector helical CT scanners and isotropic imaging acquisition techniques, the reconstructed images have no discernible loss of resolution or contrast as compared to source transaxial data. The use of contrast agents (both intravenous and enteric) in pediatric CT scanning depends on the condition being evaluated. For assessment of the mediastinum and lymphoid tissues, the presence of contrast is considered helpful, if not essential, to better characterize lymph nodes relative to adjacent vascular structures. In addition, the use of contrast-enhanced CT scanning remains the standard of care to accurately measure the size of lymphoid tumors to determine response to therapy [5, 6]. Although concerns regarding reactions to iodinated intravenous contrast agents are frequently raised, the rate of adverse reactions, including acute allergic or anaphylactoid reactions, asthmatic reactions, and vasovagal reactions, are exceedingly rare [7]. The presence of a prior contrast reaction does, however, predict subsequent recall-type allergic reactions, and clinicians and radiologists should be aware of the increased potential for adverse events in these patients and provide appropriate premedication as indicated. Awareness by radiologists and clinicians of guidelines for the use of iodinated contrast agents is important so that imaging protocols can be modified as needed [8].

Over the past 10 years, there has been a heightened awareness of the potential risk posed by CT scanning from ionizing radiation doses used [9]. When comparing the effective dose for a pediatric chest CT to a chest radiograph, some estimates indicate the CT scan is the equivalent of tens to hundreds of chest radiographs [10]. While it is clear that the use of multiple CT scanning phases and the need for multiple sequential CT examinations increases the relative radiation risk, a more extensive discussion of the radiation risk estimates associated with CT scanning in pediatric patients is beyond the scope of this chapter and can be reviewed in a number of recent publications [11–14]. It is reasonable to conclude that opinions vary widely and uncertainty about the absolute risk of cancers associated with ionizing radiation in the diagnostic CT dose range remains [15]. Nonetheless, the principle that guides the use of CT scanning in pediatric patients is adherence to the ALARA (*a*s *l*ow *a*s *r*easonably *a*chievable) guidelines, which seek to balance the relative risk of exposure to ionizing radiation against the potential benefit from the diagnostic information obtained. Namely, every effort should be made to adjust the CT doses to the patient's body size and clinical indications and to minimize scanning of body regions that are not involved or not suspected as harboring disease.

Most major manufacturers now have new dose-reducing automatic tube current modulation technologies as well as iterative image reconstruction algorithms that allow scans to be performed at much lower doses and for the doses to be adjusted dynamically, accounting for the differing tissue densities being imaged [16]. While the technical parameters used in CT scanning are ultimately the responsibility of the radiologist, clinicians ordering CT scans should be aware of these considerations in determining the need for CT and whether the clinical indications warrant the particular examination being ordered.

## Magnetic Resonance Imaging

Magnetic resonance imaging (MRI), in contrast to the *transmission* technologies such as conventional radiography, fluoroscopy, and CT, belongs to the group of *emission* technologies. MRI consists of dynamic interactions between a strong external magnetic field, the application of radiofrequency waves, and subsequent reception of low level radiofrequency (RF) emissions from hydrogen nuclei within the body [17]. Once the patient is placed in a magnetic field, the hydrogen nuclei become aligned in the orientation of the magnetic field. When they are bombarded with radiofrequency pulses, the hydrogen nuclei absorb the RF energy. Once the RF waves are turned off, the hydrogen nuclei begin to release the absorbed energy ("decay") in a manner that is related to the tissue characteristics within which the nuclei are residing. This allows exquisitely detailed images of the body's soft tissues to be acquired. There are a number of factors that can influence the signal and image quality obtained during MRI, but these are beyond the scope of this review. In general, in order to acquire a diagnostically useful image, contrast between normal tissues and diseased tissues is needed. Such contrast differences are an inherent reflection of the different tissue environments within which the protons live. Depending on the clinical indication, the MRI pulse sequences can be tailored to address specific clinical questions.

For evaluating the patient with abnormalities of the lymphoid system, characterization of normal and diseased lymph nodes can usually be accomplished well using standard T1- and T2-weighted imaging techniques in axial and at least one orthogonal (coronal or sagittal) imaging plane. The use of gadolinium-based contrast agents can be helpful in further characterizing tissue abnormalities. In some instances, the presence of iron or hemosiderin deposition may be helpful in rendering a differential diagnosis and gradient echo or T2-weighted images, which are sensitive to the local magnetic field inhomogeneities induced by the presence of paramagnetic compounds such as iron, can be utilized [18, 19].

Pediatric whole-body MRI techniques with rapid scanning sequences can now be accomplished typically in 30 min or less and have been advocated for staging and screening patients with abnormalities of the lymphoid system [20, 21]. The use of parallel imaging techniques and the ability to simultaneously receive RF information using multiple receiver coils allows for more rapid imaging and improved temporal and spatial resolution. The increased ability to perform rapid MRI studies for a wide variety of pediatric indications is particularly important for young children in whom an MRI examination of 30 min or more may require sedation in order to minimize patient motion.

The use of diffusion-weighted imaging has recently gained attention for body imaging techniques [22–24]. Diffusion-weighted imaging was initially developed for characterizing sites of brain ischemia in neuroradiologic applications. For oncologic purposes, the ability to evaluate tissue density and tumor cellularity based on changes in the restricted diffusion of water molecules within a particular region, has been helpful in characterizing and evaluating effects of therapy [24]. While diffusion-weighted imaging may aid in detecting small lymph nodes, it has not yet been able to reliably distinguish between neoplastic and non-neoplastic lymph node processes [25, 26].

The use of MR contrast agents includes both positive and negative contrast agents. Gadolinium (Gd)-based agents rely on the paramagnetic effects of Gd, which causes both T1 and T2 relaxation time shortening. The Gd ion itself is toxic and is only provided in the form of a gadolinium chelate. The pattern of tissue uptake and excretion may vary depending on the chelate used, but most commercially available Gd-based MR contrast agents are administered intravenously and are primarily excreted through the genitourinary tract. Iron- and iron oxide-based contrast agents have been specifically advocated for evaluation of the lymphoid system [19]. These agents rely on the T2 shortening effects of iron. Normal cells of the macrophage and reticuloendothelial cell lineage will typically scavenge the iron-based nanoparticles, and the use of these contrast agents has been shown in several pilot studies to be helpful in distinguishing lymph nodes involved by tumor from normal lymph nodes. Despite the potential appeal of this class of contrast agents, they have not received universal clinical acceptance.

The use of Gd-based chelates is relatively safe, although patients with underlying acute or chronic renal insufficiency have been shown to be at risk of developing nephrogenic systemic fibrosis (NSF) [27]. NSF is characterized by progressive tissue fibrosis that may be limited. On occasion, NSF may be progressive with involvement of other tissues such as the heart, lungs, and esophagus resulting in significant pathology and potentially death. Although the risk of developing NSF seems to relate to the doses of Gd chelate used and the degree of renal insufficiency, the majority of patients with renal insufficiency do not develop NSF. Nonetheless, the evaluation of renal function prior to the intended use of Gd-based contrast agents is needed in order to minimize this potential risk.

## Nuclear Medicine/Positron Emission Tomography

Functional imaging techniques in nuclear medicine are commonly used in evaluating patients with abnormalities of the lymphoid system. Although these techniques provide less anatomic and morphologic information than either CT or MRI, there is often valuable metabolic and functional information to be gathered from specific nuclear medicine techniques. As with MRI, nuclear medicine imaging relies on emission data following injection with a radiopharmaceutical agent to generate an image [28]. Depending on the pharmaceutical and isotope utilized, the agent localizes to target organs and tissues and is visualized using highly specialized detector cameras used to acquire and display images of the whole body or selected body regions. Cameras are configured to acquire both 2-D planar as well as multiplanar tomographic images and can be placed at various angles and positions to optimize image quality and lesion conspicuity.

Positron emission tomography (PET) utilizes positron-emitting radiopharmaceuticals. Following radionuclide decay in situ, emitted positrons annihilate upon contact with electrons near the point of tissue localization releasing two 511 keV photons traveling in opposite directions. These high-energy photons can be imaged using coincidence detection techniques to permit precise identification of the initial site of radiopharmaceutical localization and positron decay. Similarly, single photon emission computed tomography (SPECT) applies tomographic rather than planar imaging techniques to gamma particle emitting radiopharmaceuticals allowing multiplanar acquisition and projection images to be generated. These can be fused to CT and/or MRI images, which in some instances may be simultaneously acquired to allow anatomical and functional co-localization.

A wide variety of radiopharmaceuticals is available, although the main agents used in routine evaluation of children with lymphoid disorders include $^{99m}$Tc labeled methylenediphosphonate (MDP), $^{67}$Ga, and $^{18}$F-fluorodeoxyglucose (FDG). $^{99m}$Tc-MDP localizes to areas of bone turnover and is useful in assessing osteoblastic metastatic disease as well as sites of lytic bony disease. Historically, $^{67}$Ga, whic binds to transferrin receptors expressed on lymphoid cells, was used to evaluate patients with lymphoma. The use of gallium scanning has been essentially replaced by FDG PET imaging, and the latter has become standard of care in the evaluation of patients with lymphoma [29, 30] as well as a variety

of other non-neoplastic lymphoid disorders [31]. FDG PET imaging relies on the presence of $^{18}$F-fluorine as a positron-emitting radiotracer that is incorporated into the glucose analog fluorodeoxyglucose. FDG accumulates at relatively high levels in metabolically active lesions including lymphoid malignancies and inflammatory disorders, providing a very sensitive means of evaluating patients with abnormalities of the lymphoid system. Nearly all PET imaging is currently performed with integrated PET/CT scanners. This allows areas of FDG uptake at sites of concern to be fused to simultaneously acquired CT images to afford better anatomic correlation and coregistration of uptake sites. In addition, areas of background or physiologic uptake such as brown fat can be accurately identified using co-registered PET/CT images.

Other nuclear medicine imaging techniques include the use of $^{99m}$Tc-HMPAO or $^{111}$In-oxine labeled leukocytes for inflammatory imaging, although this technique is now less frequently used with the advent of FDG PET imaging. Nuclear medicine plays an important complimentary role in providing a functional characterization of patients with disorders of the lymphoid system. In many diseases, functional imaging is crucial for disease staging, response assessment, and in certain instances disease surveillance. Increasingly, however, the use of nuclear medicine techniques is closely integrated with simultaneously acquired cross-sectional imaging examinations (e.g., CT or MRI), requiring careful assessment of both the functional and anatomic imaging data for diagnostic evaluation [29, 30, 32].

## Benign Causes of Lymphadenopathy

In clinical practice, infectious and reactive etiologies are nearly always in the differential diagnosis of lymphadenopathy in a young patient [33]. The most common sites for lymphadenitis requiring imaging evaluation are the cervical, axillary, and inguinal regions. Clinically, lymphadenitis is associated with pain, tenderness, and focal lymph node enlargement [34, 35]. The most common causes of infectious lymphadenitis are summarized in Table 5.1.

Various infectious and reactive etiologies are often associated with broad histologic patterns of lymphadenopathy that include follicular, paracortical, sinusoidal, and mixed patterns [36]. While a more detailed discussion of the pathophysiologic causes that underlie these patterns is beyond the scope of this textbook, a summary of the most common etiologies associated with the various histologic patterns is listed in Table 5.2. Progressive transformation of germinal centers (PTGC) is a term used to describe a well-defined histologic pattern of follicular changes often associated with reactive lymphadenopathy. PTGC is characterized by follicles of varying sizes exhibiting disruption of the germinal center by encroaching mantle zone lymphocytes. The etiology and pathogenesis of isolated PTGC remain poorly understood. While the vast majority of PTGC changes are seen in benign reactive lymph nodes, recognition of this change is important since it is also often seen in the vicinity of nodular lymphocyte predominant Hodgkin lymphoma.

**Table 5.1** Most common infectious lymphadenitis

| Etiology | Common anatomic site | Histology | Diagnosis |
|---|---|---|---|
| *Viral* | | | |
| Epstein-Barr virus (EBV)-infectious mononucleosis | Cervical lymphadenopathy and splenomegaly | Interfollicular infiltrate with numerous immunoblasts (EBV positive) | Monospot test, and serology studies |
| Cytomegalovirus | Localized or generalized lymphadenopathy | Florid follicular hyperplasia and hyperplasia of monocytoid B-cells | Presence of CMV inclusions on infected cultured cells |
| Herpes simplex virus | Localized or multifocal lymphadenopathy | Interfollicular hyperplasia with necrotic areas with neutrophils and karyorrhectic debris | Presence of cells with glass-like inclusions in the areas of necrosis |
| *Bacterial* | | | |
| *Bartonella henselae* (Cat-scratch disease) | Regional lymphadenopathy following a skin lesion | Stellate necrotizing granulomas with palisading epithelioid histiocytes | Warthin-Starry stain, PCR, and serology |
| Common bacteria (streptococcal or staphylococcal) | Cervical lymphadenopathy | Follicular hyperplasia, and microabscesses in the lymph node | Aerobic and anaerobic tissue cultures |
| Mycobacterium tuberculosis | Supraclavicular and cervical lymph nodes | Ceseating granulomas with epitheliod histiocytes and multinucleated giant cells | Ziehl-Neelsen stain, cultures and PCR |
| Nontuberculous Mycobacteria (MAI, *M. kansasii, M. scofulaceum, M. malmoense*) | Unilateral cervical lymph nodes | Ceseating granulomas with epitheliod histiocytes and multinucleated giant cells | Ziehl-Neelsen stain, PAS + MAI and PCR |
| *Protozoal* | | | |
| Toxoplasma | Unilateral or bilateral lymph nodes | Florid follicular hyperplasia, monocytoid B-cells and clusters of epithelioid histiocytes surrounding germinal center | Characteristic cervical histologic changes and serology |

**Table 5.2** Common reactive lymphadenopathies

| Pattern | Histologic findings | Entity |
|---|---|---|
| Follicular | Numerous reactive follicles; GC with irregular shape and size<br>Tingible body macrophages; BCL2 is negative in GC | Follicular hyperplasia<br>Autoimmune disorders<br>Castlemans disease, hyaline vascular type<br>Progressive transformation of germinal centers |
| Sinusoidal | Prominent expansion of sinuses<br>Histiocytic hyperplasia<br>Plasma cell proliferation<br>Monocytoid B-cells | Sinus histiocytosis with massive lymphadenopathy (Rosai Dorfman disease)<br>Storage disease<br>Whipple disease<br>Vascular transformation of sinuses<br>Hemophagocytic syndrome |
| Interfollicular mixed | Interfollicular expansion<br>T-cell predominance<br>Immunoblasts increased in the interfollicular areas<br>Plasma cells, macrophages<br>Mixed population | Dermatopathic lymphadenopathy<br>Kimura's disease<br>Systemic lupus erythematous<br>Kicuchi's lymphadenitis<br>Inflammatory pseudotumor |
| Diffuse | Effacement of architecture<br>Mixed population<br>Immunoblastic proliferation | Drug-induced lymphadenophathy<br>Viral lymphadenitis |

## Lymphoproliferative Disorders and Neoplasms Associated with Immune Deficiency

### Lymphoproliferative Disorders and Neoplasms Associated with Primary Immunodeficiency Diseases

Primary immunodeficiencies (PID) are a rare and heterogeneous group of diseases caused by congenital defects affecting the innate and/or adaptive immunity, with impact on the humoral and/or cell-mediated immunity. The most updated classification for PID provided by the International Union of Immunodeficiencies Studies recognizes eight categories [37]: (1) combined immunodeficiencies: e.g., severe common immunodeficiency (SCID); (2) predominantly antibody deficiencies: e.g., X-linked agammaglobulinemia (XLA), common variable immunodeficiency (CVID); (3) well-defined syndromes with immunodeficiency: e.g., Wiskott-Aldrich syndrome, DNA repair defects; (4) diseases of immune dysregulation: e.g., autoimmune lymphoproliferative syndrome (ALPS), familial hemophagocytic lymphohistiocytosis; (5) congenital defects of phagocyte number, function or both: e.g., chronic granulomatous disease, severe congenital neutropenia; (6) defects in innate immunity: e.g., deficiencies impairing the interferon gamma/interleukin 12 axis; (7) autoinflammatory disorders: e.g., familial Mediterranean fever; and (8) complement deficiencies. More than 120 distinct genes have been identified, with abnormalities that account for more than 150 different forms of PID [38].

Patients with PID have a higher than usual risk of developing lymphoid malignancies, and these represent the second leading cause of death in this group [39]. The incidence of lymphoproliferative disease ranges from 1.4 to 24 % depending of the type of the PID. The diseases commonly associated with lymphoproliferative disorders or neoplasms include ataxia-telangiectasia, Wiscott-Aldrich syndrome, Nijmegen breakage syndrome, CVID, XLA, and autoimmune lymphoproliferative syndrome. In these patients, lymphoma is diagnosed at a median age of 7.1 years [39].

The pathogenesis of lymphoproliferative diseases in PIDs involves multiple mechanisms rooted in defects in DNA damage response (e.g., ataxia-telangiectasia and Wiscott-Aldrich syndrome) and immune deregulation that characteristically results in abnormal response to viral infections such as Epstein-Barr virus (EBV), hepatitis B or C viruses, and human papillomavirus [40]. The inability to eliminate infection is speculated to create an inflammatory environment that can eventually promote tumor development and growth by promoting and sustaining the acquisition of oncogenic somatic mutations [39].

Lymphoid proliferations associated with PID are heterogeneous and range in spectrum from reactive hyperplasia to non-Hodgkin and Hodgkin lymphoma. The most common presentation is at extranodal sites; namely, the gastrointestinal tract, lungs, and central nervous system. In patients with XLA and SCID, non-neoplastic lesions include a polymorphous lymphoid proliferation with plasmablasts, immunoblasts and Reed-Sternberg-like cells that result from primary EBV infection. Patients with CVID can present with lymphoid hyperplasia in the gastrointestinal tract or with lymph node follicular hyperplasia and expansion of paracortical

**Table 5.3** Most common primary immunodeficiencies associated with lymphoproliferative disorders

| Type of deficiency | Gene defect | Pathogenesis | Abnormality | Lymphoproliferative disease |
|---|---|---|---|---|
| CVID, autosomal (predominantly antibody deficiency) | *ICOS, CD19, BAFFR* | Defects in B-cell maturation and differentiation | Reduced B cells; low IgG and IgA | GI tract and lungs (HHV8 implicated in granulomatous interstitial lung disease), increased risk of B cell, extranodal NHL |
| SCID (combined immunodeficiency) | X-linked, γ chain mutations; JAK3, AR; ADA, AR | Abnormal interleukin signaling in XSCID and JAK3 mutations; accumulation of dATP in defective ADA | Low or absent T-cells and NK cells and nonfunctional B cells | Fulminant primary EBV Infection, lymphadenopathy, hepatosplenomegaly. Lymphoma development not well documented |
| Hyper IgM syndrome, X-linked (predominantly antibody deficiency) | CD40/CD40L ligand mutation | Defective B cell and dendritic cell signaling; CD40L required for isotype class-switching from IgM to IgG or IgA | Low or absent IgG, IgA; normal or increased IgM, cytopenias | Predominantly abdominal adenopathy; lack germinal of centers. Lymphoma development not well documented |
| Ataxia-telangiectasis, AR (well-defined syndromes with immunodeficiency) | AT gene mutation (11q22–23), encodes for protein kinase | Defective DNA repair and deregulation of cell division and apoptosis, abnormal function and development of lymphocytes | IgA, IgE, IgG2 decreased; progressive decrease in T-cells; normal B cell numbers | T-cell acute lymphoblastic leukemia/lymphoma in children; T-prolymphocytic leukemia in young adults; Hodgkin lymphoma-like lymphoproliferative disorders |
| X-linked lymphoproliferative syndrome (well-defined syndromes with immunodeficiency) | SH2D1A mutations (Xq25), that encodes for SAP protein | Uncontrolled T-cell proliferation; underlying mechanisms is not yet entirely understood | B cells normal or reduced. Defective lysis and polarization following EBV infection | Fulminant IM; extranodal B cell NHL, particularly of the terminal ileum |
| Autoimmune lymphoproliferative syndrome (well-defined syndromes with immunodeficiency) | Defects in the Fas/FasL signaling | Defects in apoptotic pathway | Autoimmune cytopenias, adenopathy and splenomegaly | Increased risk for HL, including NLPHL |
| Wiskott-Aldrich, AR (well-defined syndromes associated with immunodeficiency) | WAS mutation (Xp11.22–23) | Abnormal cytoskeletal architecture of hematopoietic cells | Decrease in T-cells, normal B cells; decreased IgM | 7 % develop NHL; CNS involvement has been reported in this setting; Lymphomatoid granulomatosis |

areas by immunoblasts infected by EBV. In patients with ALPS, lymphadenopathy results from follicular hyperplasia with or without progressive transformation of germinal centers. Overt lymphomas generally have clonal IgH rearrangement whereas non-neoplastic or polymorphous lymphocytic proliferations may show either oligoclonal or monoclonal IgH rearrangements. The presence of clonality in patients with PID does not always indicate the presence of lymphoma and correlation with clinical and imaging findings is particularly important.

The lymphomas that can occur in patients with PID are generally classified like those that arise in non-immunosuppressed patients. Diffuse large B-cell lymphoma is the most common type, followed by Burkitt lymphoma. Lymphomatoid granulomatosis involving the lungs shows T-cell background infiltrate and neoplastic B-cells, and is most commonly seen in patients with Wiscott-Aldrich syndrome. Classical Hodgkin lymphoma is less common than diffuse large B-cell lymphoma in PID patients and has been reported in patients with ataxia-telangiectasia syndrome and Wiscott-Aldrich syndrome. Peripheral T-cell lymphoma is rare and has been described in patients with ALPS. The EBV virus has been demonstrated to be present in most of the cases [41]. A summary of the most common PID types associated with lymphoproliferative disorders and neoplasms is listed in Table 5.3.

## Imaging Features

Imaging features associated with PID vary by the type and severity of the immunodeficiency. Patients with XLA do not produce immunoglobulin but do have normal T-cell function and normal thymic development. Radiographically, this disorder is most frequently associated with the sequelae of recurrent pulmonary infections such as bronchiectasis, pulmonary parenchymal scarring and heterogeneous or mosaic patterns of lung aeration and attenuation (Fig. 5.2). Bacterial infection can also occur at other sites such as the sinuses and genitourinary tract; however, these are not as commonly encountered as pulmonary infections [42]. Patients with *IgA deficiency* develop pulmonary and GI infections and may have underlying allergic and autoimmune disorders. In comparison to XLA, the imaging findings are less severe and bronchiectasis,

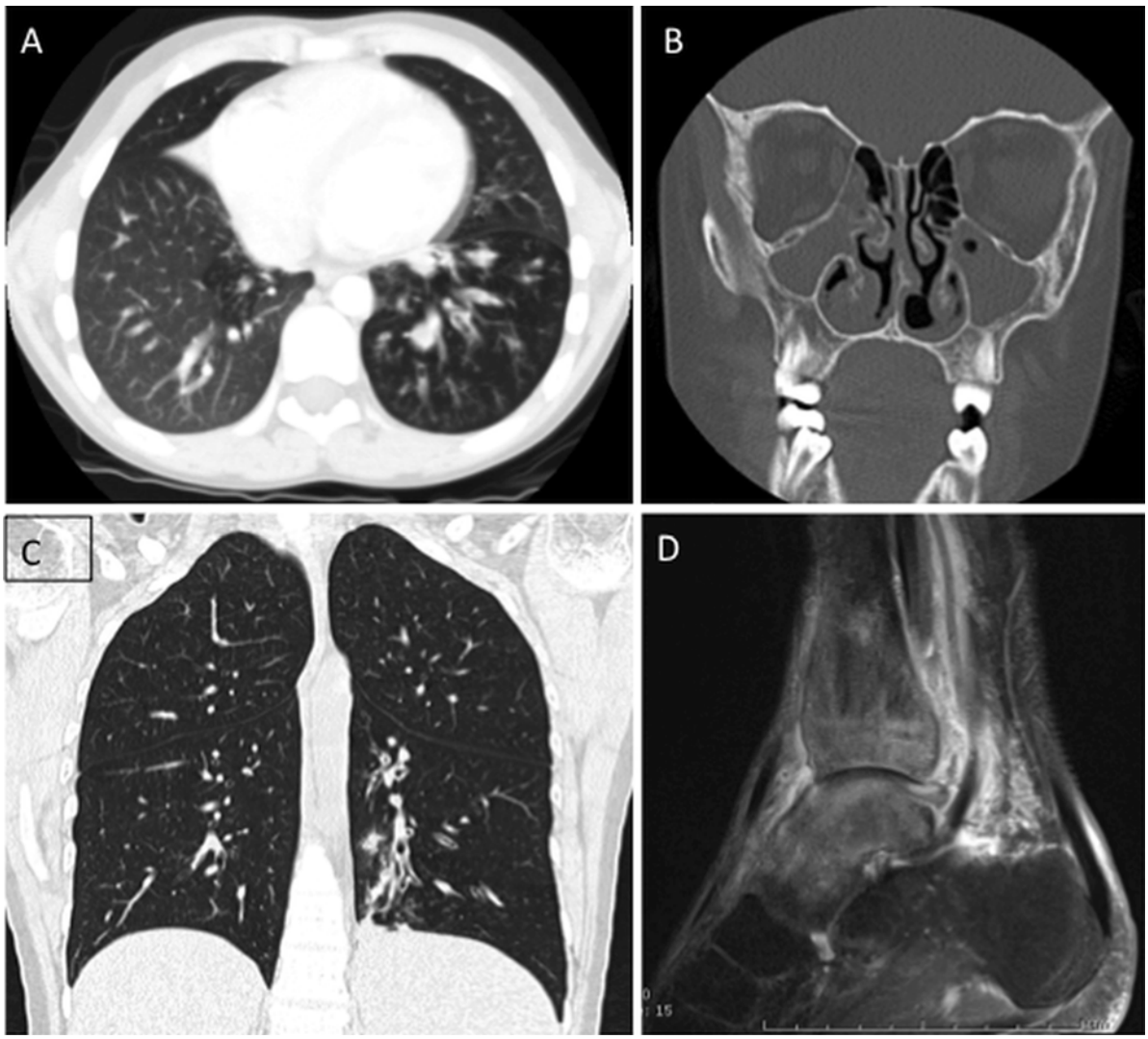


**Fig. 5.2** X-linked agammaglobulinemia. Three examples of findings in patients with XLA. 9-year-old with chronic cough and sinus infection with chest CT showing mosaic lung attenuation and air trapping in the left lower lobe (**a**) and near complete opacification of the maxillary sinuses (**b**). Chest CT in a 32-year-old patient with XLA and respiratory symptoms shows left lower lobe bronchial wall thickening, bronchiectasis, and evolving consolidation (**c**). Ankle MRI (**d**) in a 30-year-old patient with XLA revealed osteomyelitis and tenosynovitis related to chronic infection

for example, is less common. Patients with CVID, as with XLA, may also have recurrent infections, bronchiectasis, and bronchial wall thickening. In contrast to the other PID, patients with CVID may also develop lymphadenopathy and splenomegaly in addition to a more generalized lymphoproliferative process (Fig. 5.3), presumably because of varying degrees of associated T-cell functional abnormalities [42, 43].

DiGeorge syndrome (DGS) and SCID are the most severe of the PID syndromes. *DiGeorge syndrome*, also known as thymic hypoplasia, results in primary T-cell deficiency secondary to abnormal thymic development [42]. Patients with DGS have other findings including hypertelorism and micrognathia, which may be apparent radiologically. Other associated anomalies include a host of cardiovascular anomalies such as abnormalities of the aortic arch and tetralogy of Fallot. Apart from the narrow mediastinum resulting from absent thymic tissue, there are no other specific imaging findings to indicate the diagnosis of DGS. *Severe combined immunodeficiency* syndrome results from absent T- and B-cell function, as well as diminished natural killer cell function. As with DGS, the combination of deficiencies in both humoral and cellular immunity in patients with SCID leads to recurrent and severe opportunistic infections [43].

Patients with Wiskott-Aldrich syndrome and ataxia telangiectasia have a high incidence of developing malignancy, particularly leukemia and lymphoma [44, 45] (Fig. 5.4). In addition, patients with ataxia telangiectasia are at an

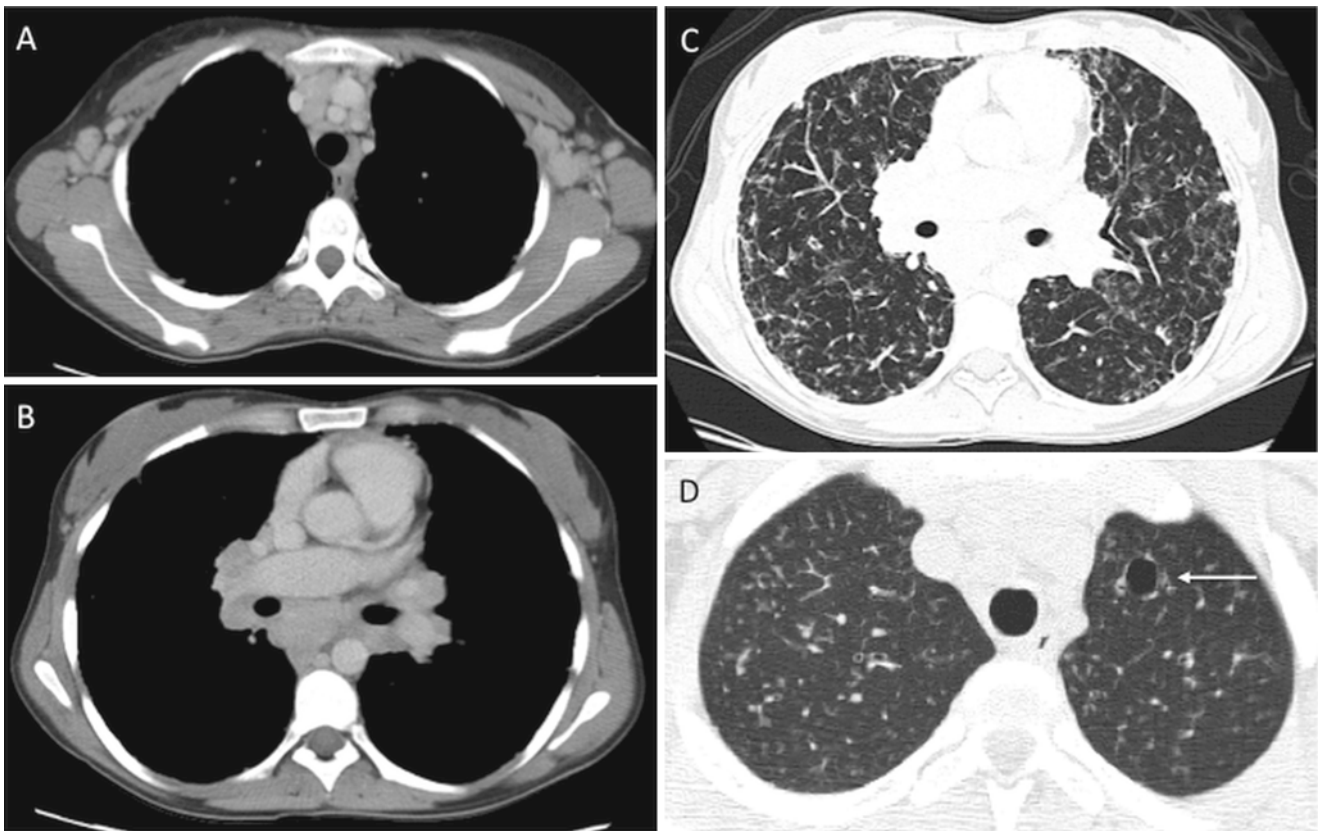


**Fig. 5.3** Common Variable Immunodeficiency (CVID) (**a**–**c**) and Hyper-IgE syndrome (**d**). Chest CT in a 26-year-old patient with CVID (**a**–**c**) shows axillary (**a**) and mediastinal/hilar lymphadenopathy (**b**), in addition to extensive parenchymal lung disease (**c**), with ground glass opacities, reticular thickening and areas of air trapping related CVID. Chest CT in patient with hyper-IgE syndrome reveals a small pneumatocele (*arrow*), characteristic of this disease, in the left upper lobe, as well as background diffuse nodular opacities consistent with underlying infection

increased risk of radiation-induced malignancy, which creates unique challenges for surveillance imaging studies. Because imaging examinations in these populations of patients are aimed at screening for malignancy or characterizing active or chronic sites of infection, the results are often nonspecific, prompting multiple follow-up imaging evaluations. As such, techniques that require repeated exposure to ionizing radiation (i.e., CT) should be used judiciously [46].

## Lymphoid Neoplasms Associated with Human Immunodeficiency Virus Infection

Human immunodeficiency virus (HIV) infection and the associated acquired immune deficiency syndrome (AIDS) occur infrequently in children and often as the result of in utero transmission. A distinct group of lymphoid neoplasms arise in the setting of HIV infection. These include lymphomas that are seen in HIV-negative patients such as Burkitt lymphoma, diffuse large B-cell lymphoma, and Hodgkin lymphoma. In addition, HIV patients are affected by lymphomas that are only rarely seen outside the setting of HIV: primary effusion lymphoma and plasmablastic lymphoma. The introduction of highly active antiretroviral therapy (HAART) has resulted in a dramatic decrease in the incidence of high grade lymphomas in HIV patients.

Most patients present with advanced stage disease and extranodal involvement. Extranodal sites usually include the gastrointestinal tract, central nervous system (CNS), liver and bone marrow, as well as more unusual sites such as oral mucosa and body cavities. Lymph nodes can also be involved. Epstein-Barr virus is identified in approximately 40 % of HIV-associated lymphomas, but this percentage varies significantly between the different types of lymphomas. Distinction between neoplasia and infection on imaging studies may be difficult occasionally; for example, CNS involvement by toxoplasmosis is a rare complication in pediatric HIV patients and can be difficult to distinguish from lymphoma [47].

## Post-transplant Lymphoproliferative Disorders

Post-transplant lymphoproliferative disorders (PTLD) are lymphoid or plasma cell disorders that develop in a recipient of a

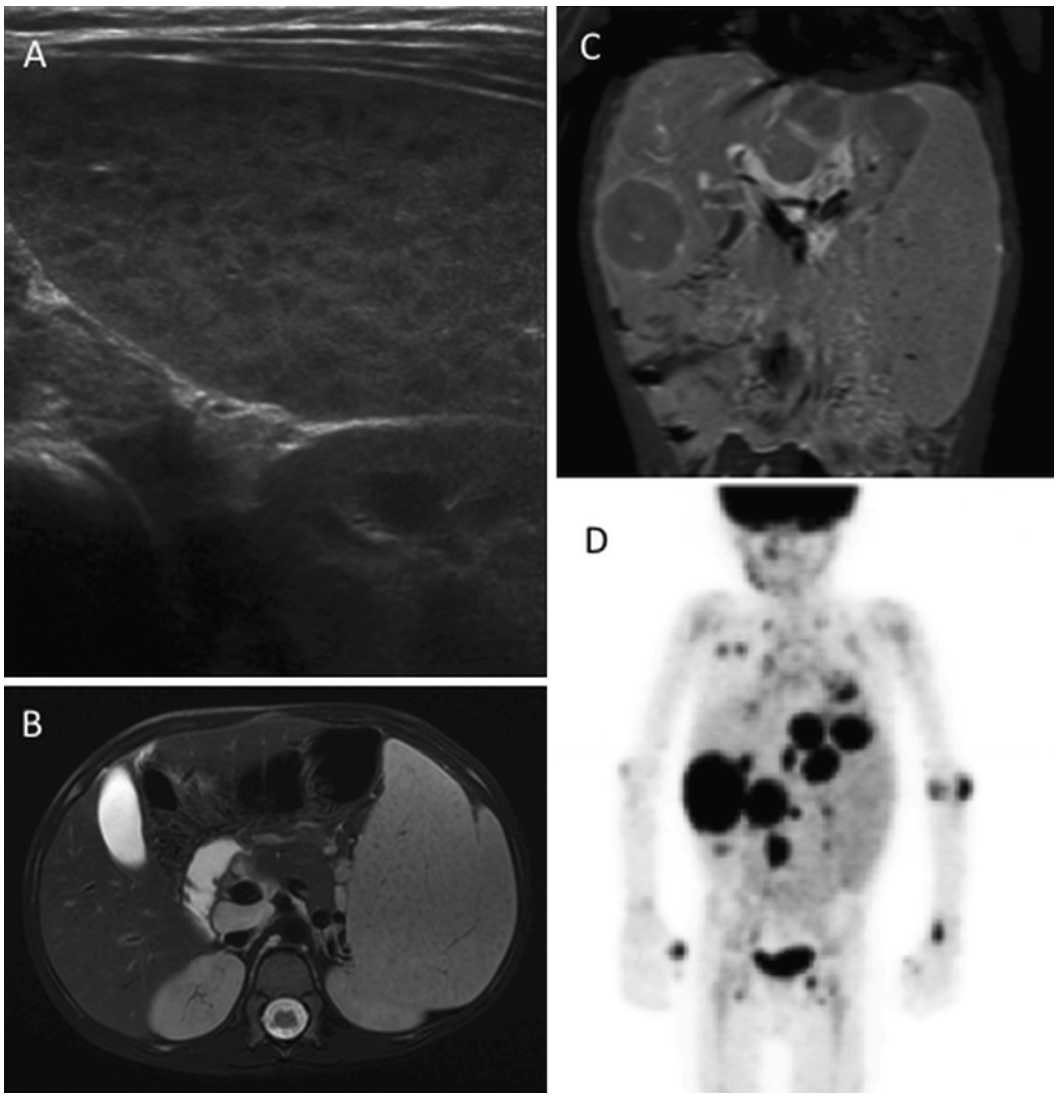


**Fig. 5.4** A 6-year old with ataxia telangiectasia initially presented with splenomegaly. Ultrasound showed diffuse splenic enlargement with innumerable hypoechoic lesions, concerning for lymphoproliferative disease (**a**). Over the next 2 months subsequent MRI confirmed splenic involvement (**b**), in addition to showing multifocal hepatic involvement (**c**). Biopsy revealed large cell lymphoma. FDG PET shows extensive abnormality of the abdomen, lungs, and skeleton (**d**)

solid organ or allogeneic stem cell transplant as a result of iatrogenic immunosuppression. The spectrum of PTLD is clinically and histologically variable. Three broad categories of PTLD are recognized: (1) early lesions (infectious mononucleosis-like and plasmacytic hyperplasia); (2) polymorphic PTLD; and (3) monomorphic PTLD. The latter includes lymphomas that also occur in non-immunosuppressed patients such as Hodgkin lymphoma and plasma cell myeloma. When compared to the adult population, the incidence of PTLD in children is higher, especially following solid organ transplant. The risk for development of PTLD is significantly associated with the occurrence of primary EBV infection after transplantation [48, 49].

Imaging of PTLD patients is directed at establishing the extent of involvement and should include cross-sectional imaging, either CT or MRI, of the entire torso as well as FDG PET imaging to establish the overall extent of disease [50]. Both CT and PET can be used to monitor response to therapy and/or immunomodulation. FDG PET has been shown to be superior to conventional imaging techniques in the early evaluation of PTLD response to therapy [50].

Routine screening for PTLD (e.g., EBV serologic studies or quantitative assessment of viral RNA) facilitates early diagnosis and treatment by reduction of immunosuppression. Lymph nodes as well as extranodal sites (tonsil, gastrointestinal tract, lungs, spleen and liver can be involved (Fig. 5.5). In solid organ transplant recipients, PTLD may affect the allograft itself and needs to be differentiated from rejection or infection. Detection

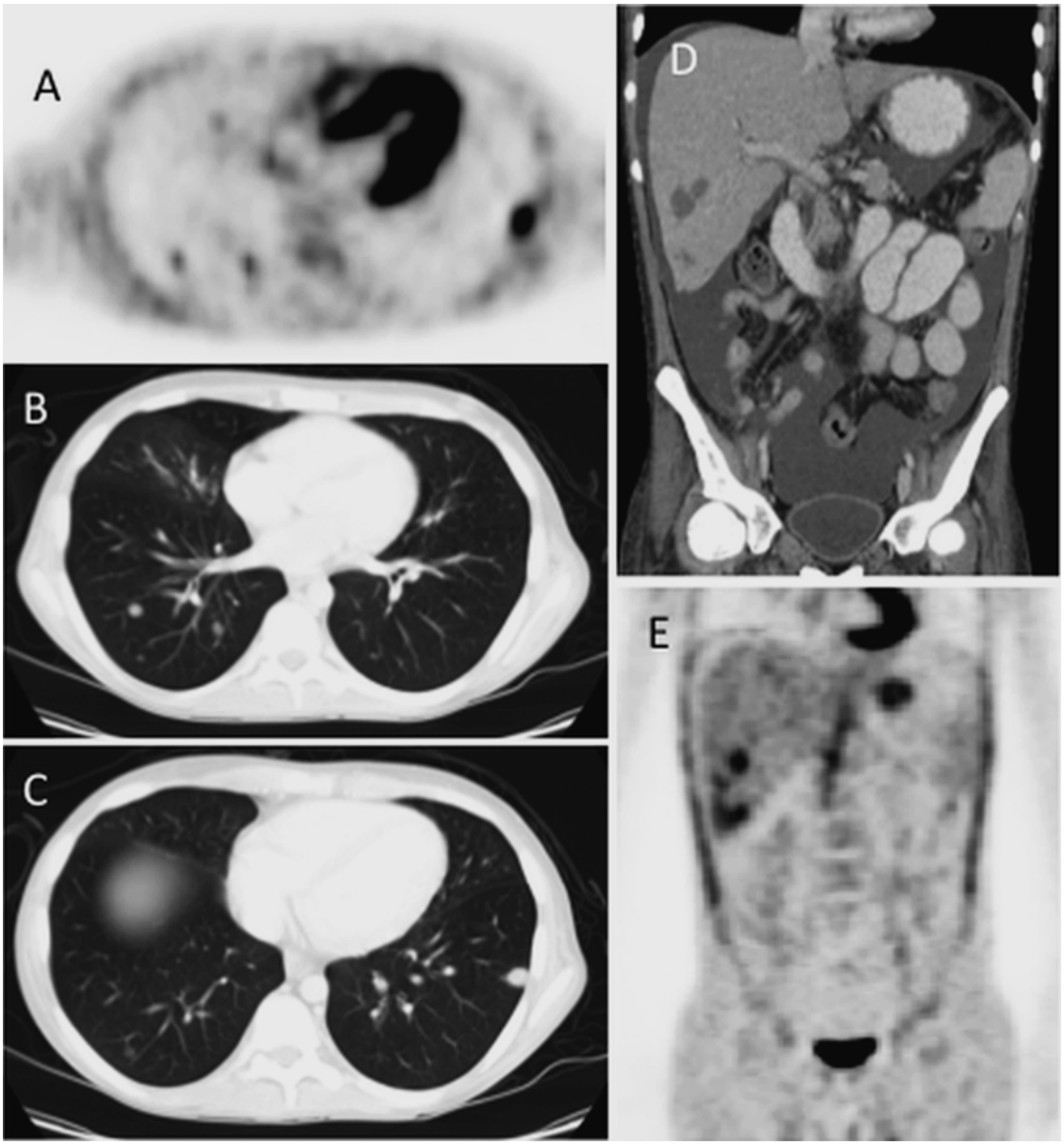


**Fig. 5.5** PTLD involving lung and liver: 16-year old with AML s/p BMT with development of pulmonary PTLD. FDG-PET (**a**) and Chest CT (**b**, **c**) show multiple FDG avid lung lesions. Abdominal CT (**d**) and accompanying FDG-PET (**e**) show multiple hepatic lesion as well as ascites, all consistent with multi-focal sites of PTLD involvement

of EBV-encoded RNA in the lesion generally favors PTLD. Early lesions, including infectious mononucleosis-like PTLD are more frequent in children and usually involve tonsils and adenoids. They have a good prognosis and respond to reduction of immunosuppressive treatment. However, the polymorphous PTLD is the most common type affecting pediatric transplant recipients. Some cases of polymorphic PTLD and most cases of monomorphic PTLD require additional treatment that includes monoclonal antibodies against B-cell antigens (e.g., rituximab), chemotherapy, and more recently cellular immunotherapy (EBV-specific cytotoxic T-cell immunity).

## Overview and Classification of Lymphoid Tumors

Lymphoma represents the third most common pediatric malignancy [51]. Lymphoid malignancies comprise 11 % of total cancers diagnosed in children and 13 % in adolescents and young adults (15–39 years) [52]. The classification of lymphoid neoplasms has undergone a bewildering series of changes over the course of several decades. Those classifications have been universally supplanted by the World Health Organization (WHO) classification. Distinct entities in the WHO classification

**Table 5.4** Common lymphoid neoplasms in children and young adolescents

| |
|---|
| *Precursor lymphoid neoplasms* |
| B-lymphoblastic leukemia/lymphoma, NOS |
| B-lymphoblastic leukemia/lymphoma with recurrent genetic abnormalities |
| T-lymphoblastic leukemia/lymphoma, NOS |
| *Mature B-cell neoplasms* |
| Nodal marginal zone lymphoma |
| Extranodal marginal zone lymphoma of mucosa-associated lymphoid tissue (MALT lymphoma) |
| Pediatric follicular lymphoma |
| Diffuse large B-cell lymphoma, NOS |
| Lymphomatoid granulomatosis |
| Primary mediastinal (thymic) large B-cell lymphoma |
| ALK positive large B-cell lymphoma |
| Burkitt lymphoma |
| *Mature T-cell neoplasms* |
| Epstein-Barr virus (EBV) positive T-cell lymphoproliferative disease of childhood |
| Systemic EBV + T-cell lymphoproliferative disease of childhood |
| Hydroa vacciniform-like lymphoma |
| Extranodal NK/T-cell lymphoma, nasal type |
| Enteropathy associated T-cell lymphoma |
| Hepatosplenic T-cell lymphoma |
| Subcutaneous panniculitis-like T-cell lymphoma |
| Primary cutaneous gamma-delta T-cell lymphoma |
| Peripheral T-cell lymphoma, NOS |
| Anaplastic large cell lymphoma |
| ALK positive |
| ALK negative |
| *Hodgkin lymphoma* |
| Nodular lymphocytic predominant Hodgkin lymphoma |
| Classical Hodgkin lymphoma |
| Nodular sclerosis |
| Mixed cellularity |
| Lymphocyte-rich |
| Lymphocyte-depleted |
| *Immunodeficiency –associated lymphoproliferative disorders* |
| Lymphoproliferative diseases associated with primary immunodeficiency |
| Lymphomas associated with HIV infection |
| Post-transplant lymphoproliferative disorders |
| Plasmacytic hyperplasia and infectious-mononucleosis-like PTLD |
| Polymorphic PTLD |
| Monomorphic PTLD |
| Classical Hodgkin lymphoma PTLD |
| *Histiocytic neoplasms* |
| Langerhans cell histiocytosis |
| Disseminated Juvenile xanthogranuloma |

are defined on the basis of morphologic, immunophenotypic, molecular, and clinical features. Lymphoid neoplasms in the current WHO classification that generally affect children and adolescents are summarized in Table 5.4.

## Precursor T and B Neoplasms

Together, precursor T and B neoplasms represent the most common malignancies in childhood. These neoplasms are derived from precursor lymphoid cells (lymphoblasts) arrested at an early stage of differentiation. B lymphoblastic leukemia/lymphoma accounts for approximately 85 % of cases while T lymphoblastic leukemia/lymphoma accounts for the remaining 15 % [53].

Lymphoid precursor neoplasms may either involve the bone marrow and blood (lymphoblastic *leukemia*) or exhibit a predominantly tissue-based distribution (lymphoblastic *lymphoma*). An arbitrary cutoff of ≥25 % blasts in the blood and/or bone marrow is used to define lymphoblastic leukemia. Since such a distinction has no known diagnostic or prognostic relevance, the current WHO classification employs the term lymphoblastic leukemia/lymphoma.

The prognosis of patients with precursor T and B neoplasms is based on many parameters that include molecular and cytogenetic features in addition to response to induction chemotherapy. In general, patients with T lymphoblastic leukemia/lymphoma tend to have worse outcomes than those with B lymphoblastic leukemia/lymphoma.

## T Lymphoblastic Leukemia/Lymphoma

### Clinical Features and Epidemiology

T lymphoblastic leukemia/lymphoma is a neoplasm of lymphoid progenitors committed to the T lineage. The disease commonly affects males in the second decade of life, and whites are more commonly affected than Asians or African Americans [54]. Patients with ataxia-telangiectasia have an increased predisposition to developing T lymphoblastic leukemia/lymphoma [45]. Up to 85 % of children and adolescents with T lymphoblastic leukemia/lymphoma present with a mediastinal mass and/or lymphadenopathy without leukemia [55, 56]. The majority of patients have symptoms of mediastinal involvement, including pain, facial swelling, and respiratory compromise. Depending on the size of the mediastinal mass, there may be a significant compression of the airway, cardiac, and central vascular structures.

### Imaging Features

Patients with T lymphoblastic leukemia/lymphoma and a large mediastinal mass often have their initial disease suspected based on chest radiograph (Fig. 5.6a, b). These rapidly proliferating tumors can enlarge quickly and present one of the few oncologic emergencies one may encounter in the imaging suite [57]. The presence of a pericardial effusion may result in cardiac tamponade. Care should be taken with

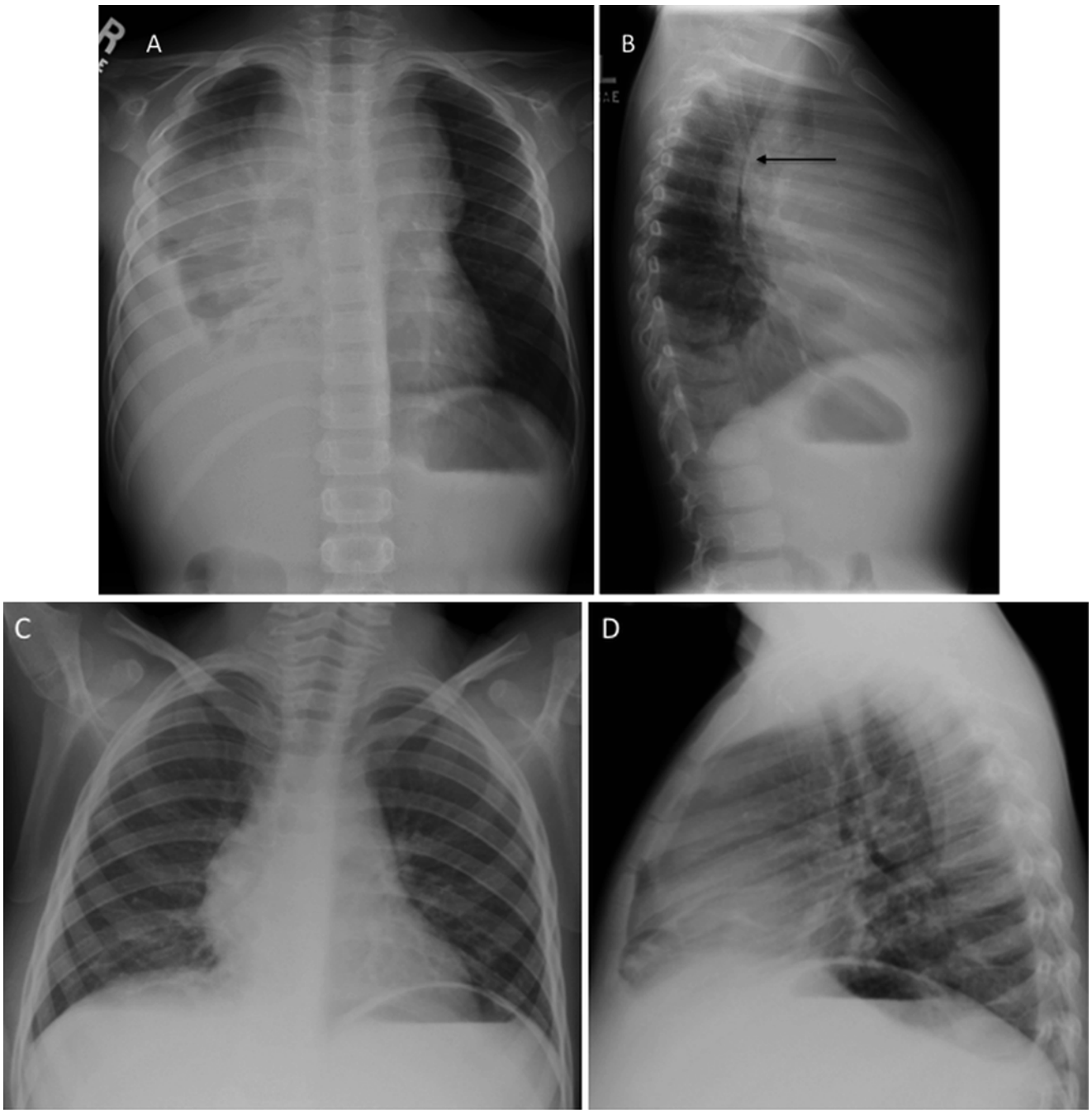


**Fig. 5.6** T-lymphoblastic lymphoma: 5-year old with wheezing, fatigue, and pallor. AP and lateral CXR at diagnosis shows large mediastinal mass with significant tracheal narrowing evident on the lateral projection arrows and a large right pleural effusion (**a**, **b**). The patient could not lie flat for biopsy; pleural fluid aspirate showed T-Cell ALL. After just 6 days of therapy mediastinal mass has nearly resolved and effusions are gone (**c**, **d**)

supine positioning of these patients and with sedation given the increased risk of respiratory compromise and impaired venous return.

Once appropriate therapy is instituted, patients with Tlymphoblastic leukemia/lymphoma typically have a rapid shrinkage in their mediastinal mass and improvement in their symptoms (Fig. 5.6c, d). There is no clear prognostic role for CT characterization of the mediastinal mass apart from establishing the extent of disease and sites of disease of involvement that may require urgent intervention. CT scans at the time of diagnosis may demonstrate extensive abdominal visceral involvement and intra-abdominal lymphadenopathy (Fig. 5.7). Some studies have shown that early resolution of the mediastinal mass, either by chest radiograph [58] or by

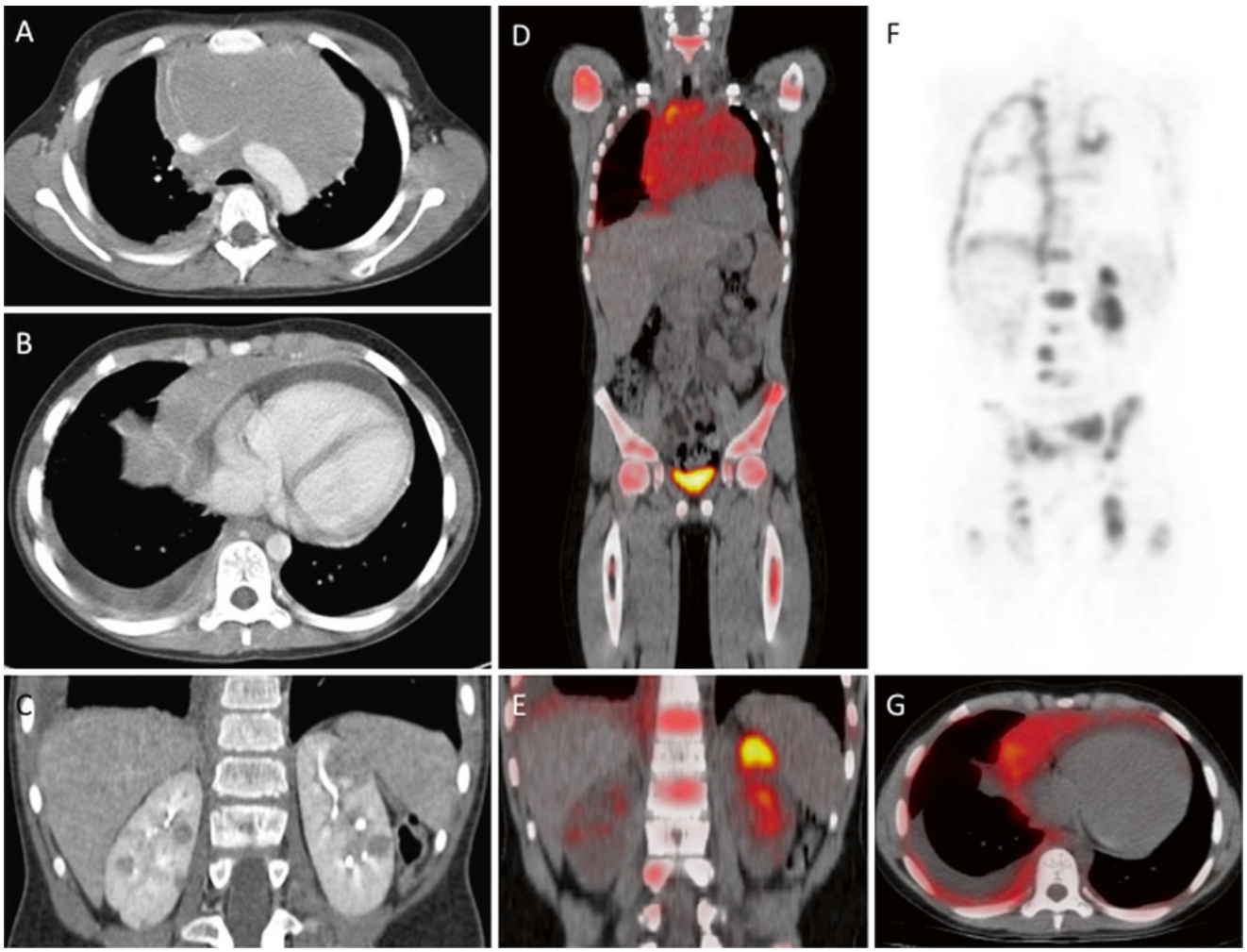


**Fig. 5.7** T-lymphoblastic lymphoma, CT and FDG PET: 10-year old with T-ALL, mediastinal mass compressing major vessels (**a**), pleural effusion and pericardial effusion (**b**) and extensive visceral (bilateral renal (**c**) and bony disease (**e**, **f**). FDG PET/CT confirms multifocal sites of involvement by metabolically active tumor and in particular shows the extent of bone involvement (**d**–**g**)

CT [59] is associated with improved outcome, presumably reflecting patients with more chemosensitive disease.

Although these rapidly dividing tumors are quite metabolically active and typically FDG avid (Fig. 5.7), staging and post-treatment evaluation by FDG PET imaging is not used frequently in patients with precursor lymphoid neoplasms.

## Pathology

The neoplastic cells have scant to moderate cytoplasm, irregular nuclear contours, and a dispersed chromatin pattern. The latter is best appreciated on Wright-Giemsa-stained preparations. A similar pattern is noted on hematoxylin-and-eosin-stained tissue sections. Characteristically, the neoplastic cells have high rates of mitosis and apoptosis with frequent areas of increased background macrophages imparting a so-called starry-sky pattern (Fig. 5.8).

Immunohistochemistry or flow cytometry immunophenotyping demonstrates expression of one or more T lineage markers including CD1a, CD2, CD3, CD4, CD7 and CD8 (Fig. 5.9). Of these, CD3 is regarded as the *bona fide* T lineage-specific marker. In addition, the neoplastic cells are often positive for CD34, TdT, and CD99. It should be noted that CD99 expression may be positive in other small round cell tumors that are usually part of the differential diagnosis [60]. T-LBL can be further subclassified into groups representing stages of T-cell maturation and differentiation (Table 5.5). Early T-cell precursor (ETP) acute lymphoblastic leukemia/lymphoma represents approximately 15 % of precursor T neoplasms and is characterized by high frequency of relapses following standard chemotherapy [61]. This recently described entity is characterized by CD3 expression (cytoplasmic ± surface using flow

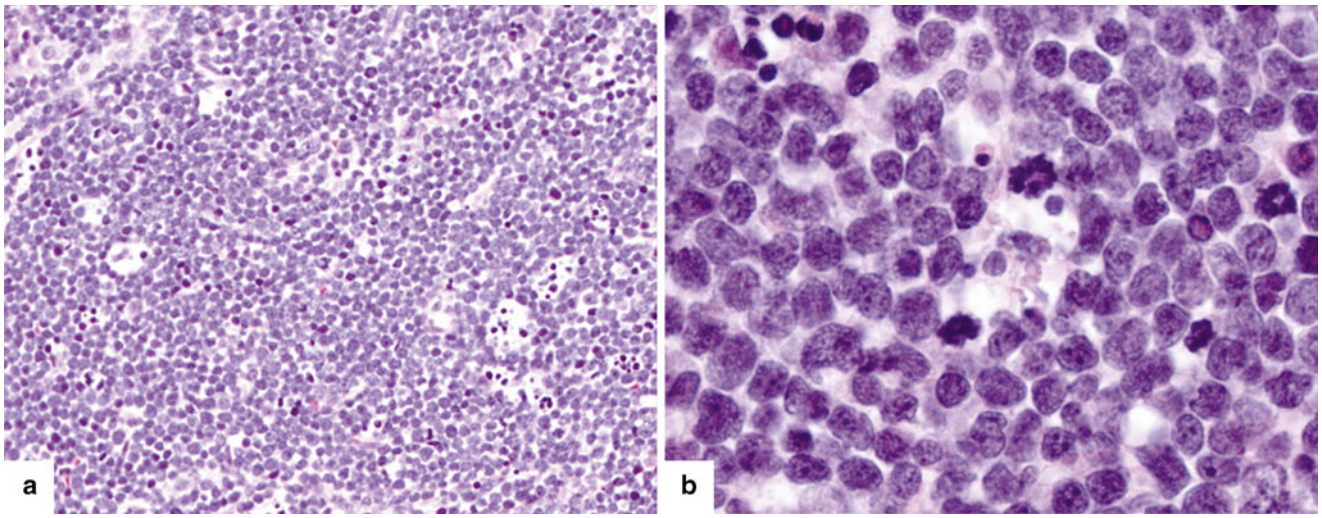


**Fig. 5.8** (**a**) Precursor T-cell ALL diffusely involving the lymph node with numerous mitoses and tingible-body macrophages imparting a "starry-sky" appearance. (**b**) The blasts have characteristic features including small to intermediate size, scant amount of cytoplasm, irregular nuclear membranes, finely dispersed chromatin, and inconspicuous nucleoli

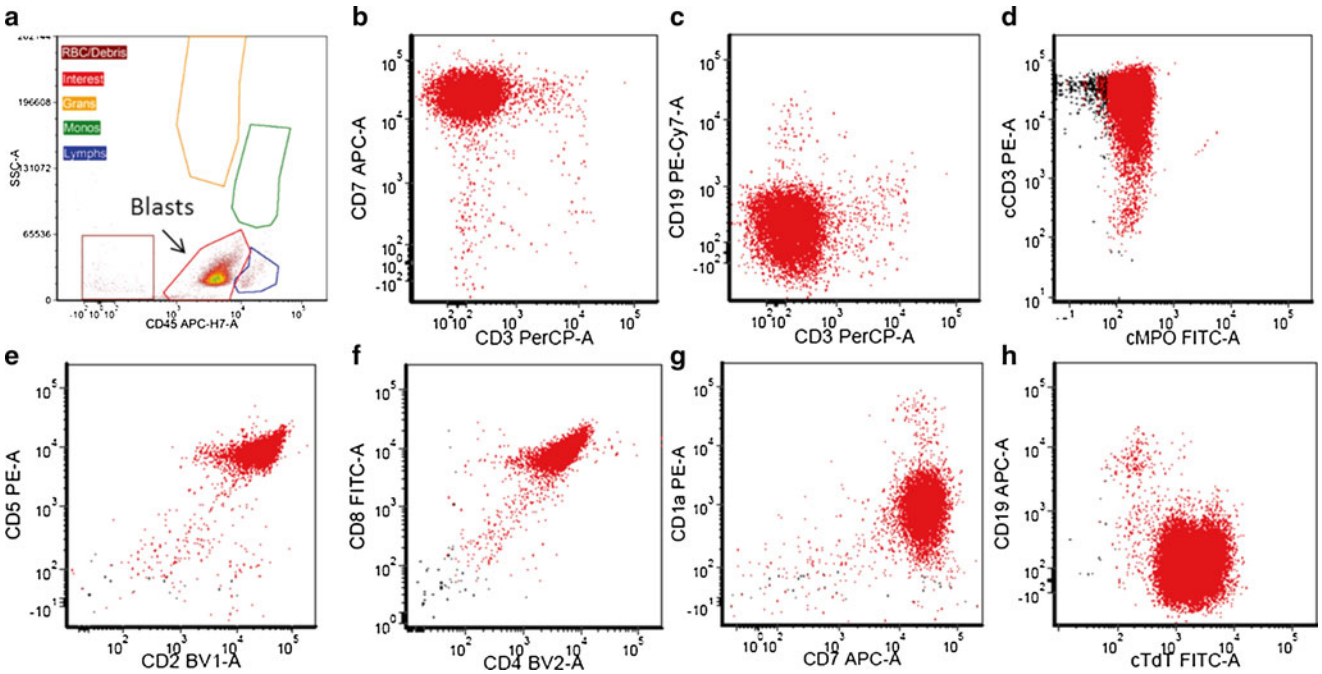


**Fig. 5.9** Precursor T-cell ALL immunopheotype. The patient is a 14-year-old male with diffuse lymphadenopathy. A core biopsy reveals a diffuse infiltrate of mononuclear cells with blast morphology. Flow cytometry was performed on a cell suspension that showed increased blasts defined by dim CD45 expression and low side scatter (SSC-A) properties (**a**). The blasts expressed bright CD7 (**b**), and they were negative for CD19 (**c**). They also expressed cytoplasmic CD3 that confirmed T-cell lineage, while they were negative for MPO (**d**). The blasts also expressed CD2, CD5 (**e**), and were double positive for CD4 and CD8 (**f**). They were also positive for CD1a (**g**) and TdT (**h**), and negative for B-cell (CD19) and myeloid (MPO) antigens

**Table 5.5** T-ALL Immunophenotype associated with T-cell maturation and differentiation

| Stage | Immunophenotype |
|---|---|
| Pre-thymic stage | Common lymphoid progenitor cell (pro-T) expressing CD34, TdT and HLA-DR and are negative for cytoplasmic CD3 (cCD3) |
| Subcupsular cortical stage | Early T-cell precursors (pre-T) that express CD2, cCD3, CD7, TdT and are double negative (CD4- and CD8-). TCR gene at germ line configuration |
| Cortical stage | Common thymocyte phenotype: CD1a, CD2, cCD3, CD7, TdT and double positive for CD4 and CD8. TCR gene rearrangement identified |
| Medullary stage | Mature medullary thymocytes loose expression of TdT and CD1a, and express both cytoplasmic and surface CD3 and either CD4 or CD8 (single positive thymocytes) |

**Table 5.6** B-ALL with recurrent genetic abnormalities (2008 WHO classification)

| Translocation | Fusion product | Frequency (%) | Prognosis | Immunophenotype |
|---|---|---|---|---|
| t(9;22)(q34;q11.2) | *BCR-ABL1* | 2–4 % in children | Poor | CD25+, CD117−, CD13+, CD33+, CD10+, CD19+, TdT+, CD34+, CD9+ |
| t(v;11q23)<br>t(4;11)(q21;q23)<br>t(19;11)(p13;q23)<br>t(9;11)(p22;q23) | *MLL*<br>*AF4-MLL*<br>*ENL-MLL*<br>*AF9-MLL* | Most common<br>Also seen in T-ALL<br>Common in AML | Poor | CD19+, CD10−,CD24−, CD15/65+, CD9+ |
| t(12;21)(p13;q22) | *TEL-AML1 (ETV6-RUNX1)* | 25 % of cases, common in children | Favorable | CD34+, CD13+, CD9− |
| Hyperdiploidy >50 chromosomes (most common +21, +X, +14, +4) | | 25 % of cases, common in children | Favorable | CD34+, CD45− |
| Hypodiploidy <46 chromosomes | – | <45 chromosomes 1 % | Poor | |
| t(5;14)(q31;q32) | *IL3-IGH@* | <1 % | Unknown | Eosinophilia |
| t(1;19)(q23;p13.3) | *E2A-PBX1 (TCF3-PBX1)* | 6 % | Improved with current intensive therapies | CD9 + strong, CD34−, cμ heavy chain |

*BCR* breakpoint cluster region, *ABL1* abelson murine leukemia viral oncogene holog 1, *MLL* mixed lineage leukemia, *AF4* AF4/FMR2 family, member 1, *ENL* MLLT1 myeloid/lymphoid/leukemia or mixed lineage leukemia translocated to 1, *AF9* ALL-1 fused gene from chromosome 9, *TEL (ETV6)* translocation, ETS, leukemia, *AML1 (RUNX1)* acute myeloid leukemia 1 gene (RUNT-related transcription factor), *IL-3* interleukin 3, *IGH@* immunoglobulin heavy chain, *E2A (TCF3)* immunoglobulin enhancer-binding factor E12/E47 (transcription factor 3), *PBX1* pre-B leukemia transcription factor 1

cytometry), lack of expression of CD1a, and aberrant expression of stem cell myeloid markers (CD34, CD33, CD13, and CD117).

## B Lymphoblastic Leukemia/Lymphoma

### Clinical Features and Epidemiology

B lymphoblastic leukemia/lymphoma, in contrast to its T counterpart, usually has limited tissue involvement at presentation [56, 62]. The majority of patients present with peripheral blood and bone marrow disease, with skin, testes, and lymph nodes being among the most common sites of extramedullary involvement. Various molecular/cytogenetic B lymphoblastic leukemia/lymphoma groups are recognized in the WHO classification (Table 5.6).

### Imaging Features

Extensive thoracic or abdominal involvement is uncommon with B lymphoblastic leukemia/lymphoma. Accordingly, the use of FDG PET imaging for staging is generally not indicated. Typically, the initial staging evaluation is directed by symptoms and physical exam findings. For example, the presence of a testicular mass noted by ultrasound might prompt additional evaluation (Fig. 5.10).

### Pathology

The morphologic features of B lymphoblastic leukemia/lymphoma are identical to those of T lymphoblastic leukemia/lymphoma. The B-cell lineage is defined by the expression of CD19 and one or more of the following markers: CD79a, cytoplasmic CD22 and/or CD10 (Fig. 5.11). In addition, the neoplastic cells are often positive for CD34 and TdT. PAX5 is a highly specific B-cell marker that is expressed in virtually all cases of B lymphoblastic leukemia/lymphoma [63]. It should be noted that the neoplastic cells of B lymphoblastic leukemia/lymphoma might be negative for CD20 and CD45 by immunohistochemistry. B lymphoblastic leukemia/lymphoma can be further subclassified into groups representing stages of B-cell maturation and differentiation (Table 5.7).

## Mature B-Cell Neoplasms

Lymphomas account for approximately 15 % of all childhood malignancies, but their incidence varies in different age groups being low in children younger than 5 years and highest in adolescents between 14 and 19 years of age [64]. Mature B-cell neoplasms are broadly divided into two categories: Hodgkin lymphoma and non-Hodgkin lymphoma (NHL).

## Hodgkin Lymphoma

### Clinical Features and Epidemiology

Hodgkin lymphomas account for nearly 9 % of all childhood cancers and usually occur in adolescents. They are unusual in children under the age of 5 years. Hodgkin lymphomas are primary nodal malignancies characterized by relatively few

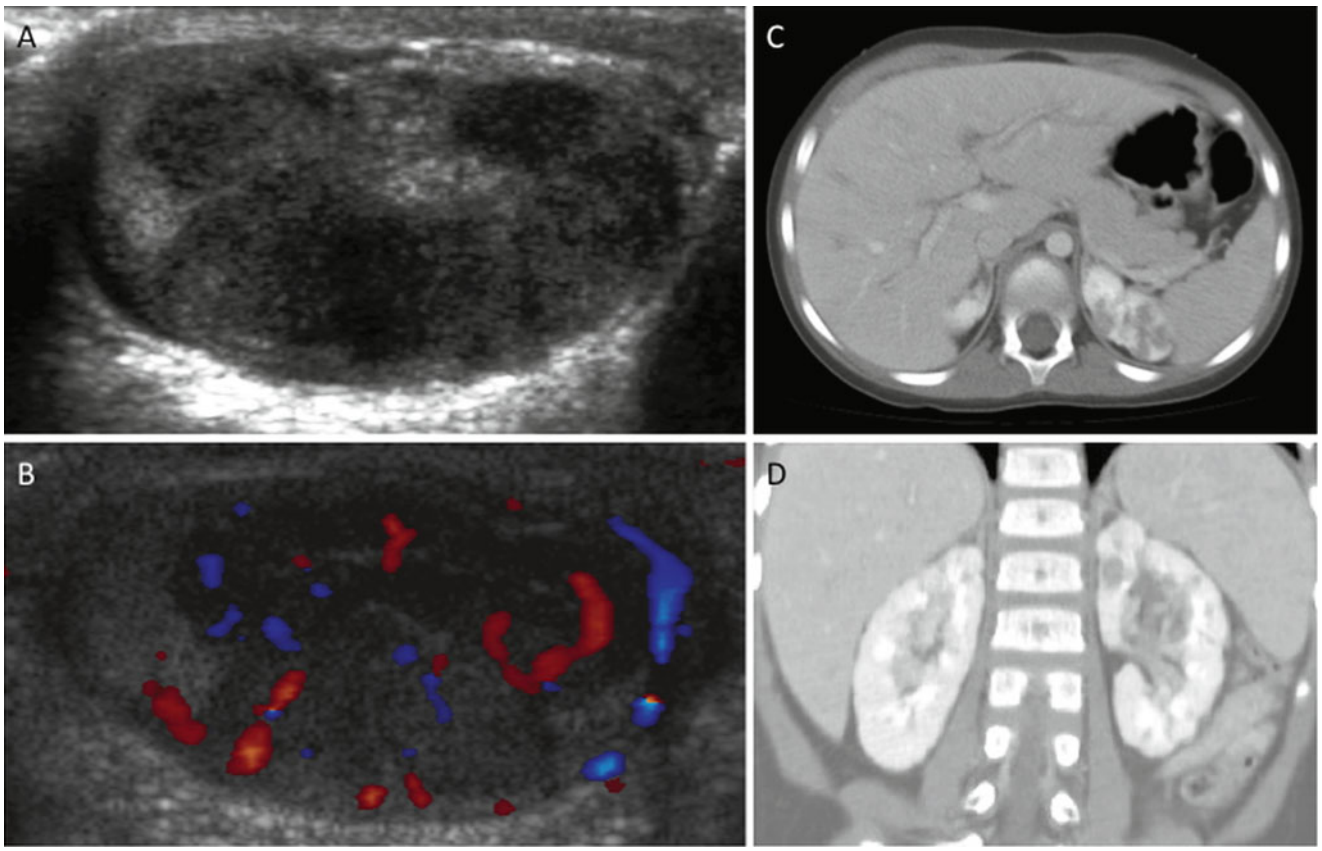


**Fig. 5.10** Pre-B lymphoblastic lymphoma: 4-year-old with bilateral asymmetric, nontender testicular enlargement detected by pediatrician at a routine check-up. (**a**, **b**) US showed multifocal testicular masses with increased color Doppler flow (b). (**c**, **d**) CT showed additional bilateral renal involvement, L>R. Biopsy revealed pre-B cell lineage lymphoblastic lymphoma; bone marrow had <5 % blasts

dispersed monoclonal lymphoid cells, most commonly of B-cell lineage, surrounded by a sizeable heterogeneous population of inflammatory cells. The WHO classification divides Hodgkin lymphomas into two broad groups with distinct differences in clinical features and behavior as well as in immunophenotype: classical Hodgkin lymphoma (CHL) and nodular lymphocyte predominant Hodgkin lymphoma (NLPHL).

Classical Hodgkin lymphoma (CHL) accounts for nearly 95 % of all Hodgkin lymphomas. Four subtypes of CHL are recognized: nodular sclerosis, mixed cellularity, lymphocyte-rich, and lymphocyte-depleted. The most common sites of involvement with CHL include the mediastinum and cervical lymph nodes. The nodular sclerosis subtype is more common in developed countries and less commonly associated with EBV, whereas the mixed cellularity subtype is more common in developing countries and is frequently associated with EBV. Nodular lymphocyte predominant Hodgkin lymphoma (NLPHL) comprises approximately 5 % of Hodgkin lymphomas. The most common sites of involvement include cervical, axillary, and inguinal lymph nodes, with only rare involvement of the bone marrow, mediastinum, or spleen [65].

Therapy selection and prognostic stratification of Hodgkin lymphoma is based on pathologic and imaging staging studies, which include bilateral bone marrow biopsies and PET/CT scans [66]. The current staging system for Hodgkin lymphoma is based on the Ann Arbor staging classification system (Table 5.8). The staging system accounts for the absence (A) or presence (B) of systemic symptoms including night sweats, weight loss, and fever. The presence extranodal extension of disease (other than to bone marrow and liver, which would result in stage 4 disease) is annotated with the letter E [67].

## Imaging Considerations

In Hodgkin lymphoma, chest radiographs are often the first examination to suggest the possibility of malignancy. These are usually obtained for vague upper respiratory or constitutional symptoms including fever, night sweats, and cough. A mediastinal mass is present in more than two thirds of patients at the time of diagnosis (Fig. 5.12). These findings typically prompt further evaluation by CT or

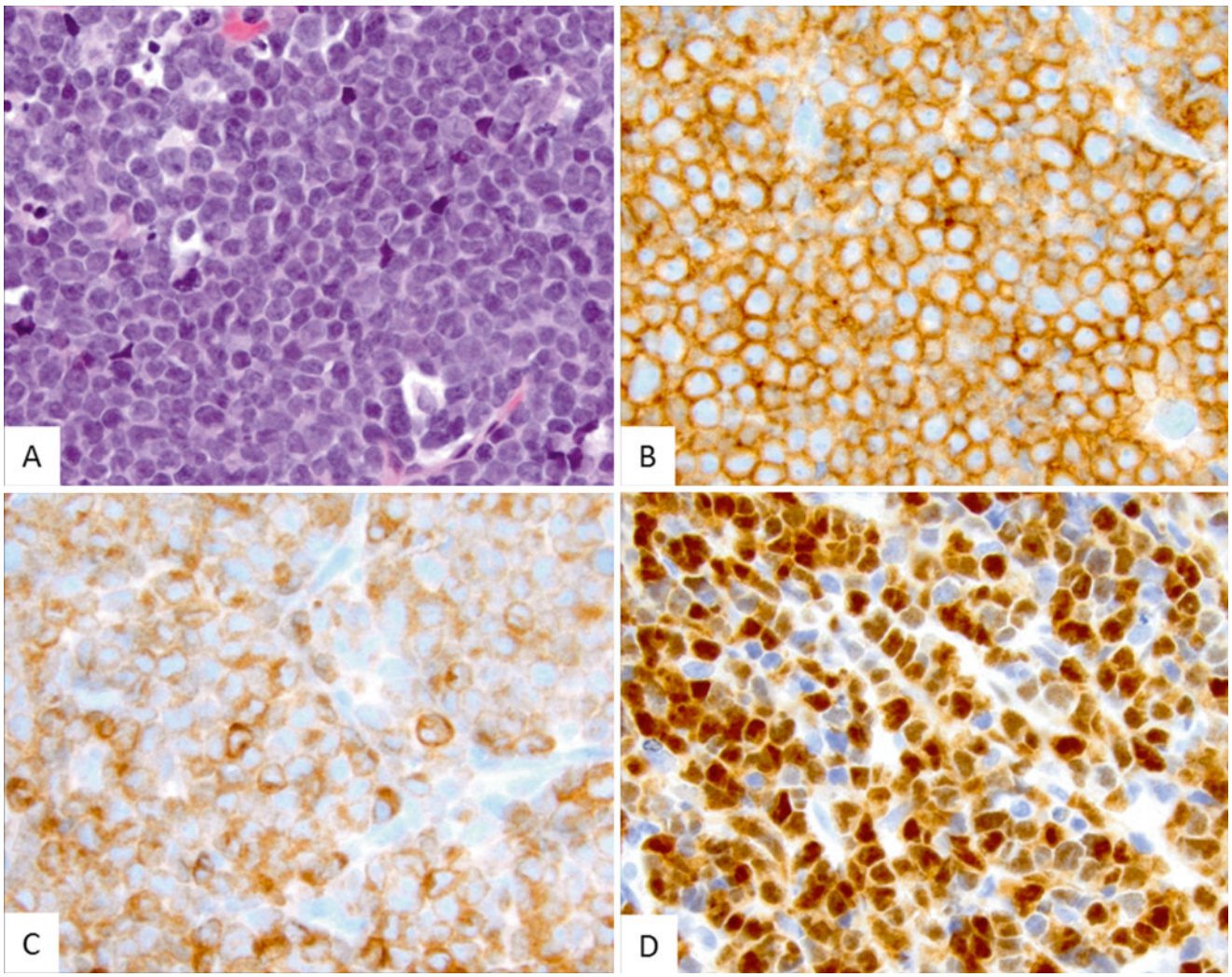


**Fig. 5.11** This case of precursor B-cell ALL reveals a neoplastic infiltrate that is morphologically identical to precursor T-cell ALL. (**a**) Immunohistochemical stains showed that the blasts expressed characteristic B-cell markers being positive for CD19 (**b**) and PAX5 (**c**), as well as for TdT (**d**)

**Table 5.7** B-ALL Immunophenotype associated with B-cell maturation and differentiation

| Stage | Immunophenotype |
|---|---|
| Pro-B stage | Early precursor B-ALL: CD10, CD19, cytoplasmic CD79a, cytoplasmic CD22, and TdT |
| Intermediate stage | Common B-ALL is characterized by expression of CD10, CD19, HLA-DR and heavy chain gene rearrangement |
| Pre-B stage | At this stage the cells express CD19, surface CD22, and cytoplasmic μ chains. Heavy chain and light chain gene rearrangement. At this stage TdT and CD34 are not expressed |

MRI. The diagnostic and staging examination should encompass all of the potential sites of lymph node involvement and should begin at the level of the skull base/Waldeyer ring and extend through the inguinal region. At the time of the staging, it is important to be aware of the potential for airway and vascular compression due to large neck and mediastinal masses. Indeed, it may be clinically contraindicated to place a patient supine for CT evaluation due to the presence of a large mediastinal mass and obvious airway narrowing that is apparent radiographically, although in some instances imaging can be accomplished with the patient prone (Fig. 5.13). The presence of greater than 50 % tracheal luminal narrowing poses a significant risk to sedation and anesthesia and should be a major consideration in the staging and diagnostic evaluation [68]. In addition to characterizing the extent of disease, the imaging evaluation should also help identify easily accessible lymph nodes for diagnostic sampling.

By imaging alone, it is not possible to distinguish between the subsets of Hodgkin lymphoma. One exception is nodular

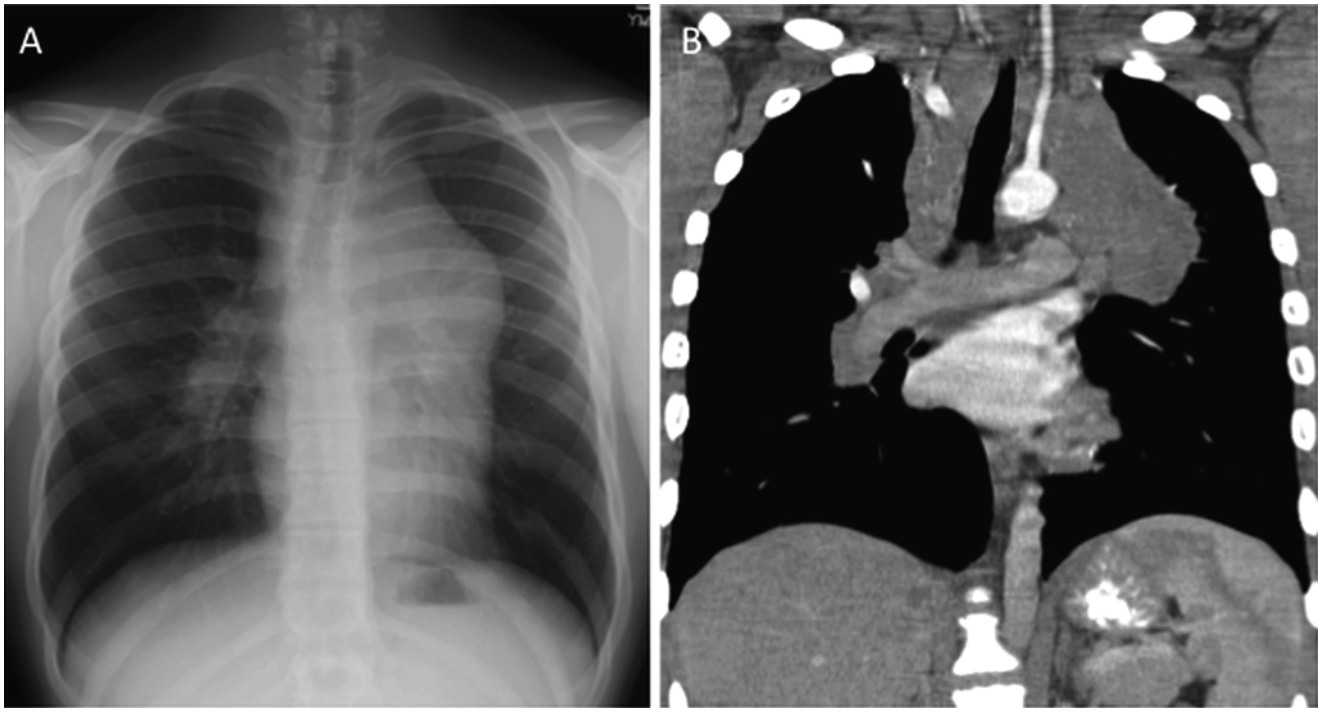


**Fig. 5.12** Hodgkin lymphoma: 17-year old presented to the emergency room with chest pain and airway symptoms. (**a**) CXR shows a large mediastinal mass and rightward tracheal deviation. (**b**) Coronal CT image confirms extensive mediastinal, paratracheal, and hilar nodal involvement. Biopsy confirmed nodular sclerosis classical Hodgkin lymphoma

lymphocyte predominant Hodgkin lymphoma, which may be suggested by the presence of localized disease. Indeed, it is not uncommon for a single site of NLPHL to be completely removed at the time of surgical excisional biopsy. In Hodgkin lymphoma, hematogenously spread metastatic disease to the lung is uncommon, and is seen in less than 5 % of the patients [69]. It is not uncommon for pulmonary disease to be present; however, this is usually seen in association with ipsilateral hilar or mediastinal nodal involvement and likely reflects contiguous extension as opposed to hematogenous spread. This may be important in determining the stage of the patient, since true hematogenous spread resulting in pulmonary parenchymal nodules would indicate stage 4 disease (Fig. 5.14a, b), whereas a localized mediastinal disease with ipsilateral contiguous parenchymal involvement via peribronchovascular lymphatics would be considered stage 2-E (2-extension) disease (Fig. 5.14c, d). Pericardial and pleural effusions may be seen in Hodgkin lymphoma. It is also important for the radiologist to be alert for the presence of cardiophrenic lymph nodes and to distinguish these from upper abdominal lymph node involvement. Involvement of the abdominal viscera is relatively unusual. Liver involvement, when present, is almost always associated with splenic involvement. Isolated splenic involvement occurs in 30–40 % of the patients with Hodgkin lymphoma [69]. Often, the extent of splenic involvement may be difficult or impossible to determine by CT and is only suggested by FDG PET imaging [70]. Bone marrow involvement in Hodgkin lymphoma is rare and bone marrow aspiration has been almost completely replaced by FDG PET imaging for the purpose of staging the bone marrow for tumor involvement [71] (see below discussion).

*Imaging modalities used in staging*: CT scanning is still the imaging modality of choice for staging children with Hodgkin lymphoma, although several recent studies have advocated the use of MRI for this purpose [32]. FDG PET imaging is considered standard of care in the staging of children with suspected Hodgkin lymphoma [72]. Hodgkin lymphoma is typically a metabolically active tumor (Fig. 5.15) and FDG PET has increased sensitivity for detecting small sites of hypermetabolic lymph node involvement that may influence disease staging, particularly in areas difficult to characterize by cross-sectional imaging, such as the hepatic hilum and retroperitoneum, and visceral sites of involvement such as the spleen. The ability to co-register simultaneously acquired PET/CT images has further advanced the use of PET imaging in pediatric Hodgkin lymphoma staging [72] (Fig. 5.16). The overall consensus from multiple studies is that FDG PET imaging combined with co-registered, simultaneously acquired cross-sectional imaging, either by CT or

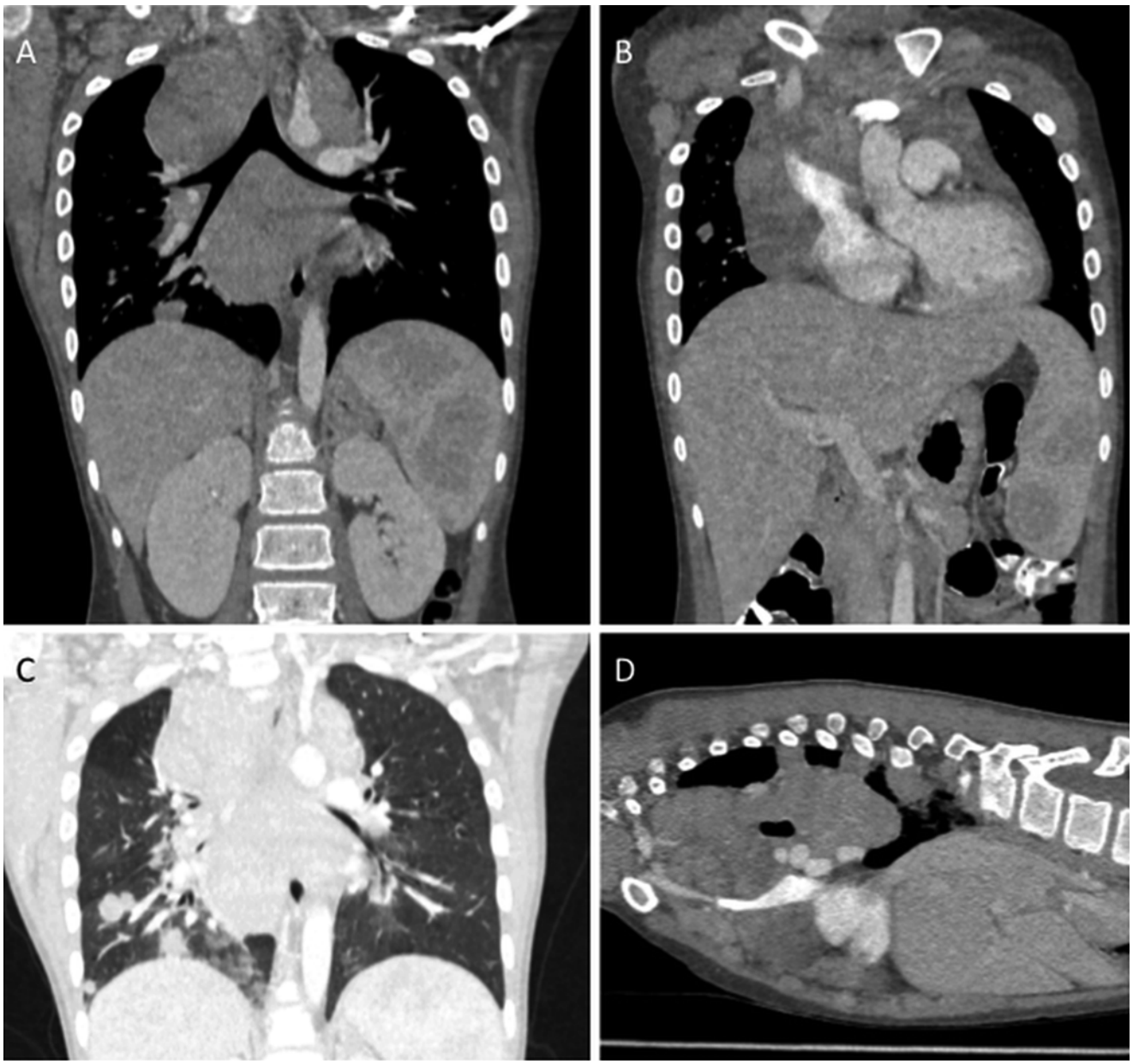


**Fig. 5.13** Patient with HL and CT images at diagnosis showing extensive mediastinal, hilar, subcarinal, and splenic involvement (**a**, **b**). CT images reviewed under lung windows show parenchymal lung nodules and heterogeneous lung attenuation, with attendant compression of the bronchi. The imaging was performed prone (**d**) based on clinical concern for airway and vascular compression, which the CT confirms, showing significant SVC narrowing (**b**) and tracheal compression (**a**, **c**)

by MRI, provides the greatest sensitivity and specificity for staging the patient with suspected lymphoma [72–75]. The combined images retain the sensitivity of FDG PET at identifying sites of radiographically occult disease, while at the same time, improving the specificity of the PET imaging, allowing sites of background or physiologic uptake to be accurately localized and distinguished from malignancy.

At the time of diagnosis, diffuse homogeneous low-level bone marrow uptake is commonly seen and should not be interpreted as diffuse marrow involvement. Rather, this likely represents reactive marrow hyperplasia secondary to the underlying Hodgkin lymphoma [71], and is readily distinguishable from the focal areas of FDG uptake seen in patients with bone marrow involvement by lymphoma (Fig. 5.17). Based on imaging, there are no specific or characteristic FDG PET features to distinguish between the different forms of Hodgkin lymphoma and biopsy is required to make this distinction.

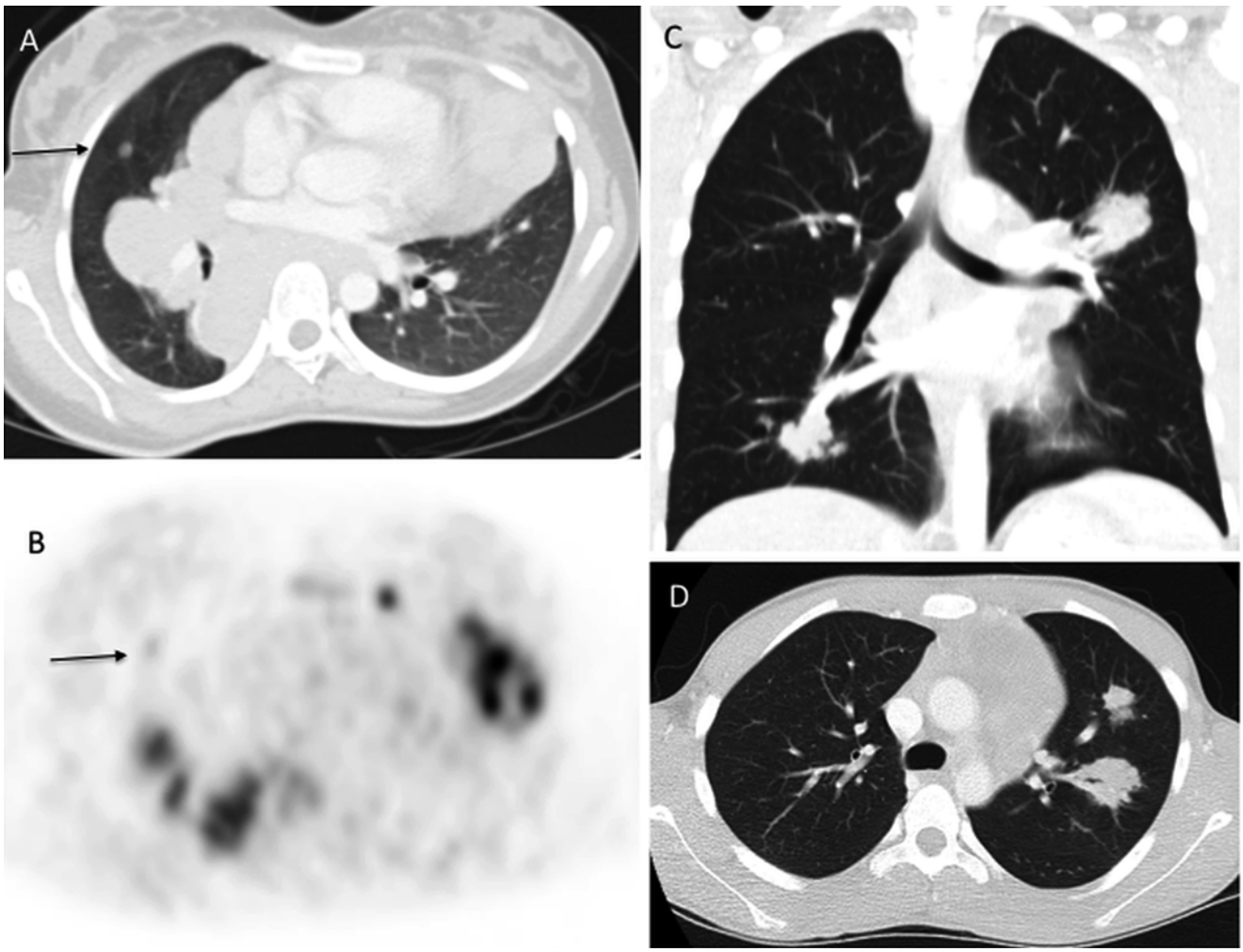


**Fig. 5.14** Lung nodules in HL. (**a**, **b**) CT (a) and FDG PET (b) focal parenchymal lung nodule (*arrows*) that is FDG avid and distinct from the more centrally located mediastinal mass. This is in contrast to the parenchymal abnormalities shown by CT in (**c**) and (**d**) that extend from sites of mediastinal and hilar involvement, consistent with local extension along peribronchovascular lymphatics, rather than hematogenously spread disease

The use of bone scintigraphy in Hodgkin lymphoma is rarely performed, and has been replaced by FDG PET imaging [71]. The use of intravenous contrast agents for either CT or MRI evaluation is still considered necessary in the staging evaluation of Hodgkin lymphoma patients, even when hypermetabolic FDG PET avid disease is present. The presence of contrast allows for a more accurate measurement of disease at the time of diagnosis (Fig. 5.18), which has been shown to be important in response assessment [6] and in terms of providing accurate measurement to establish the presence of bulky disease. Furthermore, the presence of vascular invasion or thrombosis is also difficult to detect in the absence of contrast agent administration.

Chest radiographs are often still required by clinical protocols for determining the presence of mediastinal bulk disease, and typically are obtained at the time of initial disease presentation. Many clinical protocols still require an upright PA chest radiograph to determine the maximal transthoracic diameter of the mediastinal mass, with bulk disease being defined as a mediastinal mass greater than 1/3 the transthoracic diameter [76], as measured at the level of T5/T6. The Ann Arbor staging system is still used to classify patients with childhood Hodgkin lymphoma (Table 5.8). The Cotswold modification of the Ann Arbor staging system incorporates CT imaging criteria and specifies that lymph nodes detected by CT that are greater than 10 cm in transaxial diameter are to be considered sites of bulk disease [76], although different pediatric cooperative groups use different size cut-offs for determining bulk disease (e.g., the Children's Oncology Group considers lymph nodes masses >6 cm as indicative of bulk disease).

*Response assessment*: Patients with Hodgkin lymphoma typically enjoy greater than 90 % 5-year overall survival, with even higher rates for patients with low stage disease [69, 77]. As a

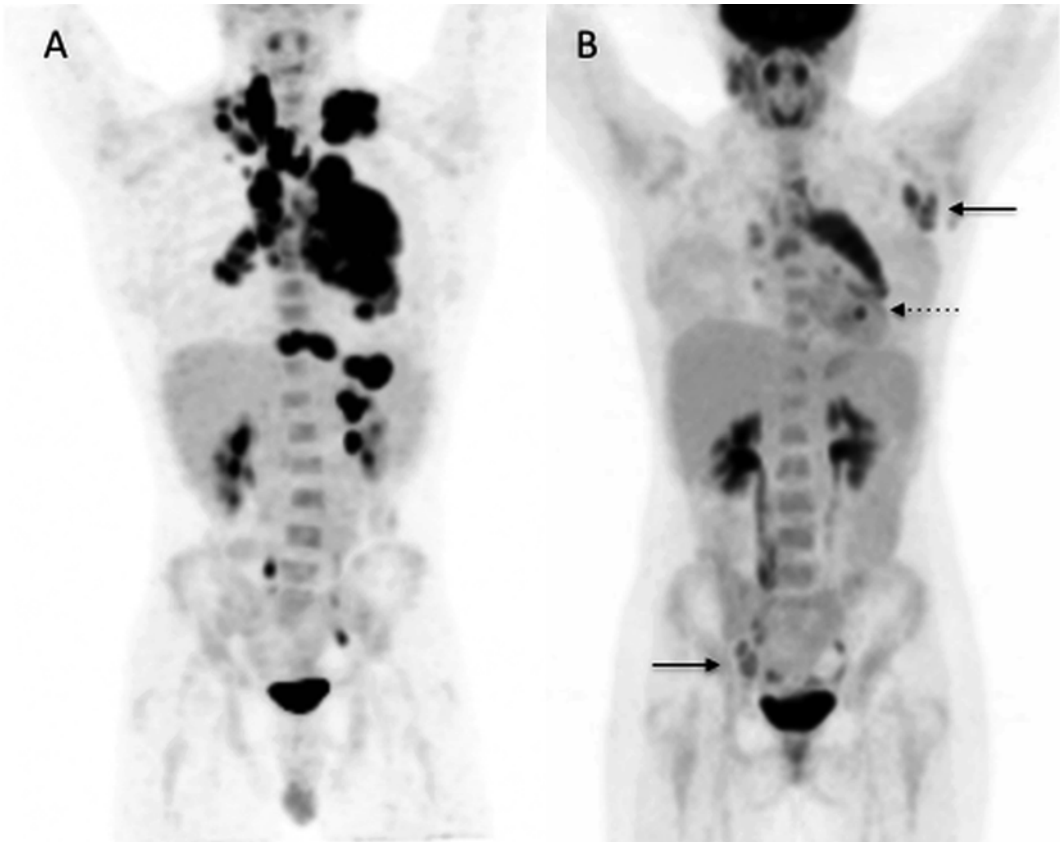


**Fig. 5.15** FDG PET in Hodgkin Lymphoma. Two patients showing intensely FDG avid disease. (**a**) This patient has supraclavicular, hilar, and mediastinal disease with separate foci of disease in diaphragmatic nodes. (**b**), This patient, in addition to having mediastinal and hilar disease, also has FDG avid lesions in the left axilla and in the right iliac chain (*arrows*), as well as the left lower lobe of the lung (*dashed arrow*), emphasizing the importance of PET in identifying multifocal sites of disease involvement

result, objective measures of treatment response have gained increasing attention in an effort to develop early, objective, and prospectively evaluable end points to identify patients who are responding early to therapy, in an effort to predict which patients will have a durable response to therapy [29, 78]. There is some evidence to suggest that a brisk early response to chemotherapy may be a determinant of tumor chemosensitivity and predict an overall good outcome [78–80]. The ability to monitor changes in metabolic activity within the mediastinal mass using FDG PET imaging has provided a valuable surrogate for assessing early response to therapy [72, 75]. There have been multiple studies both in adult and pediatric patients showing that patients with early responses to therapy based on decreases in FDG PET uptake have improved event free and overall survival as compared to those who have residual PET abnormalities after the initial two cycles of therapy [81, 82]. These results have led to implementation of a response-based treatment paradigm where early interim FDG PET scanning could be an excellent prognostic indicator for predicting chemosensitivity of the tumor and ultimately clinical outcome (Fig. 5.19). Subsequent studies, evaluating both change in size of the mediastinal mass and change in the metabolic activity, have suggested that outcomes will likely be best predicted by a combination of factors including resolution of FDG uptake and significant change in size of the patient's sites of disease involvement as measured by CT and/or MRI [5, 6].

In an effort to arrive at a consensus regarding definitions of disease and treatment response in adult patients with lymphoma, an international team of experts reviewed the available data to arrive at the so-called international harmonization project criteria for determining PET and CT responses in lymphoma [83, 84]. These are shown in Table 5.9, based on a revision of previous malignant lymphoma response criteria and have been recently updated as the Lugano Classification [85, 86]. Although these proposals for classification, staging, and response assessment have not yet been validated in pediatric patients, the main challenge that remains for clinicians and diagnostic imagers is developing objective criteria for assessing FDG PET response. There have been a number of proposals aimed at distinguishing residual low-level neoplastic FDG activity from background uptake [72]. The use of standardized uptake value measurements is still considered

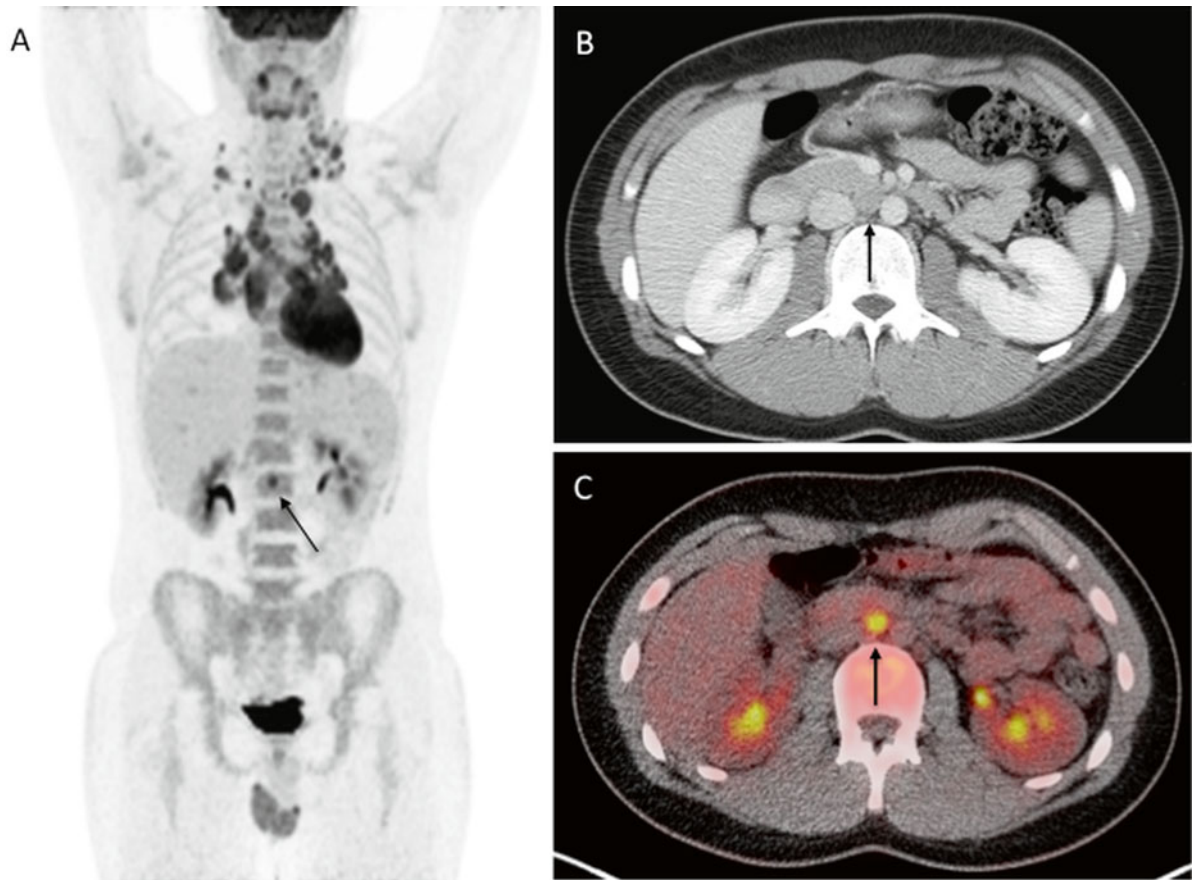


**Fig. 5.16** Impact of FDG-PET on disease staging: (**a**) Coronal FDG PET MIP image showing extensive mediastinal disease and bilateral supraclavicular disease. In addition, a tiny focus of uptake below the diaphragm (*arrows*) localized to an aortocaval node on the fused PET/CT image (**c**). With the benefit of the PET images for review, the small aortocaval lymph node could be readily identified on the diagnostic CT obtained earlier (*arrow*) (**b**)

experimental and has not been universally accepted. The criteria receiving the greatest acceptance have been based on a 5-point scale, with uptake greater than mediastinal blood pool, but less than liver, considered to be background, with uptake greater than the liver considered suspicious for residual activity [85–87]. These criteria must, however, be validated in larger treatment trials.

*Surveillance*: Also at issue is the use of imaging for disease surveillance and the frequency with which surveillance should be performed. In a study of over 200 pediatric patients with intermediate and high risk lymphoma, it was found that the sole predictor of overall survival in these patients was time to relapse [88]. Those patients who relapsed within the first year after completing therapy had lower overall survival than those patients who had relapses after the first year. Furthermore, relapses that occurred beyond 1 year off therapy, whether they were detected by physical exam, laboratory findings or routine surveillance imaging (Fig. 5.20), were equally likely to have a good clinical outcome. Based on this, it was proposed that routine surveillance CT imaging beyond 1 year after therapy be eliminated, since it is unlikely to impact overall survival and adds additional cost and radiation exposure to patients who are likely to have an overall good outcome [88–91].

## Pathology

### Classical Hodgkin Lymphoma

The lymph node architecture is often effaced in classical Hodgkin lymphoma. The neoplastic Hodgkin-Reed-Sternberg (HRS) cells are typically large and dispersed among background inflammatory cells, which include variable numbers of small lymphocytes, plasma cells, eosinophils and histiocytes. Reed-Sternberg cells are binucleated neoplastic cells with round to oval nuclear contours, a prominent eosinophilic nucleolus within each of the nuclei, and abundant amphophilic or basophilic cytoplasm. Neoplastic cells without characteristic Reed-Sternberg features are referred to as Hodgkin cells (Fig. 5.21).

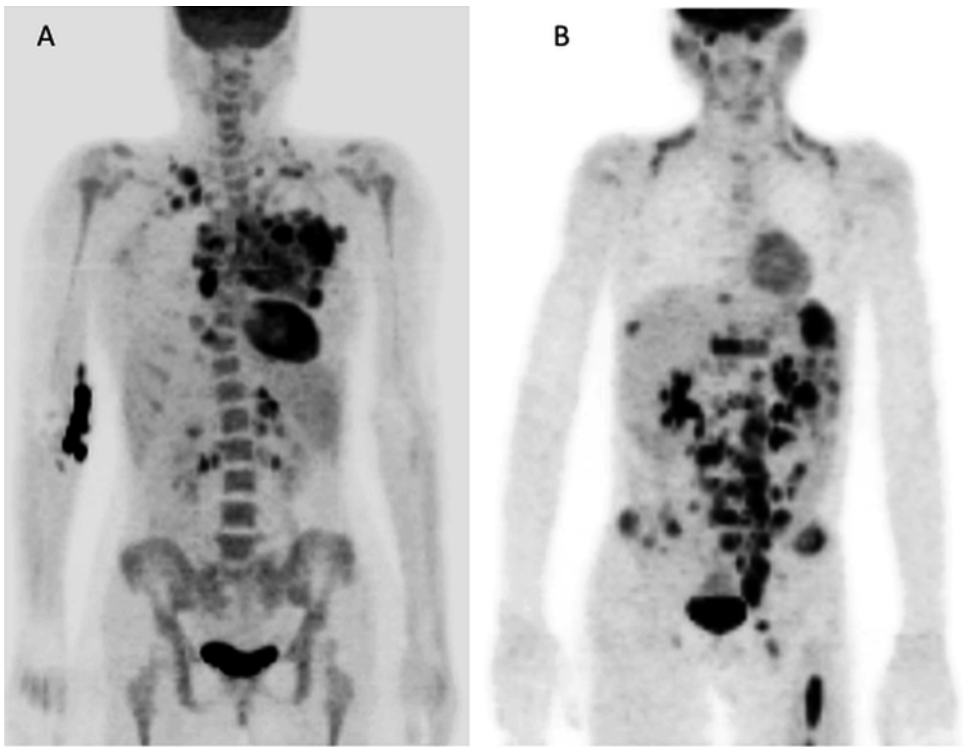


**Fig. 5.17** Bone marrow involvement in HL. Two examples of bone marrow signal abnormalities on PET scans of patients with HL. In (**a**) diffuse low level uptake throughout the bone marrow is commonly seen at the time of diagnosis (see also Fig. 5.16) and felt to be related to non-specific inflammatory changes in the bone marrow. This is in contrast to intense focal bone marrow uptake (**b**), seen in the vertebral bodies, pelvis, and left femur, related to lymphomatous involvement of the bone marrow

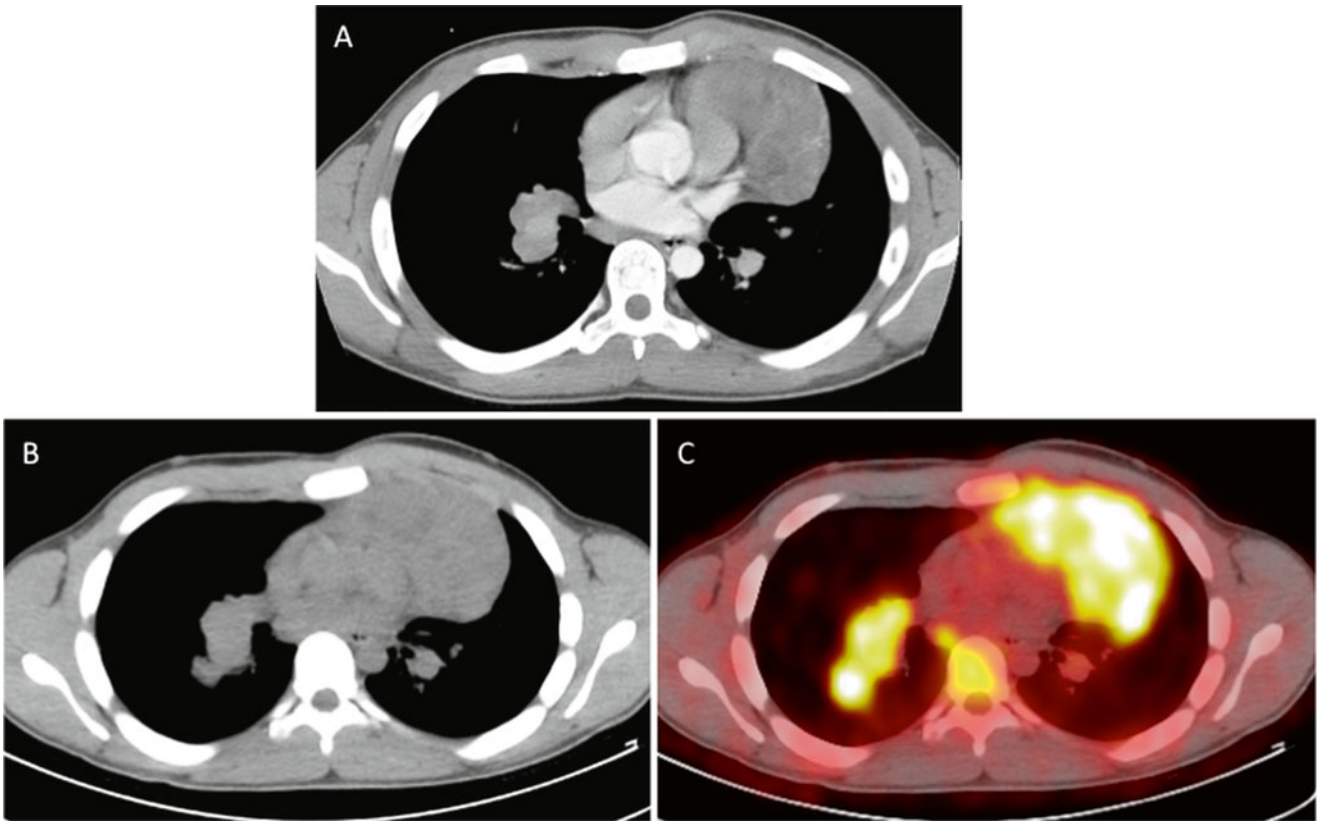


**Fig. 5.18** Comparison of contrast-enhanced versus non-contrast CT/Ac: Contrast enhanced (**a**), non-enhanced (**b**) and fused PET/CT (**c**) show the importance of IV contrast in defining the boundary between normal structures and sites of disease, allowing accurate measurements to be made

**Table 5.8** Lymphoma staging—Hodgkins lymphoma

| Ann Arbor classification for staging |
|---|
| Stage I: |
| Involvement of single lymph node region (I) or localized involvement of a single extralymphatic organ or site (IE) |
| Stage II: |
| Involvement of two or more lymph node regions on the same side of the diaphragm (II), or localized contiguous involvement of a single extralymphatic organ or site and its regional lymph node(s), with involvement of one or more lymph node regions on the same side of the diaphragm (IIE) |
| Stage III: |
| Involvement of lymph node regions on both sides of the diaphragm (III) |
| These may also be accompanied by localized contiguous involvement of an extralymphatic organ or site (IIIE), by involvement of the spleen (IIIS), or both (IIIE + S) |
| Stage IV: |
| Disseminated (multifocal) involvement of one or more extralymphatic organs or tissues, with or without associated lymph node involvement, or |
| Isolated extralymphatic organ involvement, with distant (non-regional) nodal involvement |
| "A" Symptoms: Lack of "B" symptoms |
| "B" Symptoms: at least one of the following: |
| Unexplained weight loss >10 % |
| Unexplained recurrent fever >38° |
| Drenching night sweats |

*Nodular sclerosis classical Hodgkin lymphoma* is characterized by a nodular growth pattern formed by thick collagen bands that partially or completely encase nodular areas of tumor and result in a thickened lymph node capsule. In this variant, HRS cells may occasionally retract from surrounding tissues in formalin-fixed material forming lacunar cells (Fig. 5.22). The syncytial variant of nodular sclerosis CHL refers to cases with prominent aggregates of HRS cells often associated with increased histiocytes and necrosis. *Mixed cellularity classical Hodgkin lymphoma* is characterized by effacement of the lymph node architecture with a diffuse infiltrate of HRS cells in a mixed inflammatory background without nodular collagen fibrosis. The histiocytes in the mixed inflammatory background may show epithelioid features and may form loose clusters or granulomas (Fig. 5.23). Reed-Sternberg cells are more commonly seen in this variant. *Lymphocyte-rich classical Hodgkin lymphoma* is uncommon in children. It is characterized by a nodular or, less commonly, diffuse growth pattern in which the inflammatory infiltrate consists almost exclusively of small lymphocytes. Residual germinal centers with HRS cells localized to the mantle zone are a feature that has been described in lymphocyte-rich CHL. *Lymphocyte-depleted classical Hodgkin lymphoma* is the rarest of the CHL subtypes and seldomly encountered in the pediatric age group. This subtype is characterized by an enriched HRS population and/or depletion of non-neoplastic inflammatory cells.

By immunohistochemistry, HRS cells in the various subtypes of CHL share similar immunophenotypic features. Nearly all cases are positive for CD30, MUM1/IRF4, and PAX5. Immunoreactivity for PAX5 by HRS cells is typically weak in comparison to non-neoplastic background B-cells. Nearly 80 % of cases are positive for CD15, while CD20 positivity is seen in nearly 20 % of cases. Lack of CD45 (LCA, leukocyte common antigen) expression is seen in all cases, and loss of OCT2 and/or BOB1 expression can be demonstrated in most cases (Fig. 5.24). An association exists between CHL and Epstein-Barr virus (EBV), but the prevalence of such an association varies by subtype and epidemiologic factors. It should be noted that while a mature B-cell at the germinal center stage of differentiation is believed to be the cell of origin in the vast majority of CHL cases, rare cases of demonstrable peripheral T-cell derivation have been reported.

### Nodular Lymphocyte Predominant Hodgkin Lymphoma

A nodular growth pattern, with or without a diffuse component, is characteristic of NLPHL. The neoplastic cells—known as LP cells (for lymphocyte predominant; formerly, L&H cells for *l*ymphocytic and/or histiocytic)—are large, with distinctively multilobated nuclei with prominent nuclear membrane folds, chromatin clearing, and multiple basophilic nucleoli. The LP cells have been also called "popcorn" cells. They are typically scattered in nodular arrangements within a background that is rich in small lymphocytes and histiocytes, as well as follicular dendritic cells (FDC) (Fig. 5.25). Adjacent lymph nodes or lymph nodes that are partially involved by NLPHL may occasionally exhibit reactive follicular hyperplasia with PTCG.

LP cells are usually positive for CD20, CD79a, CD45, and BCL6, and they are negative for CD30 and CD15. Characteristically, background small lymphocytes consist predominantly of B-cells and CD4+/CD57+ T-cells that express markers of germinal center T-cells. Another feature of NLPHL is the presence of expanded nodular meshworks of FDC that may be highlighted using CD21, CD23, and CD35.

### Prognosis

In the general population, approximately 60 % of patients present with localized disease (Ann Arbor stage I or II). The clinical stage and the response following two courses of chemotherapy evaluated by FDG-PET studies are the most important prognostic factors in CHL. Patients with low stage disease (stage IA and IIA) have a long-term survival between

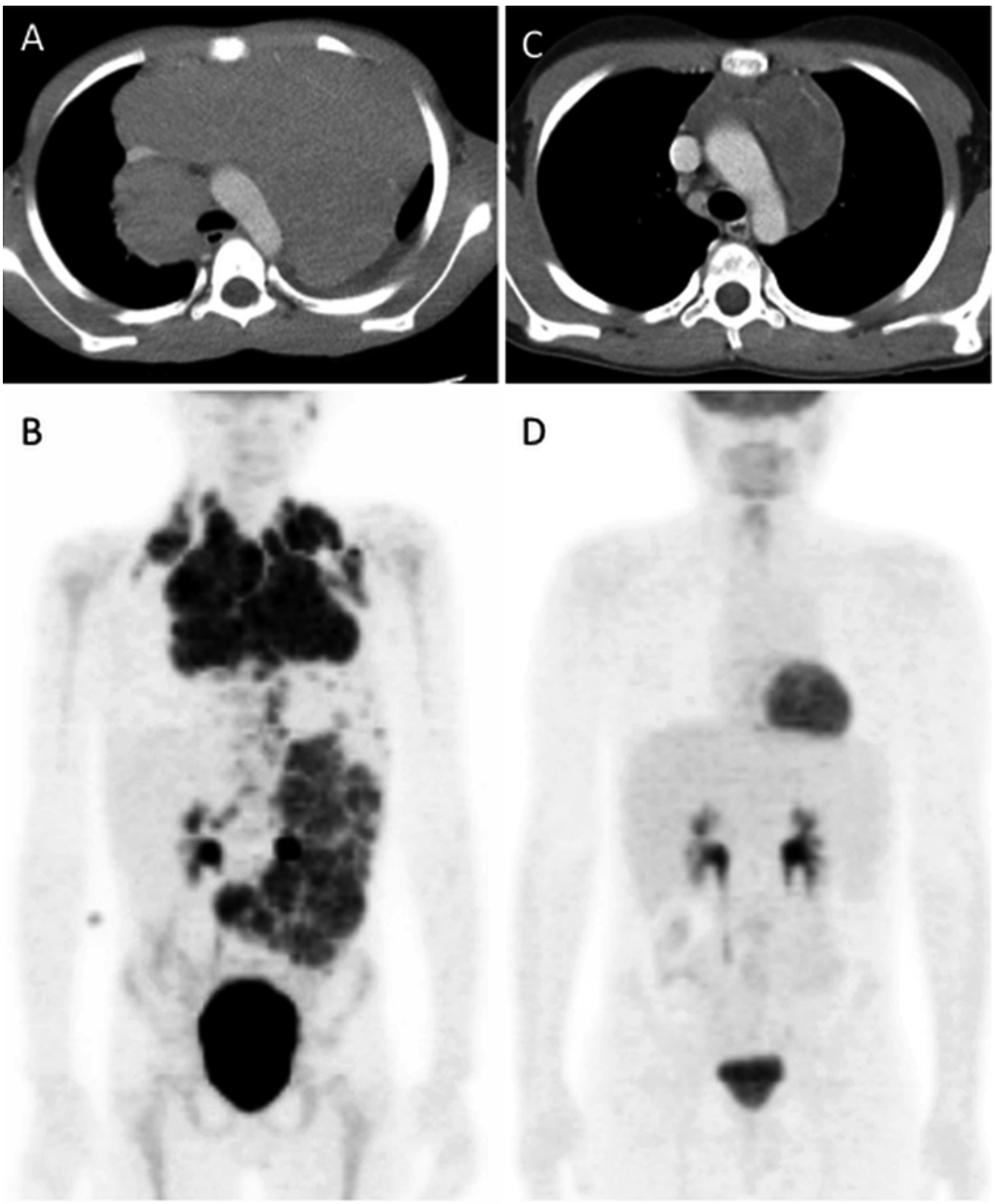


**Fig. 5.19** PET versus CT response. This patient had extensive disease at baseline (**a**, **b**), with a complete metabolic response to therapy after 2 cycles of treatment (**d**). Although there has been >70 % shrinkage of the mediastinal mass, there is still residual "disease" seen on CT (**c**) and—depending on the response criteria being used—this patient may not be considered to be in CR, emphasizing the challenge of using both anatomic and metabolic criteria for response

80 and 95 %, while patients presenting at a higher stage (stage III and IV) with B symptoms have a cure rate of 60–65 % [92]. Patients with NLPHL generally have a favorable prognosis, and the disease is responsive to therapy even after relapse. In some institutions, patients with stage I disease, especially if young, are not treated following resection of involved lymph nodes. Over 80 % of patients are alive at 10 years.

## Non-Hodgkin Lymphomas

Non-Hodgkin lymphomas in children are represented predominantly by mature aggressive B-cell lymphomas, most commonly Burkitt lymphoma followed by diffuse large B-cell lymphoma occurring in older children. Low grade indolent B-cell lymphomas are less frequent in children

compared to adults. The difference in incidence, prognosis and response to treatment for the different groups of B-cell lymphomas between children and adults support possible difference in the pathogenesis [93].

**Table 5.9** Summary of new Harmonization Project Criteria for PET and CT in determining response in lymphoma

| Response | Criteria |
|---|---|
| CR | FDG-PET completely negative |
| | Residual lymph nodes/nodal masses allowed, if FDG-negative |
| | Bone marrow biopsy negative |
| | Splenic/liver involvement must disappear |
| | No new sites of disease |
| PR | FDG positivity should be present in at least one previously involved site |
| | Regression of measurable disease; no new sites of disease |
| | ≥50 % decrease in SPD of 6 dominant LNs/nodal masses |
| | ≥50 % reduction in splenic/hepatic nodules, if present |
| | Even if CR by other criteria, positive bone marrow biopsy is considered PR |
| SD | Failure to achieve PR, but not meeting PD criteria |
| PD/relapse | Any lesion increased in size by ≥50 % from nadir |
| | Any new lesion |
| | PET should be positive in new/progressed lesions if ≥1.5 cm |

*Notes:* New criteria include PET in definition of CR. PET considered positive if uptake is greater than mediastinal blood pool (lesions >2 cm), or above local background (lesions <2 cm)

From an imaging standpoint, the staging and response assessment of patients with NHL lymphoma are very different from the Ann Arbor system used in patients with Hodgkin lymphoma [55]. In childhood NHL, the St. Jude staging system (Table 5.10) is still widely used. Depending on the type of lymphoma, e.g., T-lymphoblastic leukemia/lymphoma, FDG PET imaging may not be indicated for staging or response assessment. Otherwise, the imaging evaluation is similar to that utilized for Hodgkin lymphoma patients and should include cross-sectional imaging either by CT or by MRI, and FDG PET imaging as indicated [94]. For patients with primary bone lymphomas, MRI may also be required to further assess the sites of skeletal involvement. For lymphomas primarily involving the cutaneous and subcutaneous tissues, there is very little role for imaging.

## Diffuse Large B-Cell Lymphoma

### Clinical Features

Diffuse large B-cell lymphoma (DLBCL) is a heterogeneous category of mature B-cell neoplasms characteristically comprised of large transformed mature B cells that grow in a diffuse pattern. It represents approximately 10 % of NHL of childhood [95]. Most children with DLBCL present with localized disease involving extranodal sites. Mediastinal large B-cell lymphoma is a rare but distinct variant of DLBCL

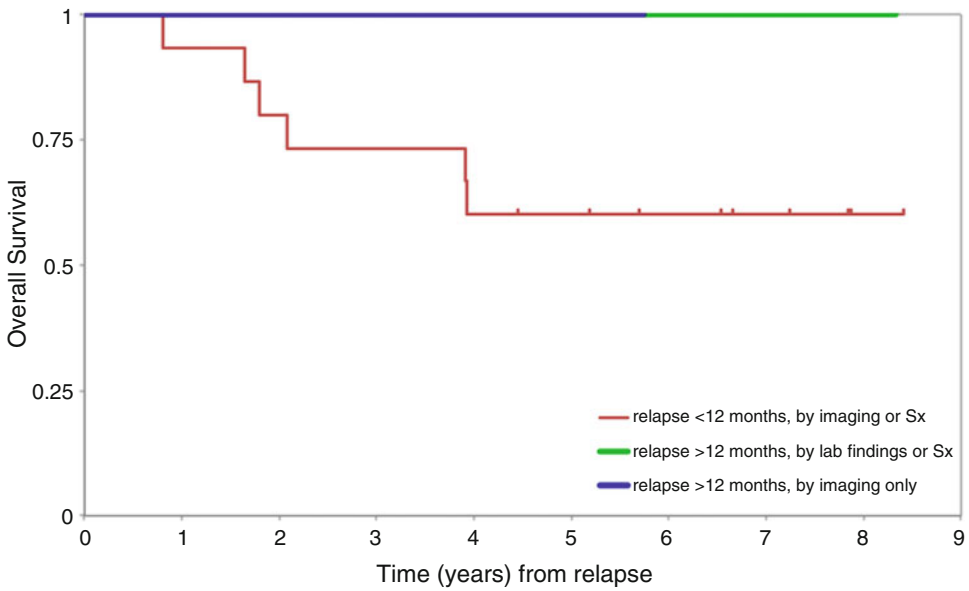


**Fig. 5.20** Overall survival in HL following relapse, based on method of relapse detection: 216 patients were enrolled on the multi-institutional Children's Oncology Group Trial 9425 from 1997 to 2001. 25 patients relapsed. When patients were grouped based on method of relapse detection; (1) Relapse within the first 12 months, detected either by imaging, Sx or clinical findings (*red line*); (2) Relapse beyond 12 months, detected by Sx or clinical findings (*green line*); or (3) Relapse beyond 12 months, detected by imaging only, with no Sx or clinical findings (*blue line*)]. Six patients died, all of them within the first year off therapy, independent of the method of detection, showing that the most important predictor of survival was time to relapse. Surveillance imaging beyond 1 year after completing therapy had no impact on outcome (reproduced with permission [88])

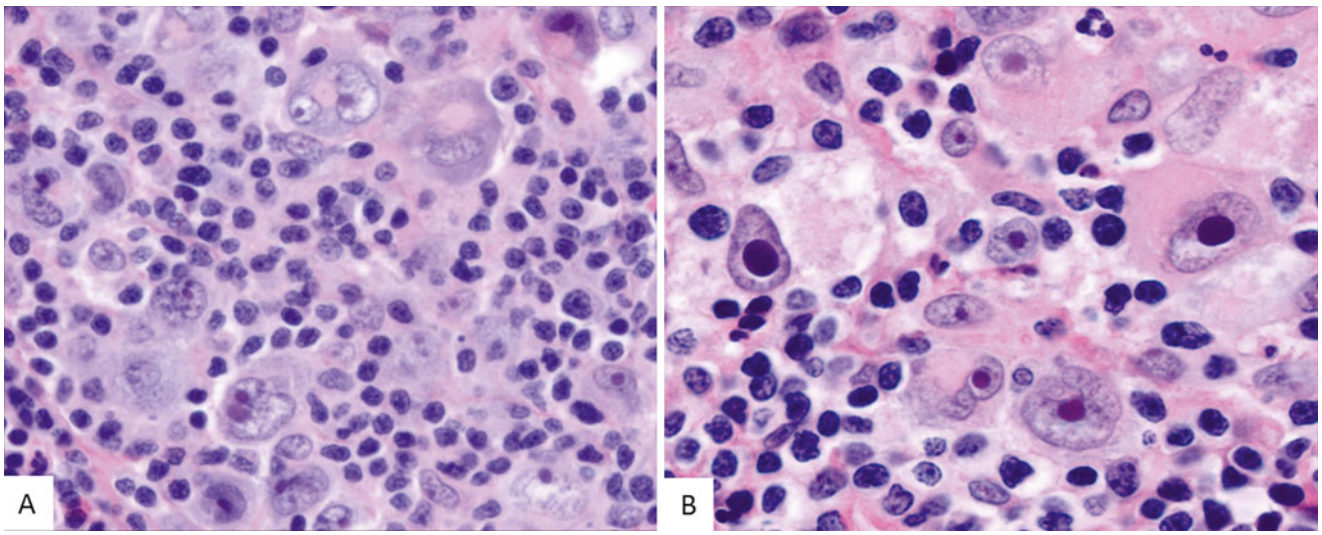


**Fig. 5.21** The neoplastic cell of classical Hodgkin lymphoma. (**a**) The Reed-Sternberg (RS) cells are giant cells with binucleated or multinucleated nuclei with macronuclei present in the separate nuclei or nuclear lobes. (**b**) The Hodgkin cells represent the mononuclear variant of the RS cells with prominent large nucleoli

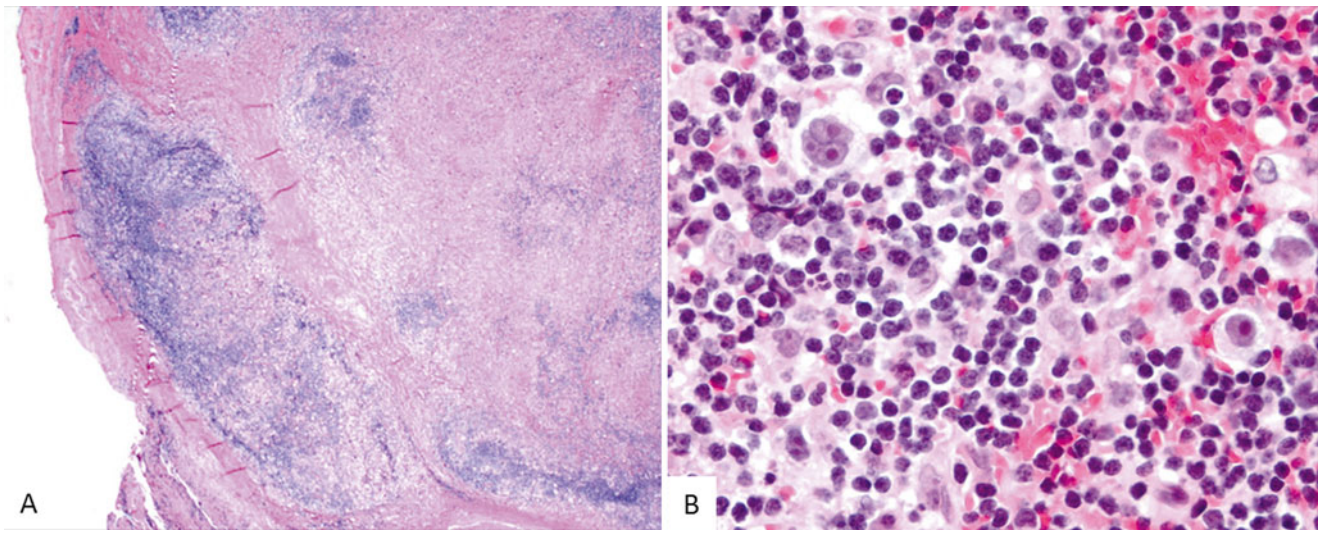


**Fig. 5.22** Classical Hodgkin lymphoma, nodular sclerosis (NS) subtype. (**a**) A lymph node involved by CHL with neoplastic nodules surrounded by broad collagen bundles. (**b**) Neoplastic cells are identified in the nodules including lacunal cells that are considered characteristic of this subtype of CHL. The lacunar cells are only identified in formalin-fixed tissues due to retraction artifact

that arises from mature thymic B-cells and is generally associated with worse outcomes compared to non-mediastinal DLBCL [96].

## Imaging Features

DLBCL commonly presents with localized disease. Anterior mediastinal or cervical/supraclavicular lymphadenopathy may be present and is more characteristic of DLBCL than other NHL subtypes. The mediastinal mass may appear somewhat more diffuse and aggressive by imaging, but is not specifically distinguishable from mediastinal masses present in other lymphoid malignancies such as Hodgkin lymphoma [97]. In some patients DLBCL tends to be associated with aggressive clinical features such as pericardial and malignant pleural effusions (Fig. 5.26). In addition, pulmonary parenchymal involvement and bone involvement, which are unusual in Hodgkin lymphoma, are more commonly seen in DLBCL. A characteristic of DLBCL is renal involvement [98].

Because of the difficulty in establishing the extent of visceral involvement by CT scanning alone, the use of PET-CT has increased the sensitivity with which sites of tumor involvement outside of the mediastinum are detected. The use of FDG PET imaging for response assessment, while not

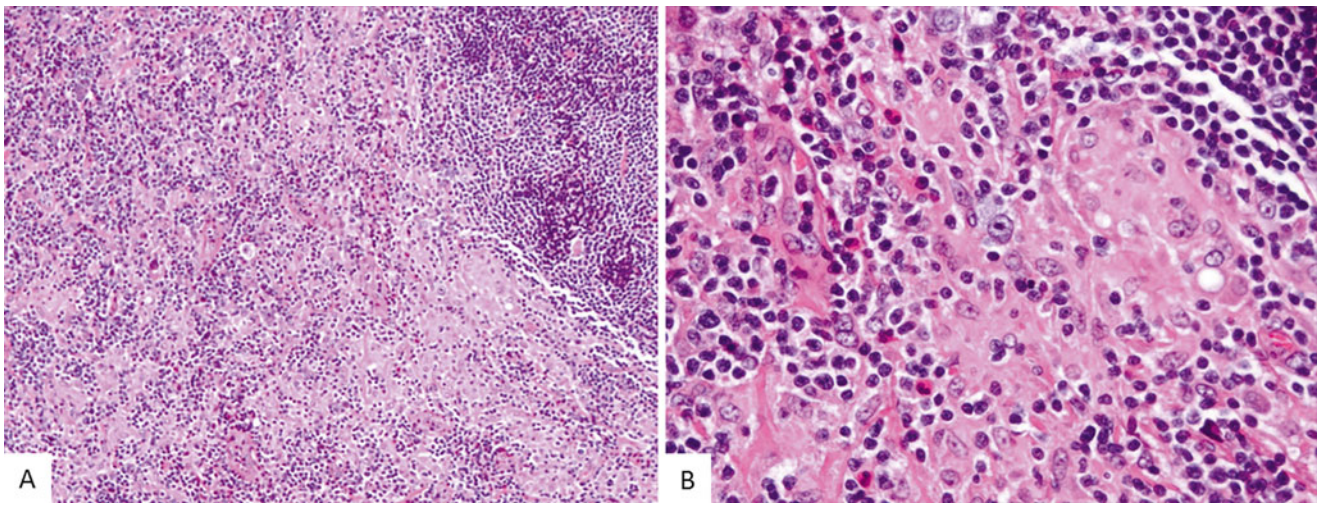


**Fig. 5.23** Classical Hodgkin lymphoma, mixed cellularity (MC) subtype. (**a**) The MC subtype show a diffuse pattern sparing residual follicles. (**b**) The neoplastic cells are mixed with a significant number of epitheliod histiocytes, small lymphocytes and eosinophils

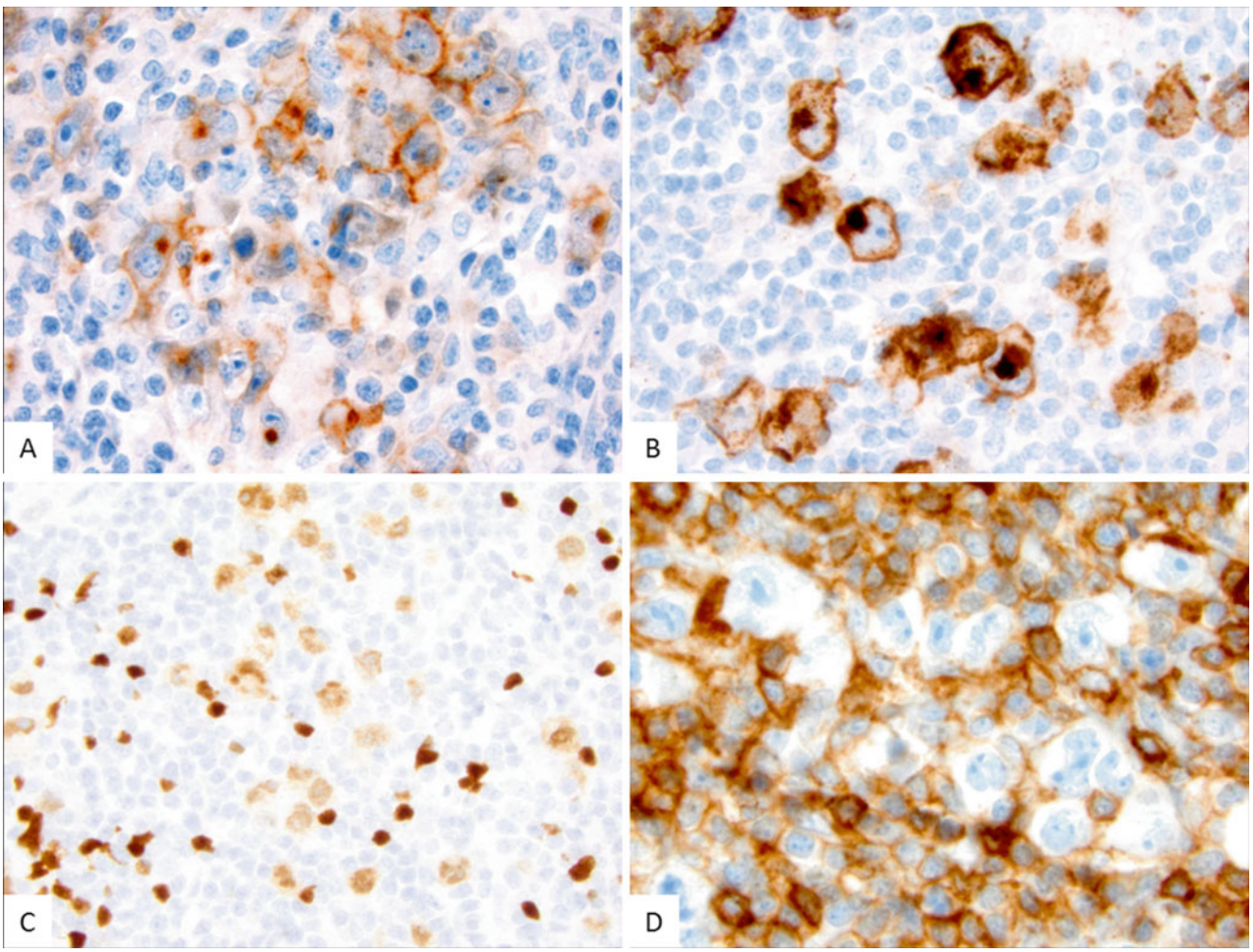


**Fig. 5.24** The HRS cells show characteristic immunophenotype including the membrane-associated and cytoplasmic (Golgi-type) CD30 (**a**) and CD15 (**b**). The neoplastic cells are positive for PAX5 (**c**) with expression weaker than the small B lymphocytes, and lack CD45 (**d**)

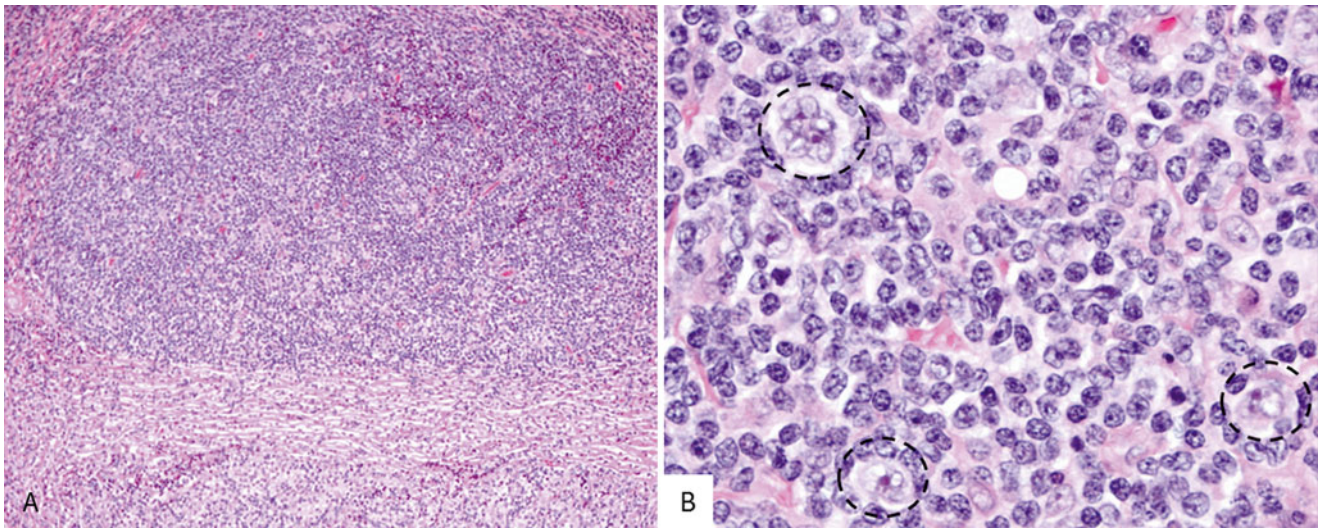


**Fig. 5.25** (**a**) Nodular lymphocyte predominant classical Hodgkin lymphoma involving the lymph node in nodular pattern. (**b**) The neoplastic nodules are large with a variable number of neoplastic L&H cells (*circled*) in a background of small lymphocytes. The neoplastic L&H cells are large with nuclear lobation, vesicular chromatin, and peripherally located small nucleoli

**Table 5.10** Lymphoma staging—non-Hodgkin lymphoma

| St. Jude classification |
|---|
| *Localized* |
| Stage I: |
| A single tumor (extranodal) or single anatomic area (nodal) with the exclusion of mediastinum or abdomen |
| Stage II: |
| A single tumor (extranodal) with regional node involvement |
| Two or more nodal areas on the same side of the diaphragm |
| Two single (extranodal) tumors with or without regional node involvement on the same side of the diaphragm |
| A primary gastrointestinal tumor, usually in the ileocecal area, with or without involvement of associated mesenteric nodes only, grossly completely resected |
| *Disseminated* |
| Stage III: |
| Two single tumors (extranodal) on opposite sides of the diaphragm |
| Two or more nodal areas above and below the diaphragm |
| All primary intra-thoracic tumors (mediastinal, pleural, thymic) |
| All extensive primary intra-abdominal disease |
| All paraspinal or epidural tumors, regardless of other tumor site(s) |
| Stage IV: |
| Any of the above with initial CNS and/or bone marrow involvement (based on Murphy, Seminars in Oncology (1980) 7; 332–339) |

specifically validated in the setting of pediatric NHL [40], can be helpful to assess response to therapy and evaluate sites of suspicious disease recurrence.

## Pathology

The morphologic features of DLBCL are variable. In the pediatric population, the centroblastic, immunoblastic, T-cell/histiocyte rich, and anaplastic variants are most commonly seen (Fig. 5.27). Plasmablastic lymphoma, a rare variant of DLBCL, is seldomly seen in children but should be considered in the setting of immunodeficiency. ALK-positive large B-cell lymphoma is another variant characterized by t(2;17)(p23;q23) resulting in *ALK-CLTC* fusion leading to aberrant cytoplasmic expression of the ALK protein.

The neoplastic cells in DLBCL typically express the B-cell markers CD19, CD20, CD22, and PAX5, and most cases are positive for BCL6 expression. Based on gene expression profiling data, two biologically distinct subtypes of DLBCL have been recognized; they are referred to as germinal center B-cell like (GCB) and activated B-cell like (ABC). These subtypes have distinct pathogenic features and are associated with different clinical outcomes [99]. The GCB subtype is defined commonly on the basis of CD10 and/or BCL6 expression while the ABC subtype is defined on the basis of MUM1/IRF4 expression [100]. The majority of DLBCL in children (83 %) are of the GCB subtype, positive for CD10 and BCL6 [101]. In addition, childhood DLBCL tends to be associated with high proliferation index, frequent *MYC* alterations, and infrequent BCL2 expression [102].

## Prognosis

Risk stratification using the international prognostic index (including age, performance status, LDH levels, Ann Arbor stage, and extranodal involvement) effectively predicts outcome with conventional chemotherapy in adult patients with DLBCL. However, additional studies are required to assess whether prognostic markers of DLBCL used in the adult population are predictive of outcomes in the pediatric group.

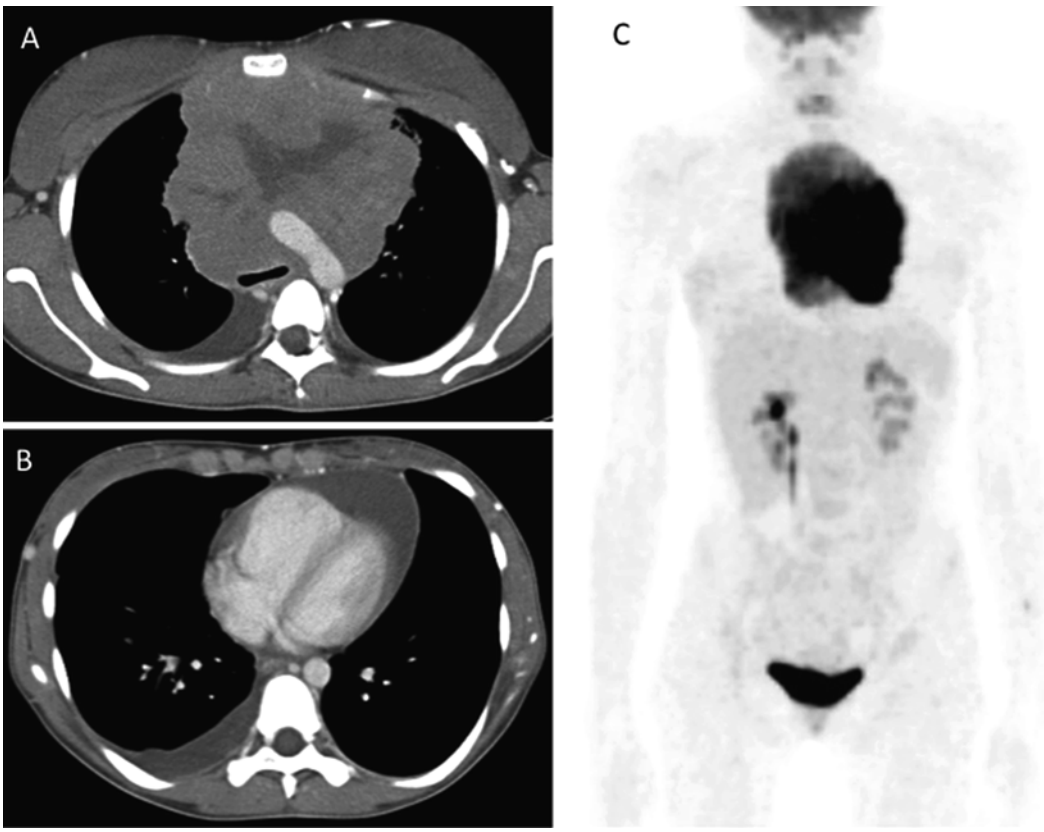


**Fig. 5.26** Diffuse large B-cell lymphoma: CT (**a**, **b**) and PET (**c**) showing aggressive appearing FDG-avid large mediastinal mass with anterior chest wall invasion and accompanying pleural and pericardial effusions

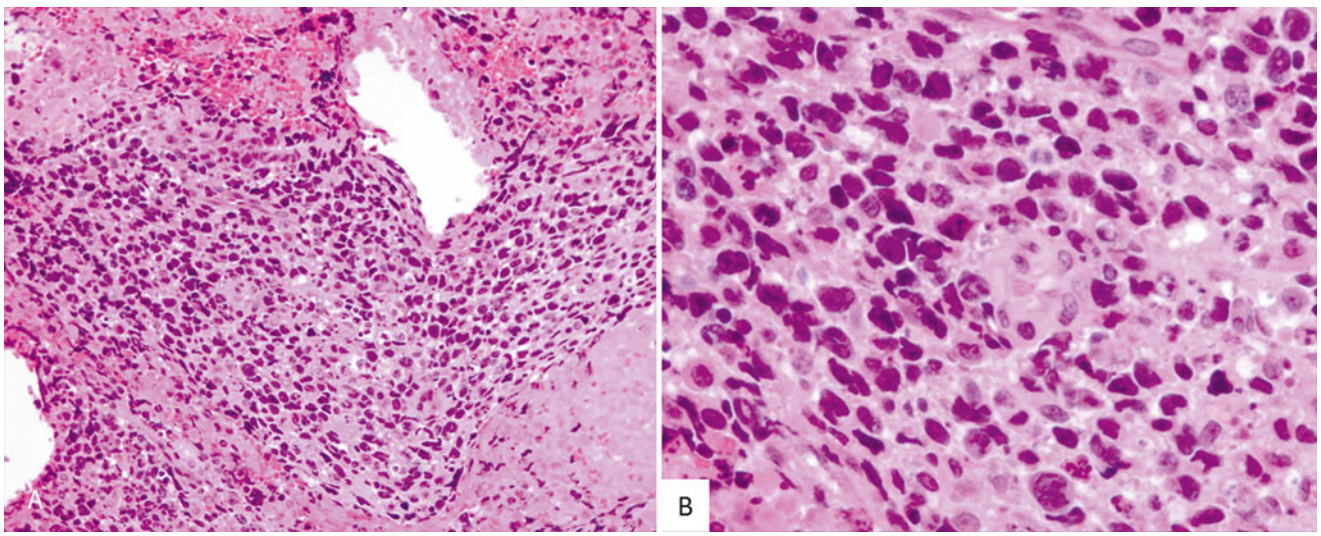


**Fig. 5.27** Diffuse large B-cell lymphoma involving bone. (**a**) Sheets of large non-cleaved cells associated with tumor necrosis. (**b**) High power view of the diffuse large B-cell lymphoma composed of large neoplastic cells with irregular nuclear membrane and moderate amounts of eosinophilic cytoplasm. Imaging studies did not identify any other anatomic site involved by tumor. This case represents a primary bone diffuse large B-cell lymphoma

## Burkitt Lymphoma

### Clinical Features

Burkitt lymphoma (BL) is a highly aggressive mature B-cell malignancy with characteristic morphologic, immunophenotypic and cytogenetic findings, and accounts for 30 % of childhood lymphomas. Three clinical variants/forms have been identified: (1) the *endemic form,* common in children in equatorial Africa, with frequent involvement of the jaw and kidneys; (2) the *sporadic form*; and, (3) the *immunodeficiency-associated form* observed mainly in the setting of HIV infection.

### Imaging Features

The sporadic form of BL typically presents with intra-abdominal visceral disease involvement, often with accompanying widespread extranodal involvement [56]. The initial evaluation, either by radiography, ultrasound or CT, is usually directed at characterizing the extent of abdominal involvement as part of assessing initial presenting abdominal symptoms. Peritoneal, abdominal viscera, visceral, and bowel wall involvement are common (Fig. 5.28a, b). Patients with bowel wall involvement characteristically present with intussusception. Occasionally, the diagnosis is made surgically following resection of an intussuscepted segment of bowel refractory to hydrostatic or air-enema reduction. More commonly, however, the presence of extensive intra-abdominal disease is noted on CT imaging (Fig. 5.28c–e). Abdominal involvement and isolated lymphadenopathy are less common in the endemic form of BL.

The presence of pleural effusions and ascites may also be present, with disease confirmation by cytologic examination. Testicular and isolated lymph node involvement is uncommon, whereas CSF involvement is identified in many patients. The use of diagnostic imaging either by FDG PET or by MRI is not sufficient to exclude bone marrow or CSF involvement. The use of PET imaging, however, has been advocated to evaluate the extent of disease in patients with BL [103, 104], although the rapid response to therapy that is commonly observed in these patients has limited the more widespread and systematic use of PET imaging at the time of diagnosis. There is currently no role for routine follow-up PET imaging to assess response to therapy in the absence of specific clinical concerns [103].

### Pathology

Histologically, the tumor is composed of medium-sized lymphocytes with moderate amounts of cytoplasm and round nuclei with several small nucleoli. Mitotic figures and apoptotic cells are typically abundant, and elevated numbers of reactive histiocytes with ingested cellular debris are scattered in the background imparting a "starry sky" pattern. The neoplastic cells in BL express B-cell markers and are typically positive for CD10 and BCL6 and negative for BCL2 (Fig. 5.29). Virtually 100 % of the neoplastic cells express the proliferation marker Ki-67.

Burkitt lymphoma is characterized by chromosomal translocations involving the *MYC* gene at chromosome 8q24 leading to MYC overexpression. The *IGH* gene at 14q32 is the most frequent breakpoint partner (75–85 % of cases), with t(2;8) and t(8;22) variant translocations utilizing the *IGK* and *IGL* enhancers seen in the remainder of cases. Given the wide range of breakpoints, *MYC* alterations are usually best detected by conventional cytogenetics or FISH. Alterations involving the ARF/MDM2-MDM4/p53 pathway have been reported in pediatric Burkitt lymphomas, including *TP53* mutations in ~30 % of sporadic BL [105]. The genetic alterations and gene expression profiles of pediatric BL appear to be similar to those of adult BL.

## Marginal Zone Lymphoma

### Clinical Features

Both nodal and extranodal marginal zone lymphoma (MZL) can occur in the pediatric age group, although their incidence is markedly lower than that observed among older patients. Most cases are nodal MZL that arise in males with a median age of 16 years who present with localized lymphadenopathy often involving the head and neck region [106]. Extranodal marginal zone lymphoma is rare in children and adolescents [107]. The most common sites of involvement include skin, soft tissue, conjunctiva and parotid. Most of the patients present with localized disease.

### Pathology

Histologically, MZL is composed of small lymphocytes with monocytoid and centrocyte-like features as well as varying degrees of plasmacytic differentiation (Fig. 5.30). Nodal MZL is frequently associated with PTGC. The neoplastic cells are positive for CD19 and CD20, and in up to 70 % of cases can show aberrant CD43 coexpression. CD5, CD10, and CD103 expression is typically absent, and, unlike splenic MZL, most nodal MZL cases are negative for IgD. In situ hybridization studies for Epstein-Barr virus are usually negative [106].

Extranodal MZL arising in pediatric patients resembles its counterpart in older individuals. Namely, the neoplasm is characterized by a dense infiltrate of small lymphocytes including monocytoid forms surrounding reactive lymphoid follicles with architectural distortion and glandular destruction (lymphoepithelial lesions).

Immunoglobulin heavy and light chain genes are clonally rearranged with somatic hypermutation of variable regions indicating a post-germinal center memory B-cell origin. Translocations that have commonly been associated with MALT lymphoma in adults, namely t(14;18)(q32;q21) leading to *IGH-MALT1* fusion, are also found in pediatric MALT lymphoma but at a lower frequency [108].

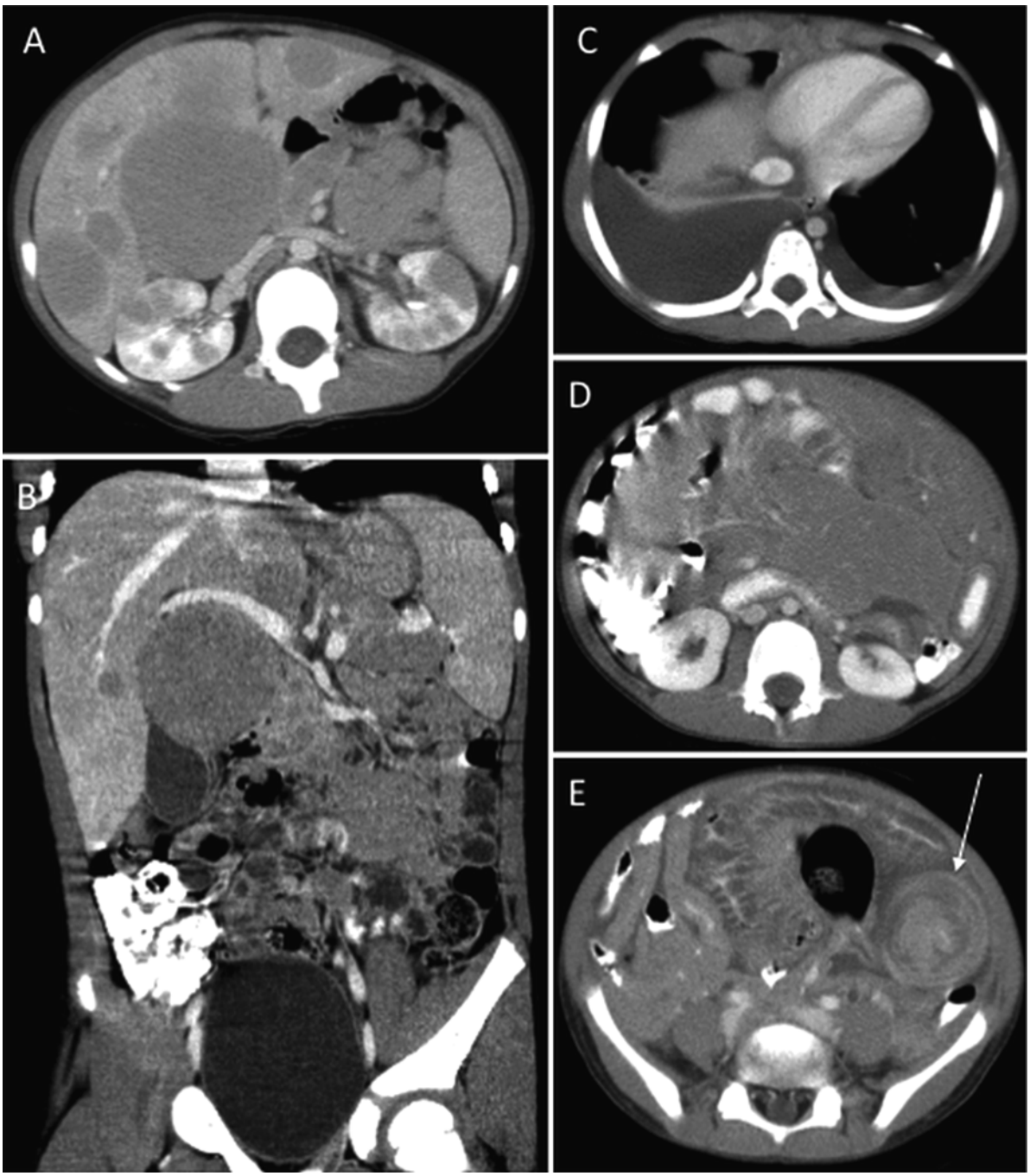


**Fig. 5.28** Burkitt Lymphoma: two examples of Burkitt lymphoma. The patient in (**a**) and (**b**) has multifocal visceral involvement of liver, kidneys and retroperitoneum, whereas the patient in **c**–**e** presented with large pleural effusions, lung lesions, in addition to extensive bowel wall thickening, mesenteric nodal involvement, and small bowel intussusception (**e**, *arrow*)

## Follicular Lymphoma

### Clinical Features

Follicular lymphoma (FL), the most common low-grade lymphoma in adults in the United States, represents 2 % of NHL in children [98]. Pediatric FL most likely represents a genetically distinct entity unrelated to adult FL, and the t(14;18), which is characteristic of the latter, is uncommon in pediatric cases [109]. The median age at presentation is 8–12 years, and males are more commonly affected than females by a ratio of 4:1. Pediatric FL usually presents as localized disease (stage I and II) [110]. The tonsils and lymph nodes of the head and neck are most commonly involved; however, cases of other extranodal involvement have been described (gastrointestinal tract, skin, testes, and parotid gland) [111]. Unlike adult FL patients, bone marrow involvement is rare in pediatric FL.

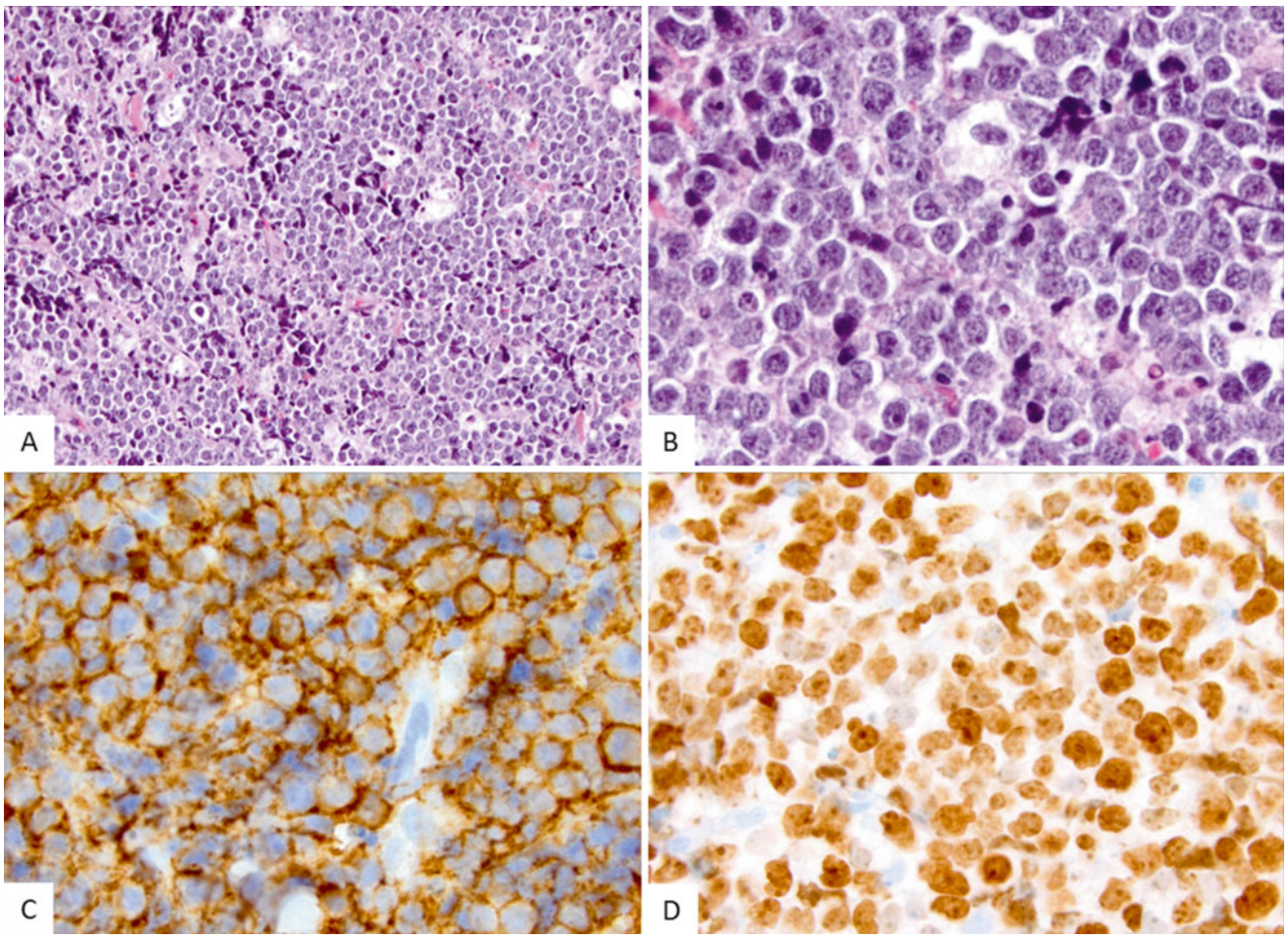


**Fig. 5.29** Burkitt lymphoma, morphologic and immunophenotypic characteristics. (**a**) A low power view shows soft tissue with diffuse monomorphous lymphoid infiltrate with "starry-sky" pattern. (**b**) The tumor cells are intermediate in size with round to oval nuclei and inconspicuous nucleoli and small amounts of cytoplasm. The neoplastic cells are positive for CD20 (**c**) and show >99 % proliferation index by Ki-67 stain (**d**)

## Imaging Features

There are no distinguishing imaging features to discriminate pediatric FL from other types of NHL. Depending on the symptoms or exam findings at the time of presentation, the initial site of disease involvement may be discovered incidentally or based on localizing exam findings (Fig. 5.31). Once the diagnosis is established, staging should include CT of the neck, chest, abdomen, and pelvis [112]. PET scanning may increase the sensitivity with which sites of distant disease are noted, although this is unusual in pediatric FL. When treatment is complete, routine off-treatment surveillance can be accomplished either by physical exam or by focused imaging of the original site(s) of disease, as indicated clinically. There is no evidence to support a high frequency of surveillance imaging or for FDG PET imaging in the routine surveillance of pediatric FL. Post-therapy PET imaging may be helpful in distinguishing scar tissue from residual neoplasm [113].

## Pathology

Histologically, FL is comprised of a heterogeneous population of centrocytes (small cleaved cells) and centroblasts (large noncleaved cells) in a predominantly follicular growth pattern. Grading is based on the overall number of centroblasts relative to centrocytes. In grade 1 and 2 FL centrocytes are predominant, while in grade 3 FL centroblasts exceed 15 per high-power-field on microscopic evaluation. Grade 3 is further subdivided into 3A and 3B on the basis of whether centrocytes are present or absent, respectively. Pediatric FL are typically grade 3A. Notably, a diffuse large B-cell component does not portend an aggressive clinical course as it does in adult FL; rather, a favorable outcome with few relapses has been reported in children treated according to the NHL-BFM protocol [110].

The neoplastic B-cells of pediatric FL express CD19, CD20, and the germinal center markers CD10 and BCL6. Most cases lack BCL2 expression. The CD21 and CD23

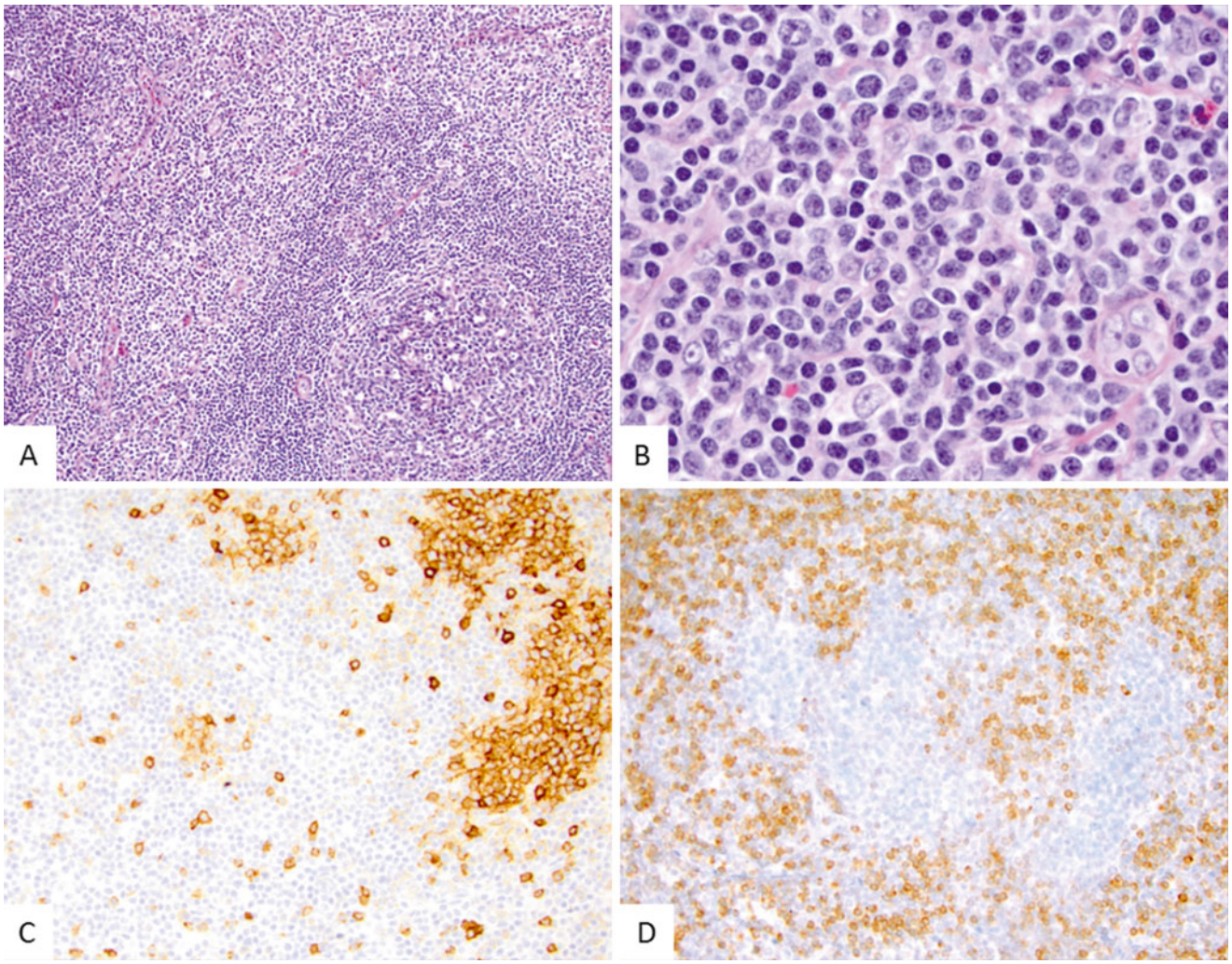


**Fig. 5.30** Nodal marginal zone lymphoma. (**a**) A low power view demonstrates distorted lymph node architecture including interfollicular expansion and variably expanded and often ill-defined follicles with irregular mantle zones. (**b**) There is a heterogeneous infiltrate in the interfollicular regions that is composed of small cleaved cells admixed with plasma cells and monocytoid B cells. (**c**) The neoplastic cells disrupt the germinal centers and are positive for CD20 (not shown), but negative for CD10 (shown) that highlights the residual germinal center B-cells. (**d**) The neoplastic cells are positive for Bcl-2 (shown) with aberrant co-expression of CD43 (not shown). The disrupted, irregular germinal center is negative for Bcl-2

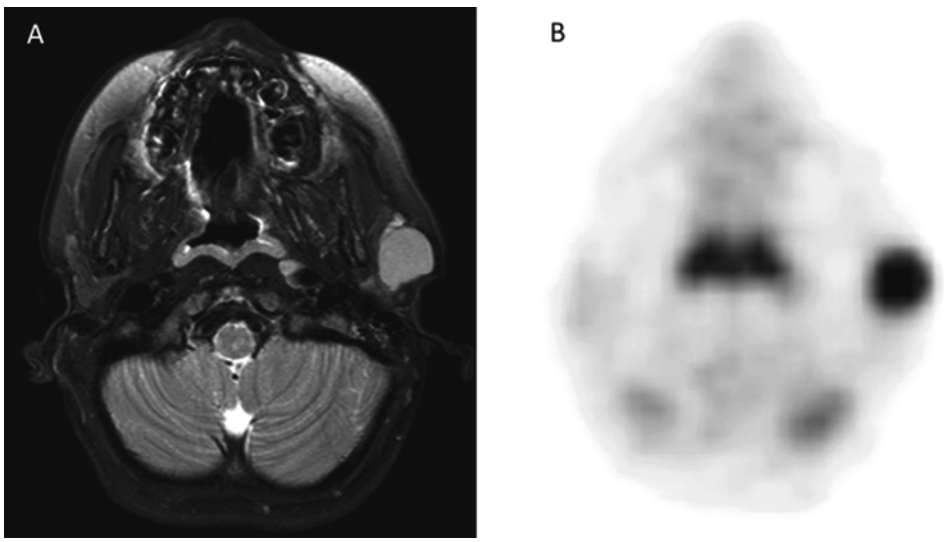


**Fig. 5.31** Follicular lymphoma of the parotid. Five-year old with palpable parotid mass. MRI shows a mildly T2 hyperintense focal lesion in the left parotid (**a**). Staging FDG PET shows intense FDG uptake in the lesion (**b**); no other sites of disease were seen

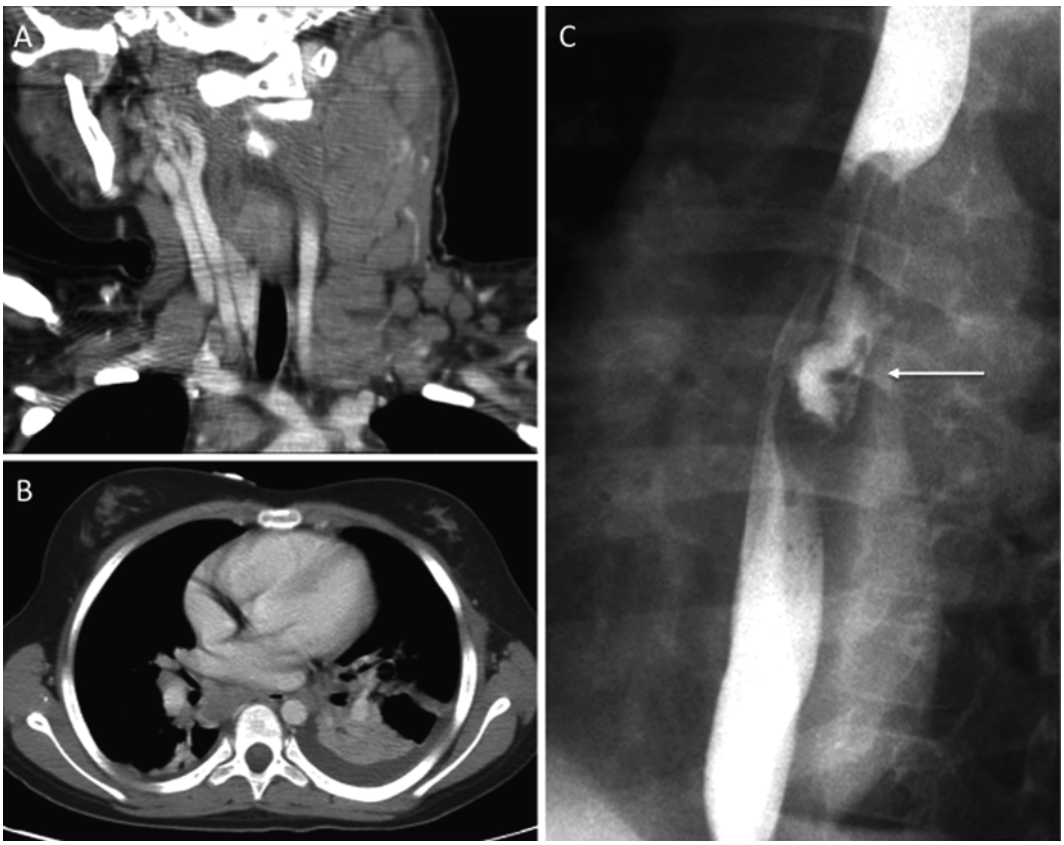


**Fig. 5.32** Anaplastic large cell lymphoma (ALCL), with varied presentations of disease. (**a**, **b**)11-year-old patient with ALCL presented with bulky neck and mediastinal disease and pleural effusions. The 5-year-old patient in (**c**) presented with dysphagia. (**c**) Barium swallow shows a large esophageal ulcer (*arrow*) which subsequent biopsy confirmed as ALCL

antigens can be used to highlight the follicular dendritic cell meshworks that correlate with the follicular growth pattern observed in most cases of pediatric FL. The proliferation index assessed by Ki-67 antigen can be high, ranging from 40 to 95 %.

The presence of the t(14;18) *IGH-BCL2* translocation that is considered the hallmark of the adult follicular lymphoma is commonly absent in pediatric cases. However, rearrangements involving the *IGH* locus, some leading to *IGH-IRF4* fusion, have been described in pediatric FL [110, 114].

## Anaplastic Large Cell Lymphoma

### Clinical Features

Anaplastic large cell lymphoma (ALCL) is a T-cell lymphoma characterized by CD30-positive neoplastic cells that are usually large and have abundant cytoplasm with pleomorphic nuclei. Although rare, making up only about 15 % of pediatric NHL, ALCL is the most common mature T-cell neoplasm in children [115]. The majority of cases that arise among young individuals are ALK-positive ALCL characterized by balanced translocations involving the *ALK* (*anaplastic lymphoma kinase*) gene at chromosome 2p23 with one of several possible partner genes, most commonly the *NPM1* gene at 5q35 encoding the nucleophosmin protein. Patients with ALK-positive ALCL often present with lymphadenopathy and/or extranodal masses, B-type symptoms, and advanced stage (III and IV). The most commonly involved extranodal sites include skin, bone, soft tissues, lung, and liver. Central nervous system and bone marrow involvement are uncommon in ALK-positive ALCL [114]. ALK-positive ALCL must be distinguished from primary cutaneous ALCL and other T-cell or B-cell lymphomas with similar features and CD30 expression. Primary cutaneous ALCL is almost always ALK negative and is rare in children.

### Imaging Features

There are no specific imaging findings associated with ALCL to distinguish it from other forms of lymphoma, although ALCL frequently presents with extensive multifocal disease and can involve the lung, skin and bone, GI tract, and abdominal viscera [97] (Fig. 5.32). A mediastinal mass may be seen in up to 40 % of the patients and

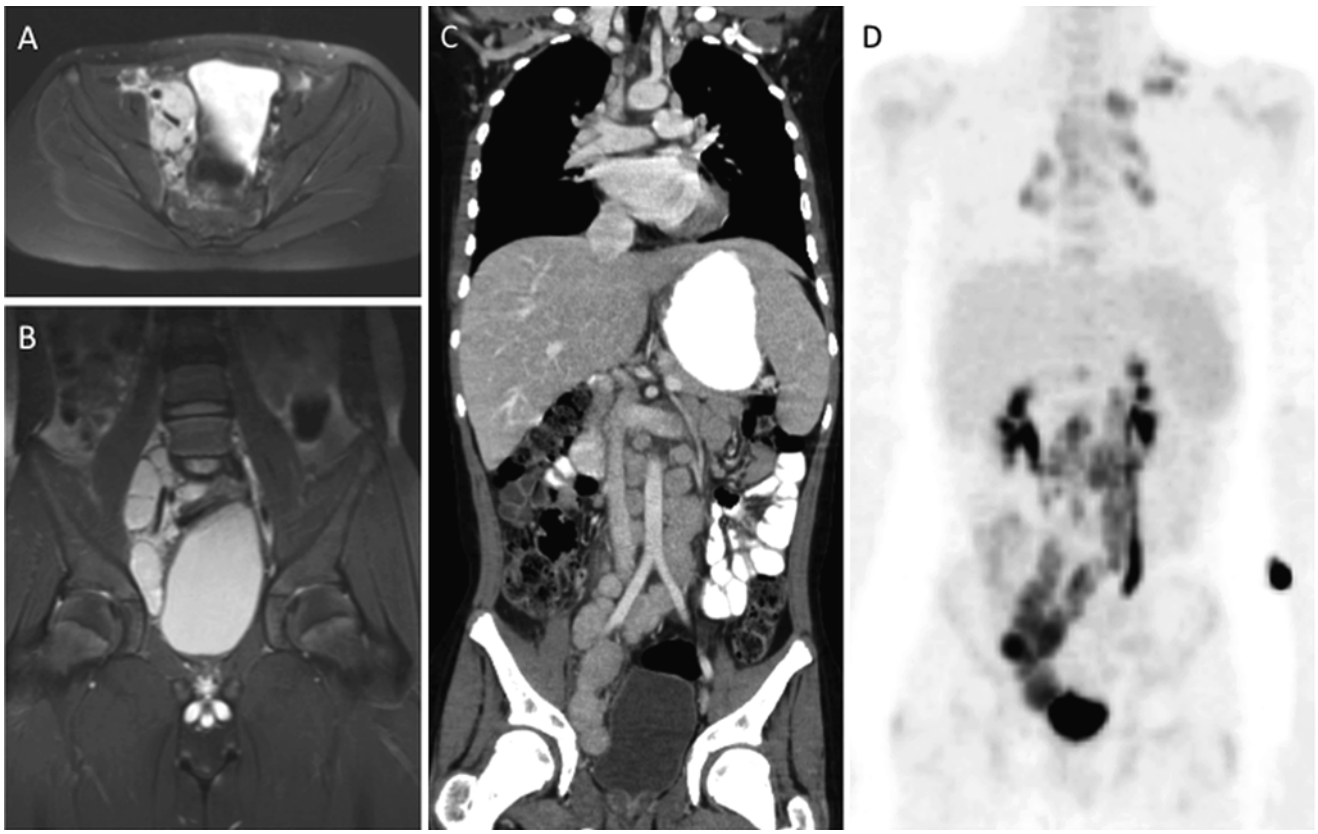


**Fig. 5.33** ALCL with FDG PET: 12-year-old presented initially with right leg/groin pain. (**a**, **b**) MRI showed diffuse pelvic lymph node enlargement. (**c**) CT confirmed extensive adenopathy in chest, abdomen and pelvis, all of which was FDG avid (**d**)

is often associated with pericardial and pleural effusion. When a mediastinal mass is present, it may be difficult to distinguish ALCL from Hodgkin lymphoma and diffuse large B-cell lymphoma. PET imaging, together with CT and/or MRI should be used for initial staging (Fig. 5.33) and can be helpful in monitoring response to therapy [115]. Experimental therapies targeting ALK can show dramatic disease response, which may be best demonstrated by FDG PET imaging [117] (Fig. 5.34). As with other NHL, disease surveillance involves a combination of clinical examination and focused imaging to evaluate for the presence of disease at original sites of tumor involvement. There is no evidence to indicate that routine surveillance by FDG PET imaging improves outcome in ALCL.

### Pathology

Typically, lymph node involvement by ALCL is predominantly sinusoidal in pattern and leads to partial or complete effacement of nodal architecture. Among the pleomorphic neoplastic cells of ALCL, a variable proportion with a horseshoe-shaped or kidney-shaped nucleus and abundant eosinophilic cytoplasm is often identified. Such cells have been referred to as *hallmark cells* and can be recognized in all morphologic variants of ALCL, including the lymphohistiocytic and small cell variants.

The neoplastic cells of ALCL are strongly positive for CD30. Although most cases are negative for CD3 expression, the majority express other T-cell associated antigens including CD2, CD5 and CD7. A subset of ALCL has a "null cell" immunophenotype, although a T-cell lineage can be established at a molecular level. Most cases are positive for the cytotoxic antigens granzyme B, TIA1, and perforin. The pattern of ALK expression by immunohistochemistry can often foretell the underlying translocation type, and cases with the NPM1-ALK fusion protein exhibit a cytoplasmic and nuclear staining pattern (Fig. 5.35).

## Histiocytic and Dendritic Cell Neoplasms

The World Health Organization classifies neoplasms of histiocytes and dendritic cells according to their putative normal counterparts: histiocytic sarcoma, tumors derived from Langerhans cells (Langerhans cell histiocytosis, Langerhans cell sarcoma), interdigitating dendritic cell sarcoma, and disseminated juvenile xanthogranuloma (JXA).

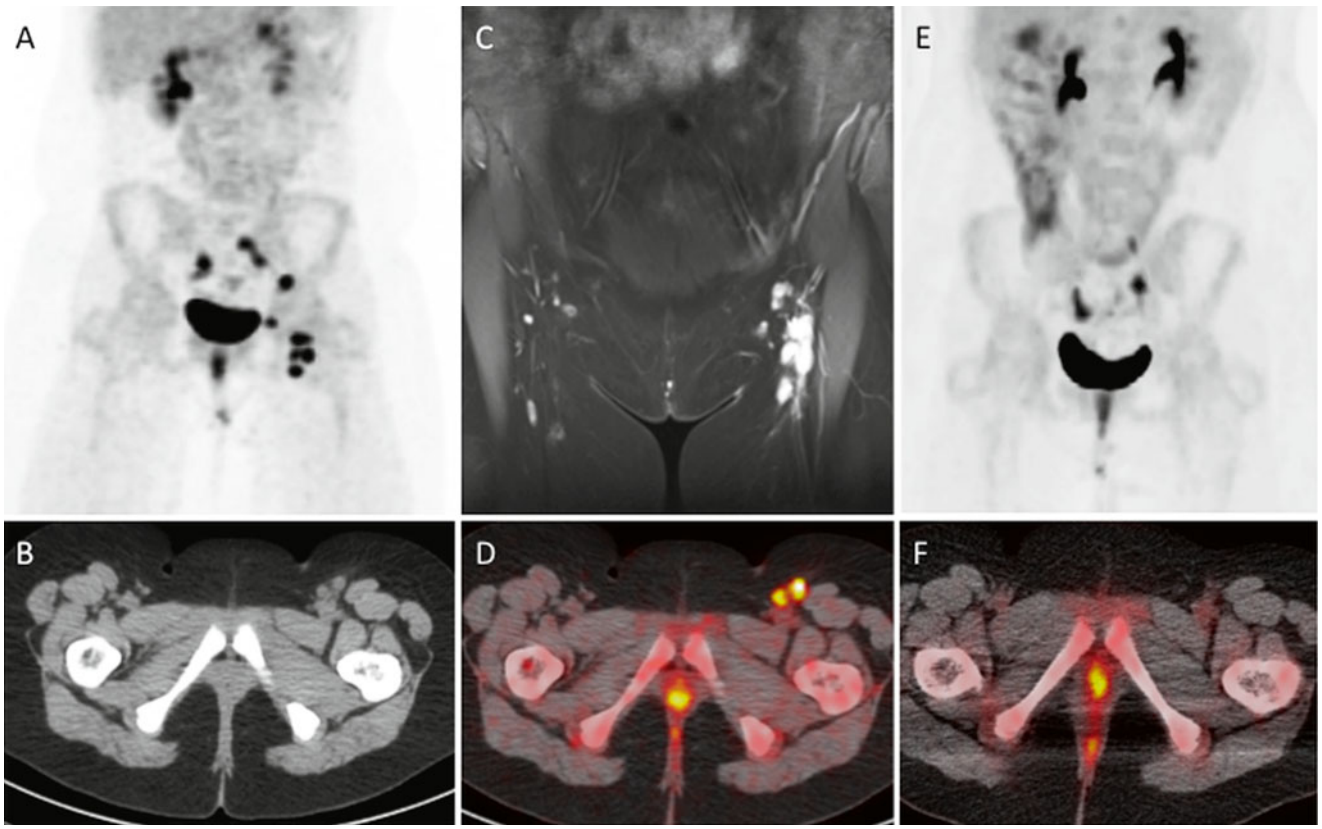


**Fig. 5.34** ALCL and ALK targeted therapy: 12-year old with recurrent ALCL being treated with experimental phase 1 agent targeted at the ALK kinase. FDG PET/CT (**a**, **b**, **d**) and MRI (**c**) at baseline (**a**–**d**) showing extensive left inguinal and external iliac chain nodal disease. After just one 4 weeks cycle of ALK-targeted crizotinib, there has been both a complete anatomic (**f**) and metabolic (**e**) response, with resolution of the nodal disease seen at baseline

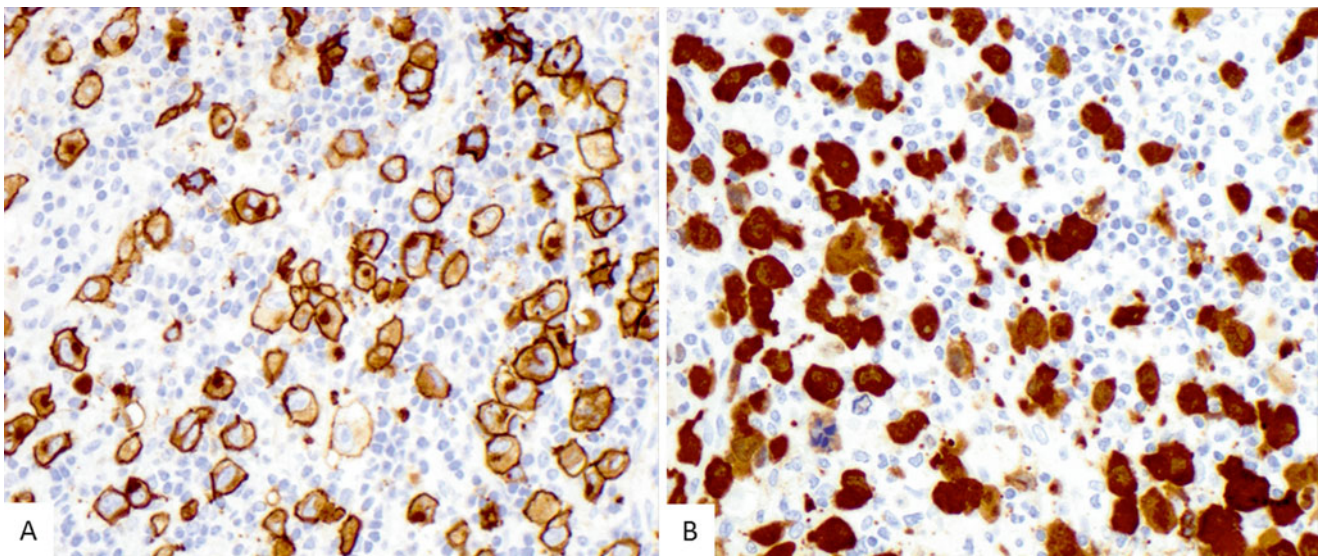


**Fig. 5.35** Anaplastic large cell lymphoma, ALK positive. (**a**) CD30 immunostain highlights the neoplastic cells of anaplastic large cell lymphoma. (**b**) ALK immunostain shows the characteristic nuclear and cytoplasmic staining that is associated with the t(2;5) translocation resulting in the aberrant expression of NPM1-ALK fusion protein

## Langerhans Cell Histiocytosis

### Clinical Features

Langerhans cell histiocytosis (LCH) is a rare group of disorders characterized by the clonal proliferation of neoplastic Langerhans cells. The disease has a wide range of clinical presentations ranging from localized to multifocal and disseminated, and it includes the entities formerly known as Letterer-Siwe syndrome (characterized by early age at diagnosis, hepatosplenomegaly, lymphadenopathy, and pulmonary involvement), Hand-Schüller-Christian syndrome (occurring in older children and associated with osteolytic bone lesions, diabetes insipidus, and a more indolent course) and eosinophilic granuloma (associated with lung involvement, osteolytic lesions, and presentation in older children and young adults) [118].

The disorder affects up to 6 per million children per year with a male-to-female ratio of 2:1. Most patients are diagnosed between 1 and 15 years of age, with a peak incidence between 1 and 4 years [119]. Disease localized to a single site is generally benign, even without treatment. The most common sites involved are bone (skull, femur, vertebra, pelvic bones, and ribs), lymph nodes, skin and lung [120]. Multisystem (disseminated) disease commonly affects infants and is often associated with constitutional symptoms, cytopenias, skin and bone lesions, and hepatosplenomegaly [121]. Patients with LCH have been stratified into high-risk and low-risk categories, with the former including liver, lung, hematopoietic system, and spleen involvement as well as onset before 2 years of age [122].

### Imaging Features

Staging evaluation is aimed at establishing the extent of disease, and most clinical protocols and practitioners require patients to undergo skeletal survey to assess for osteolytic bone lesions [120]. Depending on the clinical presentation and physical exam findings, additional imaging may include CT scan of the chest or torso, CT or MRI of the brain to assess for the presence of a focal pituitary lesion and to characterize any sites of palpable abnormality around the skull (Fig. 5.36). For bone imaging, in practice conventional radiographs are still routinely obtained and have high sensitivity for detecting lytic bone lesions (Fig. 5.37). Radiographs may not detect sites of bone marrow involvement or visceral lesions and recent studies have shown increased sensitivity of MRI and FDG PET at identifying both radiographically occult and metabolically active lesions [123, 124]. $^{99m}$Tc-MDP bone scintigraphy is not recommended routinely since purely lytic lesions may not elicit sufficient surrounding bone activity to render them visible.

Several recent studies have advocated the use of FDG PET imaging to assess for active osseous and intramedullary bone lesions, to identify occult sites of soft tissue involvement and potentially as a means of monitoring response to therapy (Fig. 5.38) [123–125]. It remains to be determined whether FDG PET/CT can replace conventional imaging and clinical examination in evaluating patients with LCH.

Once the diagnosis and extent of disease have been established, follow-up imaging should be directed at characterizing response of original sites of disease to therapy. The prognostic value of FDG PET response to therapy in LCH has not been established.

### Pathology

Regardless of anatomic site and clinical features, the morphologic features of LCH tend to be uniform and distinctive. The neoplastic cells are generally large (10–15 μm), with irregular nuclear contours resulting in grooved/folded nuclei

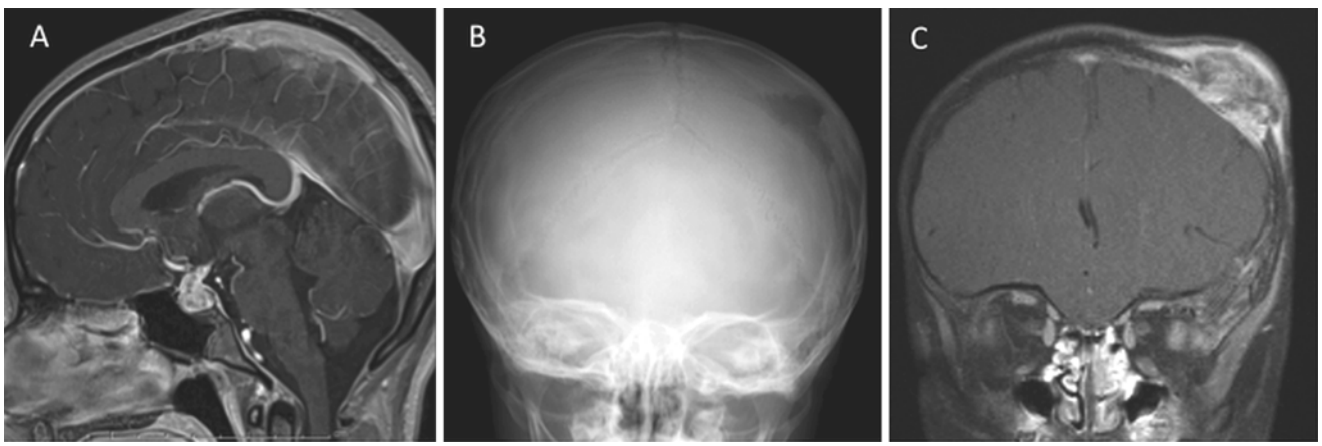


**Fig. 5.36** Langerhans cell histiocytosis (LCH): 2 examples of LCH at presentation. (**a**) 15-year old presented with headache and panhypopituitarism. Contrast enhanced MRI shows diffuse enlargement of the pituitary stalk and gland; skeletal survey revealed lytic bone lesions elsewhere. (**b**, **c**) 3-year old with palpable skull mass. Skeletal survey showed left parietal lytic skull lesion (**b**); MRI revealed a large associated soft tissue mass and intracranial extension (**c**)

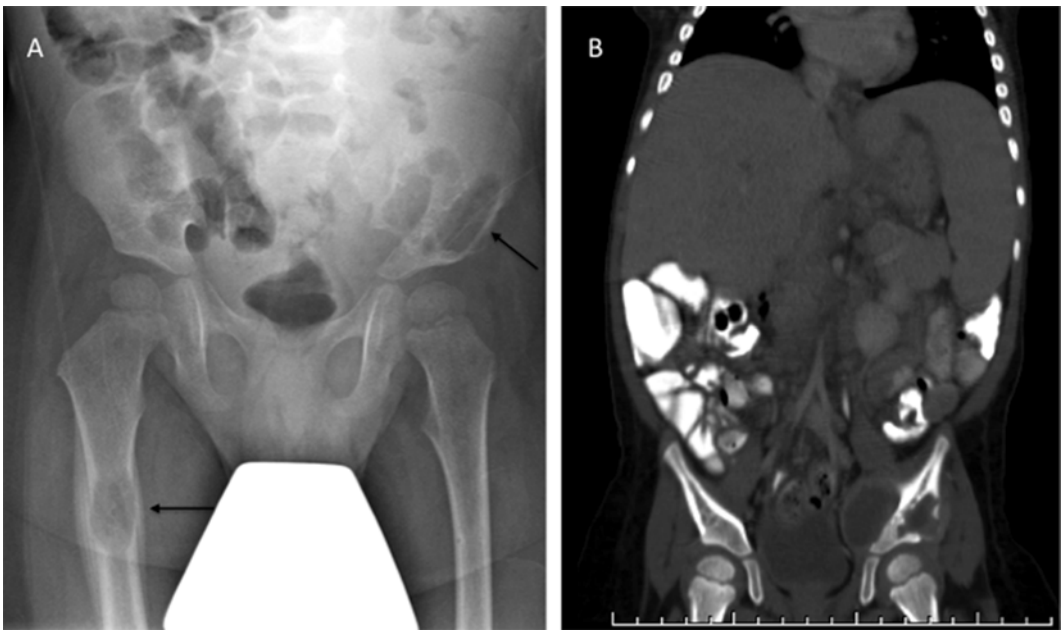


**Fig. 5.37** LCH: 20-month old with limp and leg pain. Radiographs showed lytic lesions involving the right femur and left iliac bone (**a**, *arrows*). CT (**b**) shows the lytic pelvic lesion and associated soft tissue mass, in addition to revealing hepatosplenomegaly

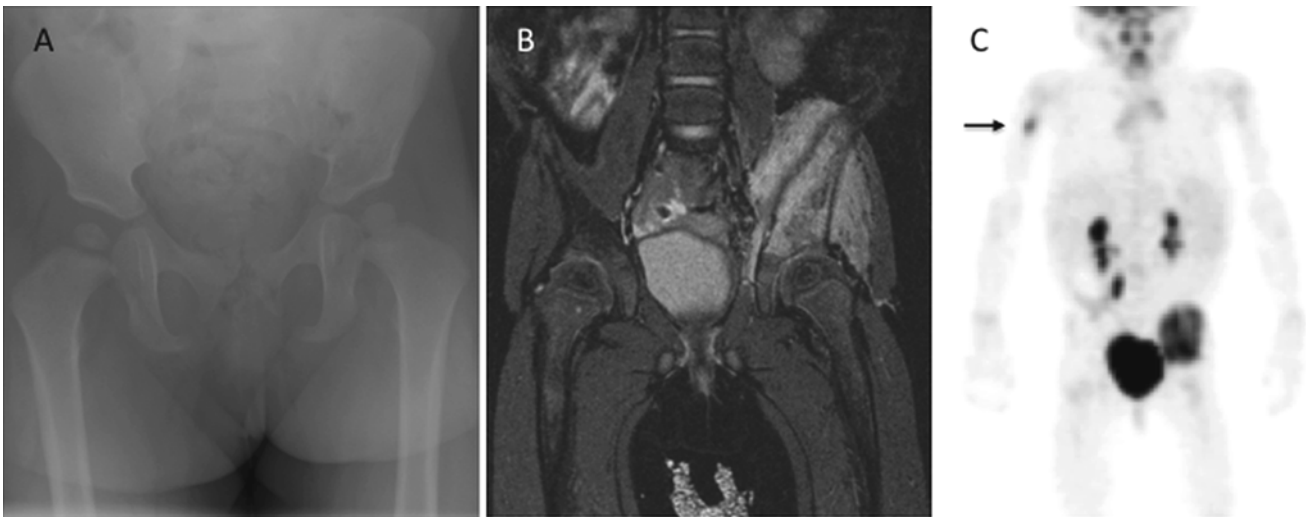


**Fig. 5.38** Sixteen-month old with LCH, who initially presented with left hip pain. Radiographs were normal (**a**). MRI shows a large left iliac crest lesion (**b**). Staging FDG PET (**c**) demonstrated the iliac crest lesion to be intensely FDG avid. In addition, a clinically occult focus of FDG-avid disease in the right humerus (*arrow*) was also demonstrated by PET

("coffee-bean" shape) (Fig. 5.39a). The nuclear chromatin is dispersed and nucleoli are often inconspicuous. The neoplastic cells of LCH cells do not have dendritic morphology and show a moderate to abundant, slightly eosinophilic cytoplasm. The identification of Birbeck granules by electron microscopy is pathognomonic of LCH.

Eosinophils are often but not invariably present and may occasionally form abscesses with central necrosis and Charcot-Leyden crystals. Neutrophils and small lymphocytes may be intermixed, while plasma cells are usually sparse. In the lymph node, LCH involvement is usually sinusoidal and paracortical in distribution, with sparing of the follicles. In the spleen, LCH involvement is usually localized to the red pulp, while in the liver there is infiltration of large bile ducts and occasionally progressive sclerosing cholangitis.

The immunophenotype of LCH cells recapitulates that of normal Langerhans cells. The neoplastic cells are typically positive for CD1a, langerin (CD207), and S-100 (Fig. 5.39b–d).

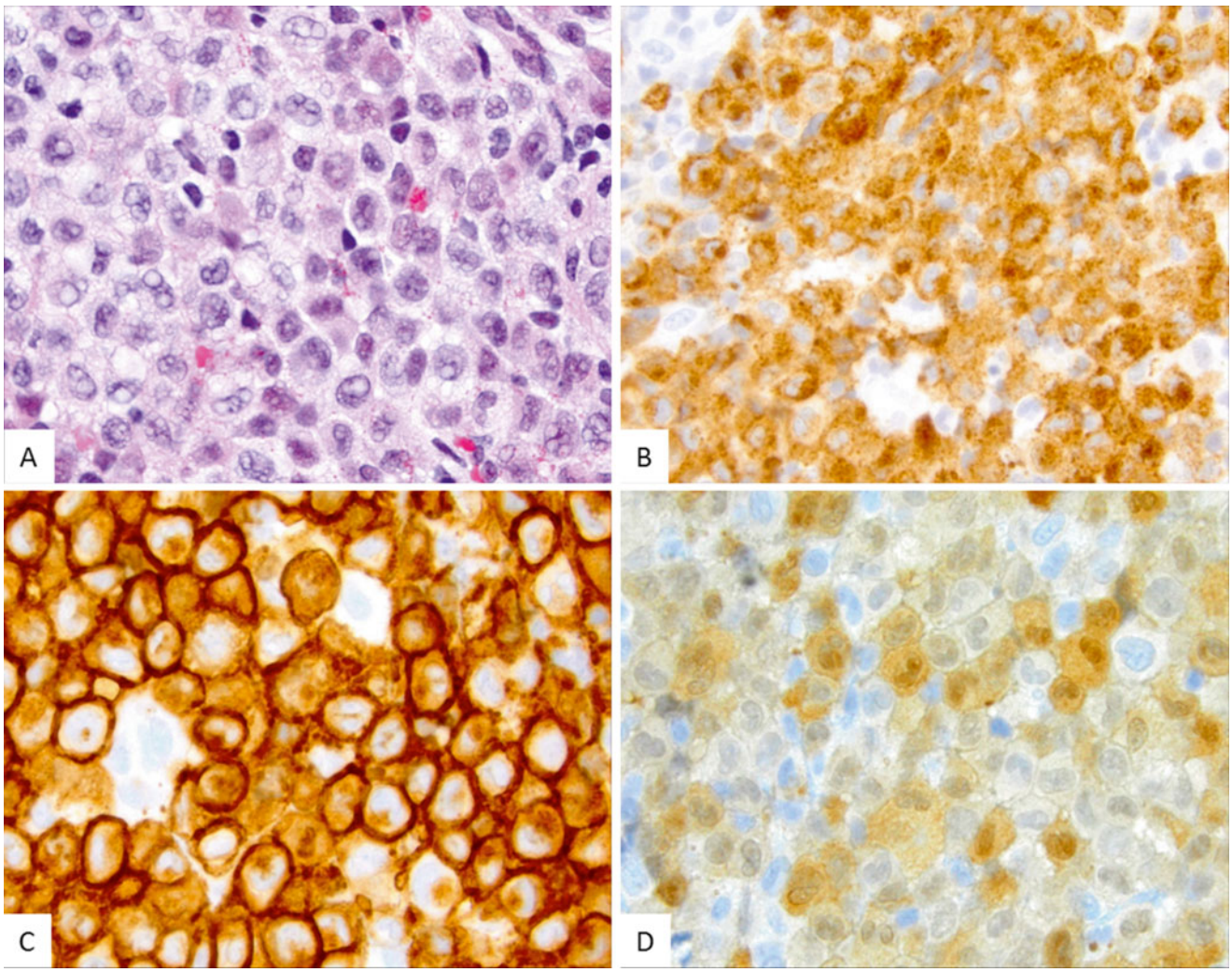


**Fig. 5.39** Langerhans cell histiocytosis, skin. (**a**) Clusters of LCH cells in the dermis with eosinophils. The LCH cells are positive for langerin (CD207) (**b**) and (**c**) CD1a. (**d**) The S100 stains the neoplastic cells in both the cytoplasm and the nucleus

## Disseminated Juvenile Xanthogranuloma

### Clinical Features

Solitary dermal juvenile xanthogranuloma (JXG) is a benign, self-limiting non-Langerhans cell histiocytosis that arises most commonly in infants and children and presents as solitary or multiple yellowish cutaneous nodules [126]. The disseminated (deep and visceral) form is a rare disease that usually (50 %) occurs during the first year of life. A subset of JXG that occurs in older children and adults and usually involves bone and lungs is termed Erdheim-Chester disease. A possible relation between disseminated JXG and Langerhans cell histiocytosis has been suggested on the basis of rare case reports describing patients with JXG and coexisting or antecedent Langerhans cell histiocytosis [127, 128]. Some disseminated JXG cases may be associated with hematologic malignancies, most commonly juvenile myelomonocytic leukemia [129, 130].

Sites of involvement by disseminated JXG include skin, mucosal surfaces (respiratory and gastrointestinal tract), kidneys, lungs, soft tissue, central nervous system, lymph nodes, and, rarely, bone. The clinical presentation is variable and depends on the site(s) of involvement. Infiltration by neoplastic cells may result in liver and/or bone marrow failure, which has been associated with macrophage activation syndrome leading to cytopenias and liver damage or even death. Involvement of the CNS and pituitary gland by disseminated JXG can results in diabetes insipidus, seizures, hydrocephalus, and mental changes mimicking LCH.

### Pathology

The neoplastic cells of JXG are small and oval shaped cells with eosinophilic cytoplasm and elongated nuclei lacking nuclear atypia. The neoplastic cells may be associated with pale foamy histiocytes, Touton giant cells, and foreign body giant cells, as well as neutrophils, lymphocytes, eosinophils, and (rarely) mast cells (Fig. 5.40). The histiocytes may contain pleomorphic nuclei, particularly in disseminated cases. Deep lesions tend to be more cellular and monotonous with fewer Touton giant cells.

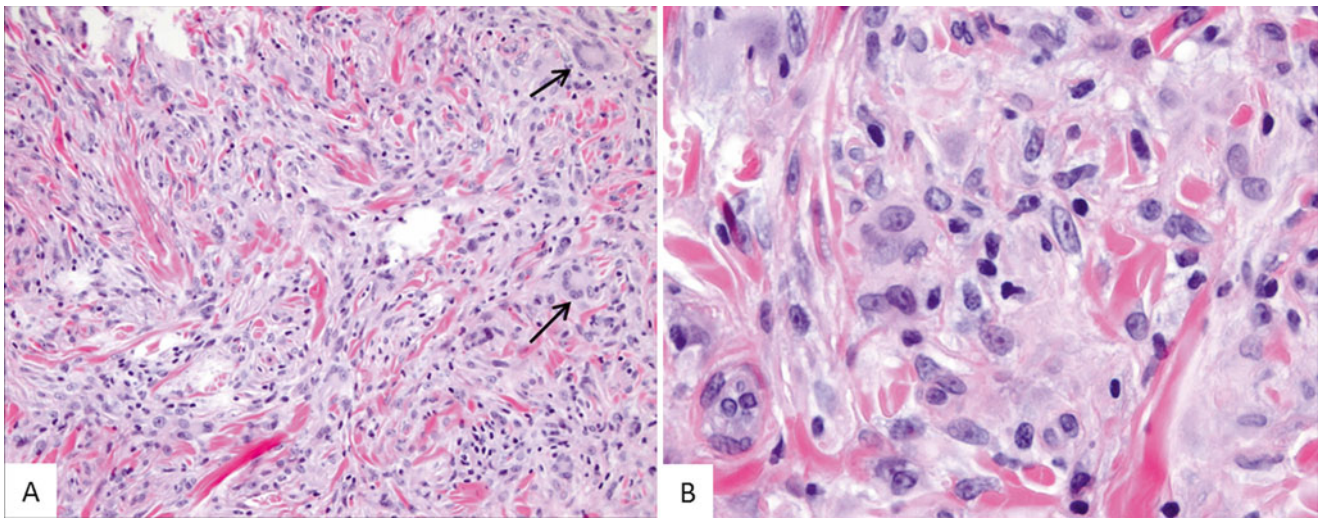


**Fig. 5.40** Juvenile xanthogranuloma, skin. (**a**) Dominant histiocytic infiltrate in the dermis with spindle cell component and occasional Touton-type giant cells (*arrows*). (**b**) High power view shows the bland cytological feature of the histiocytes without significant atypia

Electron microscopy examination of the lesions shows no specific ultrastructural features and demonstrates histiocytes with short processes and abundant cytoplasm with mitochondria, rough endoplasmic reticulum, ribosomes, lysosomes, and phagolysosomes, with occasional comma-shaped dense bodies. The absence of Birbeck bodies excludes LCH.

Immunophenotypic studies are helpful in differentiating JXA from LCH and other histiocytoses. In disseminated JXA, the neoplastic cells are positive for factor XIIIa, CD68 (coarse granular pattern), CD163, CD14, lysozyme, and vimentin. Fascin, CD4, and S-100 are variably positive. CD1a and langerin (CD207) stains are typically negative.

## Myeloid Sarcoma

### Clinical Features

Myeloid sarcoma (granulocytic sarcoma; extramedullary leukemia; chloroma) is an extramedullary proliferation of neoplastic immature myeloid cells that disrupts the local tissue architecture. Myeloid sarcoma can be a presenting feature of acute myeloid leukemia (AML) or may arise subsequently during the disease course, including relapse, in approximately 10 % of cases [131, 132]. Myeloid sarcoma is associated with certain recurrent cytogenetic abnormalities in AML, most commonly t(8;21), inv(16), and rearrangements involving chromosome 11q23 [132].

### Imaging Features

Myeloid sarcoma can involve any body part, but most typically occur in and around the orbits and subcutaneous tissues, in the sinuses, brain, spine, chest, and abdominal cavities, as well as involving the thyroid and salivary glands (Fig. 5.41) [132, 133]. When involving the brain or spinal cord, myeloid sarcoma is typically isointense or mildly hyperintense to the cerebral cortex/gray matter, but it shows intense and homogeneous enhancement following contrast injection. While the imaging features are not specific and should be confirmed by biopsy, the presence of a new mass in a patient with a prior history of myeloid malignancy should raise concern for the presence of myeloid sarcoma.

### Pathology

Histologic examination of the tumor lesions shows sheets of mononuclear cells, with or without maturation. The neoplastic cells (blasts) have round to folded nuclei, usually with fine nuclear chromatin and occasional prominent nucleoli, and scant to moderate granular cytoplasm. Touch imprint preparations and cytochemical stains for myeloperoxidase and/or nonspecific esterase can be helpful for initial assessment and proper specimen processing.

Immunophenotype by flow cytometry and/or immunohistochemistry demonstrates expression of myeloid or myelomonocytic markers such as CD4, CD13, CD33, CD34, CD43, CD45, CD117, lysozyme, and myeloperoxidase (Fig. 5.42). In pediatric cases, a panel of immunohistochemical studies can be very useful especially for differentiating from small round blue cell tumors. In such cases, the expression of CD45, CD117, myeloperoxidase, and lysozyme is particularly important in distinguishing myeloid sarcoma from lymphoblastic leukemia/lymphoma and other neoplasms such as Ewing sarcoma family tumors, rhabdomyosarcoma, Wilms tumor, and neuroblastoma [134].

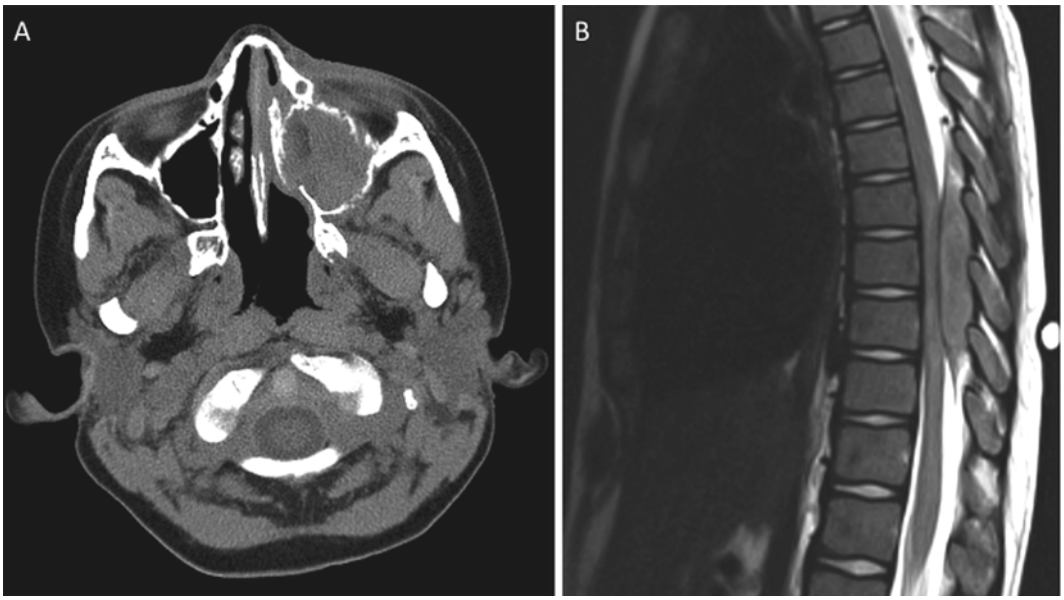


**Fig. 5.41** Myeloid sarcoma: (**a**) 6-year old presenting with left infraorbital/maxillary sinus mass, peripheral blasts, and acute myeloid leukemia (AML). Biopsy of the sinus mass showed myeloid sarcoma (aka chloroma). (**b**) 10-year old with history of AML presented with back pain and progressive lower extremity paraplegia. Spine MRI revealed an intradural extramedullary mass, found at resection to be myeloid sarcoma

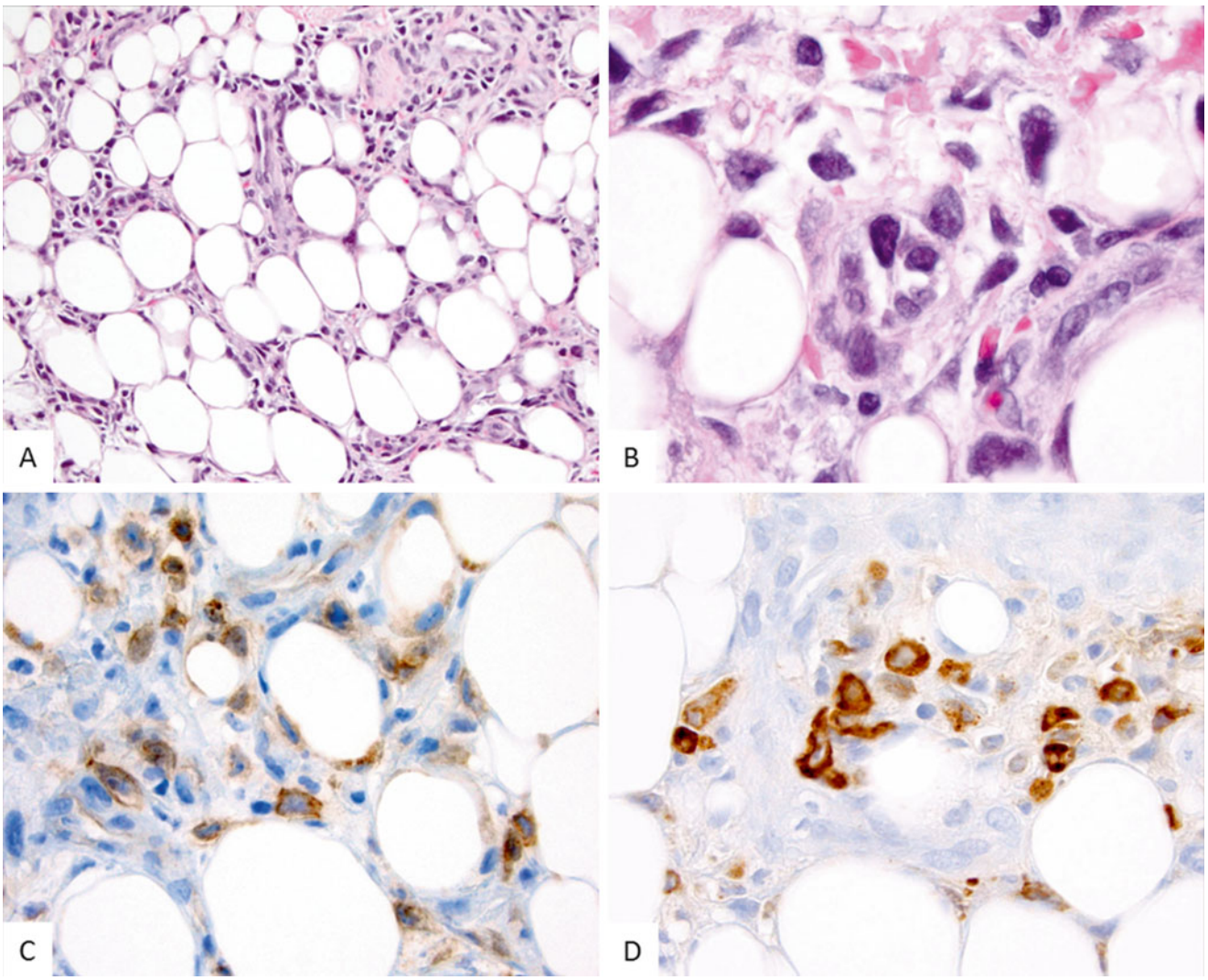


**Fig. 5.42** Myeloid sarcoma, skin. (**a**, **b**) This is a patient with a history of refractory acute myeloid leukemia status post bone marrow transplant presenting with multiple skin nodules that show atypical mononuclear infiltrate in the deep dermis and subcutaneous fat. The mononuclear cells show aberrant co-expression of immature myeloid markers including CD34 (not shown) CD117 (**c**) and MPO (**d**)

## Conclusion

There are a large and varied number of tumors involving lymphoid and hematopoietic tissues. A comprehensive radiologic imaging evaluation, together with a thorough histopathologic characterization of the type, lineage, and extent of the hematolymphoid disease, is necessary both to establish a diagnosis and to determine the extent of malignant involvement. This information, when integrated with the clinical situation, can be used to guide treatment, assess response to therapy, evaluate potential sites of relapse, and develop strategies for monitoring disease recurrence during periods of off-treatment surveillance.

## References


1. Nickoloff EL. AAPM/RSNA physics tutorial for residents: physics of flat-panel fluoroscopy systems: survey of modern fluoroscopy imaging: flat-panel detectors versus image intensifiers and more. Radiographics. 2011;31:591–602.
2. Navarro OM. Soft tissue masses in children. Radiol Clin North Am. 2011;49:1235–59. vi–vii.
3. McCarville MB. Contrast-enhanced sonography in pediatrics. Pediatr Radiol. 2011;41 Suppl 1:S238–42.
4. Dudea SM, Botar-Jid C, Dumitriu D, et al. Differentiating benign from malignant superficial lymph nodes with sonoelastography. Med Ultrason. 2013;15:132–9.
5. Kostakoglu L, Schoder H, Johnson JL, et al. Interim [(18)F]fluorodeoxyglucose positron emission tomography imaging in stage I-II non-bulky Hodgkin lymphoma: would using combined positron emission tomography and computed tomography criteria better predict response than each test alone? Leuk Lymphoma. 2012;53:2143–50.
6. Schwartz CL, Friedman DL, McCarten K, et al. Predictors of early response and event-free survival in Hodgkin lymphoma (HL): PET versus CT imaging. J Clin Oncol. 2011;29:8006.
7. Callahan MJ, Poznauskis L, Zurakowski D, et al. Nonionic iodinated intravenous contrast material-related reactions: incidence in large urban children's hospital-retrospective analysis of data in 12,494 patients. Radiology. 2009;250:674–81.
8. ACR Manual on Contrast Media, Version 9, in Radiology ACo, editor. American College of Radiology; 2013
9. Brenner DJ, Hall EJ. Computed tomography – an increasing source of radiation exposure. N Engl J Med. 2007;357:2277–84.
10. Mettler Jr FA, Huda W, Yoshizumi TT, et al. Effective doses in radiology and diagnostic nuclear medicine: a catalog. Radiology. 2008;248:254–63.
11. Brenner DJ. Slowing the increase in the population dose resulting from CT scans. Radiat Res. 2010;174:809–15.
12. Pearce MS, Salotti JA, Little MP, et al. Radiation exposure from CT scans in childhood and subsequent risk of leukaemia and brain tumours: a retrospective cohort study. Lancet. 2012;380:499–505.
13. Mathews JD, Forsythe AV, Brady Z, et al. Cancer risk in 680,000 people exposed to computed tomography scans in childhood or adolescence: data linkage study of 11 million Australians. BMJ. 2013;346:f2360.
14. Krille L, Zeeb H, Jahnen A, et al. Computed tomographies and cancer risk in children: a literature overview of CT practices, risk estimations and an epidemiologic cohort study proposal. Radiat Environ Biophys. 2012;51:103–11.
15. Nievelstein RA, Quarles van Ufford HM, Kwee TC, et al. Radiation exposure and mortality risk from CT and PET imaging of patients with malignant lymphoma. Eur Radiol. 2012;22:1946–54.
16. McCollough CH, Bruesewitz MR, Kofler Jr JM. CT dose reduction and dose management tools: overview of available options. Radiographics. 2006;26:503–12.
17. Pooley RA. AAPM/RSNA physics tutorial for residents: fundamental physics of MR imaging. Radiographics. 2005;25:1087–99.
18. Weissleder R, Elizondo G, Wittenberg J, et al. Ultrasmall superparamagnetic iron oxide: an intravenous contrast agent for assessing lymph nodes with MR imaging. Radiology. 1990;175:494–8.
19. Pandharipande PV, Mora JT, Uppot RN, et al. Lymphotropic nanoparticle-enhanced MRI for independent prediction of lymph node malignancy: a logistic regression model. Am J Roentgenol. 2009;193:W230–7.
20. Kwee TC, Takahara T, Vermoolen MA, et al. Whole-body diffusion-weighted imaging for staging malignant lymphoma in children. Pediatr Radiol. 2010;40(10):1592–602.
21. Vermoolen MA, Kwee TC, Akkerman EM, et al. Whole-body MRI, including diffusion-weighted imaging, compared to FDG-PET for staging Hodgkin's lymphoma – initial experience. Pediatr Radiol. 2010;40:1097.
22. Punwani S, Taylor SA, Saad ZZ, et al. Diffusion-weighted MRI of lymphoma: prognostic utility and implications for PET/MRI? Eur J Nucl Med Mol Imaging. 2013;40:373–85.
23. Koh DM, Collins DJ. Diffusion-weighted MRI in the body: applications and challenges in oncology. Am J Roentgenol. 2007;188:1622–35.
24. Padhani AR, Liu G, Koh DM, et al. Diffusion-weighted magnetic resonance imaging as a cancer biomarker: consensus and recommendations. Neoplasia. 2009;11:102–25.
25. Mir N, Sohaib SA, Collins D, et al. Fusion of high b-value diffusion-weighted and T2-weighted MR images improves identification of lymph nodes in the pelvis. J Med Imaging Radiat Oncol. 2010;54:358–64.
26. Roy C, Bierry G, Matau A, et al. Value of diffusion-weighted imaging to detect small malignant pelvic lymph nodes at 3T. Eur Radiol. 2010;20:1803–11.
27. Kaewlai R, Abujudeh H. Nephrogenic systemic fibrosis. Am J Roentgenol. 2012;199:W17–23.
28. Treves ST. Pediatric nuclear medicine/PET. Seacus, NJ: Springer; 2007.
29. Kelly KM, Hodgson D, Appel B, et al. Children's Oncology Group's 2013 blueprint for research: Hodgkin lymphoma. Pediatr Blood Cancer. 2013;60:972–8.
30. Kostakoglu L, Cheson BD. State-of-the-art research on lymphomas: role of molecular imaging for staging, prognostic evaluation, and treatment response. Front Oncol. 2013;3:212.
31. Zhuang H, Yu JQ, Alavi A. Applications of fluorodeoxyglucose-PET imaging in the detection of infection and inflammation and other benign disorders. Radiol Clin North Am. 2005;43:121–34.
32. Vermoolen MA, Kersten MJ, Fijnheer R, et al. Magnetic resonance imaging of malignant lymphoma. Expert Rev Hematol. 2011;4:161–71.
33. Oguz A, Karadeniz C, Temel EA, et al. Evaluation of peripheral lymphadenopathy in children. Pediatr Hematol Oncol. 2006;23:549–61.
34. Twist CJ, Link MP. Assessment of lymphadenopathy in children. Pediatr Clin North Am. 2002;49:1009–25.
35. Rosado FG, Stratton CW, Mosse CA. Clinicopathologic correlation of epidemiologic and histopathologic features of pediatric bacterial lymphadenitis. Arch Pathol Lab Med. 2011;135:1490–3.
36. Monaco SE, Khalbuss WE, Pantanowitz L. Benign non-infectious causes of lymphadenopathy: a review of cytomorphology and differential diagnosis. Diagn Cytopathol. 2012;40:925–38.

37. Chapel H. Classification of primary immunodeficiency diseases by the International Union of Immunological Societies (IUIS) Expert Committee on Primary Immunodeficiency 2011. Clin Exp Immunol. 2012;168:58–9.
38. International Union of Immunological Societies Expert Committee on PrimaryI, Notarangelo LD, Fischer A, et al. Primary immunodeficiencies: 2009 update. J Allergy Clin Immunol. 2009;124: 1161–78.
39. Filipovich AH, Mathur A, Kamat D, et al. Primary immunodeficiencies: genetic risk factors for lymphoma. Cancer Res. 1992; 52:5465s–7.
40. Terasawa T, Lau J, Bardet S, et al. Fluorine-18-fluorodeoxyglucose positron emission tomography for interim response assessment of advanced-stage Hodgkin's lymphoma and diffuse large B-cell lymphoma: a systematic review. J Clin Oncol. 2009;27:1906–14.
41. Ng SB, Khoury JD. Epstein-Barr virus in lymphoproliferative processes: an update for the diagnostic pathologist. Adv Anat Pathol. 2009;16:40–55.
42. Hollingsworth CL. Thoracic disorders in the immunocompromised child. Radiol Clin North Am. 2005;43:435–47.
43. Yin EZ, Frush DP, Donnelly LF, et al. Primary immunodeficiency disorders in pediatric patients: clinical features and imaging findings. Am J Roentgenol. 2001;176:1541–52.
44. Cotelingam JD, Witebsky FG, Hsu SM, et al. Malignant lymphoma in patients with the Wiskott-Aldrich syndrome. Cancer Invest. 1985;3:515–22.
45. Taylor AM, Metcalfe JA, Thick J, et al. Leukemia and lymphoma in ataxia telangiectasia. Blood. 1996;87:423–38.
46. Notarangelo L, Casanova JL, Conley ME, et al. Primary immunodeficiency diseases: an update from the International Union of Immunological Societies Primary Immunodeficiency Diseases Classification Committee Meeting in Budapest, 2005. J Allergy Clin Immunol. 2006;117:883–96.
47. Safriel YI, Haller JO, Lefton DR, et al. Imaging of the brain in the HIV-positive child. Pediatr Radiol. 2000;30:725–32.
48. Boyle GJ, Michaels MG, Webber SA, et al. Posttransplantation lymphoproliferative disorders in pediatric thoracic organ recipients. J Pediatr. 1997;131:309–13.
49. Webber SA, Naftel DC, Fricker FJ, et al. Lymphoproliferative disorders after paediatric heart transplantation: a multi-institutional study. Lancet. 2006;367:233–9.
50. von Falck C, Maecker B, Schirg E, et al. Post transplant lymphoproliferative disease in pediatric solid organ transplant patients: a possible role for [18F]-FDG-PET(/CT) in initial staging and therapy monitoring. Eur J Radiol. 2007;63:427–35.
51. Gurney JG, Davis S, Severson RK, et al. Trends in cancer incidence among children in the U.S. Cancer. 1996;78:532–41.
52. Jaglowski SM, Linden E, Termuhlen AM, et al. Lymphoma in adolescents and young adults. Semin Oncol. 2009;36:381–418.
53. Pui CH, Robison LL, Look AT. Acute lymphoblastic leukaemia. Lancet. 2008;371:1030–43.
54. Morton LM, Wang SS, Devesa SS, et al. Lymphoma incidence patterns by WHO subtype in the United States, 1992–2001. Blood. 2006;107:265–76.
55. Sandlund JT, Downing JR, Crist WM. Non-Hodgkin's lymphoma in childhood. N Engl J Med. 1996;334:1238–48.
56. Gross TL, Perkins SL. Malignant non-Hodgkin lymphomas in children. In: Pizzo PA, Poplack DG, editors. Principles and practice of pediatric oncology. Philadelphia, PA: Lippincott Williams & Wilkins; 2011. p. 663–82.
57. Anghelescu DL, Burgoyne LL, Liu T, et al. Clinical and diagnostic imaging findings predict anesthetic complications in children presenting with malignant mediastinal masses. Paediatr Anaesth. 2007;17:1090–8.
58. Shepherd SF, A'Hern RP, Pinkerton CR. Childhood T-cell lymphoblastic lymphoma-does early resolution of mediastinal mass predict for final outcome? The United Kingdom Children's Cancer Study Group (UKCCSG). Br J Cancer. 1995;72:752–6.
59. Termuhlen AM, Smith LM, Perkins SL, et al. Disseminated lymphoblastic lymphoma in children and adolescents: results of the COG A5971 trial: a report from the Children's Oncology Group. Br J Haematol. 2013;162:792–801.
60. Khoury JD. Ewing sarcoma family of tumors. Adv Anat Pathol. 2005;12:212–20.
61. Zhang J, Ding L, Holmfeldt L, et al. The genetic basis of early T-cell precursor acute lymphoblastic leukaemia. Nature. 2012;481:157–63.
62. Cairo MS, Raetz E, Lim MS, et al. Childhood and adolescent non-Hodgkin lymphoma: new insights in biology and critical challenges for the future. Pediatr Blood Cancer. 2005;45:753–69.
63. Oschlies I, Burkhardt B, Chassagne-Clement C, et al. Diagnosis and immunophenotype of 188 pediatric lymphoblastic lymphomas treated within a randomized prospective trial: experiences and preliminary recommendations from the European childhood lymphoma pathology panel. Am J Surg Pathol. 2011;35:836–44.
64. Hochberg J, Waxman IM, Kelly KM, et al. Adolescent non-Hodgkin lymphoma and Hodgkin lymphoma: state of the science. Br J Haematol. 2009;144:24–40.
65. Khoury JD, Jones D, Yared MA, et al. Bone marrow involvement in patients with nodular lymphocyte predominant Hodgkin lymphoma. Am J Surg Pathol. 2004;28:489–95.
66. Carbone A, Spina M, Gloghini A, et al. Classical Hodgkin's lymphoma arising in different host's conditions: pathobiology parameters, therapeutic options, and outcome. Am J Hematol. 2011;86:170–9.
67. Bradley AJ, Carrington BM, Lawrance JA, et al. Assessment and significance of mediastinal bulk in Hodgkin's disease: comparison between computed tomography and chest radiography. J Clin Oncol. 1999;17:2493–8.
68. Shamberger RC. Preanesthetic evaluation of children with anterior mediastinal masses. Semin Pediatr Surg. 1999;8:61–8.
69. Metzger ML, Krasin MJ, Hudson MM, et al. Hodgkin Lymphoma. In: Pizzo PA, Poplack DG, editors. Principles and practice of pediatric oncology. Philadelphia, PA: Lippincott, Williams and Wilkens; 2011. p. 638–62.
70. Paes FM, Kalkanis DG, Sideras PA, et al. FDG PET/CT of extranodal involvement in non-Hodgkin lymphoma and Hodgkin disease. Radiographics. 2010;30:269–91.
71. Purz S, Mauz-Korholz C, Korholz D, et al. [18F] Fluorodeoxyglucose positron emission tomography for detection of bone marrow involvement in children and adolescents with Hodgkin's lymphoma. J Clin Oncol. 2011;29:3523–8.
72. Kluge R, Kurch L, Montravers F, et al. FDG PET/CT in children and adolescents with lymphoma. Pediatr Radiol. 2013;43:406–17.
73. Furth C, Denecke T, Steffen I, et al. Correlative imaging strategies implementing CT, MRI, and PET for staging of childhood Hodgkin disease. J Pediatr Hematol Oncol. 2006;28:501–12.
74. Furth C, Steffen IG, Amthauer H, et al. Early and late therapy response assessment with [18F]fluorodeoxyglucose positron emission tomography in pediatric Hodgkin's lymphoma: analysis of a prospective multicenter trial. J Clin Oncol. 2009;27:4385–91.
75. Gallamini A, Fiore F, Sorasio R, et al. Interim positron emission tomography scan in Hodgkin lymphoma: definitions, interpretation rules, and clinical validation. Leuk Lymphoma. 2009;50:1761–4.
76. Lister TA, Crowther D, Sutcliffe SB, et al. Report of a committee convened to discuss the evaluation and staging of patients with Hodgkin's disease: Cotswolds meeting. J Clin Oncol. 1989;7: 1630–6.
77. Freed J, Kelly KM. Current approaches to the management of pediatric Hodgkin lymphoma. Paediatr Drugs. 2010;12:85–98.
78. Metzger ML, Hudson MM. Balancing efficacy and safety in the treatment of adolescents with Hodgkin's lymphoma. J Clin Oncol. 2009;27:6071–3.

79. Metzger ML, Hudson MM, Krasin MJ, et al. Initial response to salvage therapy determines prognosis in relapsed pediatric Hodgkin lymphoma patients. Cancer. 2010;116:4376–84.
80. Metzger ML, Weinstein HJ, Hudson MM, et al. Association between radiotherapy vs no radiotherapy based on early response to VAMP chemotherapy and survival among children with favorable-risk Hodgkin lymphoma. JAMA. 2012;307:2609–16.
81. Hutchings M. How does PET/CT help in selecting therapy for patients with Hodgkin lymphoma? Hematol Am Soc Hematol Educ Program. 2012;2012:322–7.
82. Kostakoglu L, Gallamini A. Interim 18F-FDG PET in Hodgkin lymphoma: would PET-adapted clinical trials lead to a paradigm shift? J Nucl Med. 2013;54:1082–93.
83. Cheson BD, Pfistner B, Juweid ME, et al. Revised response criteria for malignant lymphoma. J Clin Oncol. 2007;25:579–86.
84. Juweid ME, Stroobants S, Hoekstra OS, et al. Use of positron emission tomography for response assessment of lymphoma: consensus of the Imaging Subcommittee of International Harmonization Project in Lymphoma. J Clin Oncol. 2007;25:571–8.
85. Barrington SF, Mikhaeel NG, Kostakoglu L, et al. Role of imaging in the staging and response assessment of lymphoma: consensus of the international conference on Malignant Lymphomas Imaging Working Group. J Clin Oncol. 2014. pii: JCO.2013.53.5229. PMID: 25113771, [Epub ahead of print].
86. Cheson BD, Fisher RI, Barrington SF, et al. Recommendations for initial evaluation, staging, and response assessment of Hodgkin and non-Hodgkin lymphoma: the Lugano classification. J Clin Oncol. 2014. pii: JCO.2013.54.8800. PMID: 25113753, [Epub ahead of print].
87. Meignan M, Gallamini A, Itti E et al. Report on the Third International Workshop on Interim Positron Emission Tomography in Lymphoma held in Menton, France, 26–27 September 2011 and Menton 2011 consensus. Leuk Lymphoma 2012;53:1876-81.
88. Voss SD, Chen L, Constine LS, et al. Surveillance computed tomography imaging and detection of relapse in intermediate- and advanced-stage pediatric Hodgkin's lymphoma: a report from the Children's Oncology Group. J Clin Oncol. 2012;30:2635–40.
89. Voss SD. Surveillance imaging in pediatric hodgkin lymphoma. Curr Hematol Malig Rep. 2013;8:218–25.
90. Rathore N, Eissa HM, Margolin JF, et al. Pediatric Hodgkin lymphoma: are we over-scanning our patients? Pediatr Hematol Oncol. 2012;29:415–23.
91. Friedmann AM, Wolfson JA, Hudson MM, et al. Relapse after treatment of pediatric Hodgkin lymphoma: outcome and role of surveillance after end of therapy. Pediatr Blood Cancer. 2013;60:1458–63.
92. Venkataraman G, Mirza MK, Eichenauer DA, et al. Current status of prognostication in classical Hodgkin lymphoma. Br J Haematol. 2014;165:287–99.
93. Deffenbacher KE, Iqbal J, Sanger W, et al. Molecular distinctions between pediatric and adult mature B-cell non-Hodgkin lymphomas identified through genomic profiling. Blood. 2012;119:3757–66.
94. Toma P, Granata C, Rossi A, et al. Multimodality imaging of Hodgkin disease and non-Hodgkin lymphomas in children. Radiographics. 2007;27:1335–54.
95. Burkhardt B, Oschlies I, Klapper W, et al. Non-Hodgkin's lymphoma in adolescents: experiences in 378 adolescent NHL patients treated according to pediatric NHL-BFM protocols. Leukemia. 2011;25:153–60.
96. Gerrard M, Waxman IM, Sposto R, et al. Outcome and pathologic classification of children and adolescents with mediastinal large B-cell lymphoma treated with FAB/LMB96 mature B-NHL therapy. Blood. 2013;121:278–85.
97. Reiter A, Ferrando AA. Malignant lymphomas and lymphadenopathies. In: Orkin SH, Fisher DE, Look AT, et al., editors. Oncology of infancy and childhood. Philadelphia: Elsevier; 2009. p. 417–508.
98. Reiter A, Klapper W. Recent advances in the understanding and management of diffuse large B-cell lymphoma in children. Br J Haematol. 2008;142:329–47.
99. Morin RD, Gascoyne RD. Newly identified mechanisms in B-cell non-Hodgkin lymphomas uncovered by next-generation sequencing. Semin Hematol. 2013;50:303–13.
100. Hans CP, Weisenburger DD, Greiner TC, et al. Confirmation of the molecular classification of diffuse large B-cell lymphoma by immunohistochemistry using a tissue microarray. Blood. 2004; 103:275–82.
101. Oschlies I, Klapper W, Zimmermann M, et al. Diffuse large B-cell lymphoma in pediatric patients belongs predominantly to the germinal-center type B-cell lymphomas: a clinicopathologic analysis of cases included in the German BFM (Berlin-Frankfurt-Munster) Multicenter Trial. Blood. 2006;107:4047–52.
102. Miles RR, Raphael M, McCarthy K, et al. Pediatric diffuse large B-cell lymphoma demonstrates a high proliferation index, frequent c-Myc protein expression, and a high incidence of germinal center subtype: Report of the French-American-British (FAB) international study group. Pediatr Blood Cancer. 2008;51: 369–74.
103. Sandlund JT. Burkitt lymphoma: staging and response evaluation. Br J Haematol. 2012;156:761–5.
104. Karantanis D, Durski JM, Lowe VJ, et al. 18F-FDG PET and PET/CT in Burkitt's lymphoma. Eur J Radiol. 2010;75:e68–73.
105. Leventaki V, Rodic V, Tripp SR, et al. TP53 pathway analysis in paediatric Burkitt lymphoma reveals increased MDM4 expression as the only TP53 pathway abnormality detected in a subset of cases. Br J Haematol. 2012;158:763–71.
106. Taddesse-Heath L, Pittaluga S, Sorbara L, et al. Marginal zone B-cell lymphoma in children and young adults. Am J Surg Pathol. 2003;27:522–31.
107. Rizzo KA, Streubel B, Pittaluga S, et al. Marginal zone lymphomas in children and the young adult population; characterization of genetic aberrations by FISH and RT-PCR. Mod Pathol 23: 866–73
108. Rizzo KA, Streubel B, Pittaluga S, et al. Marginal zone lymphomas in children and the young adult population; characterization of genetic aberrations by FISH and RT-PCR. Mod Pathol. 2010;23:866–73.
109. Lorsbach RB, Shay-Seymore D, Moore J, et al. Clinicopathologic analysis of follicular lymphoma occurring in children. Blood. 2002;99:1959–64.
110. Oschlies I, Salaverria I, Mahn F, et al. Pediatric follicular lymphoma – a clinico-pathological study of a population-based series of patients treated within the Non-Hodgkin's Lymphoma–Berlin-Frankfurt-Munster (NHL-BFM) multicenter trials. Haematologica. 2010;95:253–9.
111. Setty BA, Termuhlen AM. Rare pediatric non-hodgkin lymphoma. Curr Hematol Malig Rep. 2010;5:163–8.
112. Hayashi D, Lee JC, Devenney-Cakir B, et al. Follicular non-Hodgkin's lymphoma. Clin Radiol. 2010;65:408–20.
113. Hofman MS, Hicks RJ. Imaging in follicular NHL. Best Pract Res Clin Haematol. 2011;24:165–77.
114. Salaverria I, Philipp C, Oschlies I, et al. Translocations activating IRF4 identify a subtype of germinal center-derived B-cell lymphoma affecting predominantly children and young adults. Blood 118:139–47
115. Lowe EJ, Gross TG. Anaplastic large cell lymphoma in children and adolescents. Pediatr Hematol Oncol. 2013;30:509–19.
116. Le Deley MC, Reiter A, Williams D, et al. Prognostic factors in childhood anaplastic large cell lymphoma: results of a large European intergroup study. Blood. 2008;111:1560–6.
117. Mosse YP, Lim MS, Voss SD, et al. Safety and activity of crizotinib for paediatric patients with refractory solid tumours or anaplastic large-cell lymphoma: a Children's Oncology Group phase 1 consortium study. Lancet Oncol. 2013;14:472–80.

118. Favara BE, Feller AC, Pauli M, et al. Contemporary classification of histiocytic disorders. The WHO Committee on Histiocytic/Reticulum Cell Proliferations. Reclassification Working Group of the Histiocyte Society. Med Pediatr Oncol. 1997;29:157–66.
119. Alston RD, Tatevossian RG, McNally RJ, et al. Incidence and survival of childhood Langerhans cell histiocytosis in Northwest England from 1954 to 1998. Pediatr Blood Cancer. 2007;48:555–60.
120. Degar BA, Fleming MD, Rollins BJ. Histocytoses. In: Orkin SH, Fisher DE, Look AT, et al., editors. Oncology of infancy and childhood. Philadelphia, PA: Saunders Elsevier; 2009. p. 963–88.
121. Gadner H, Grois N, Arico M, et al. A randomized trial of treatment for multisystem Langerhans' cell histiocytosis. J Pediatr. 2001;138:728–34.
122. Gadner H, Grois N, Potschger U, et al. Improved outcome in multisystem Langerhans cell histiocytosis is associated with therapy intensification. Blood. 2008;111:2556–62.
123. Mueller WP, Melzer HI, Schmid I, et al. The diagnostic value of 18F-FDG PET and MRI in paediatric histiocytosis. Eur J Nucl Med Mol Imaging. 2013;40:356–63.
124. Phillips M, Allen C, Gerson P, et al. Comparison of FDG-PET scans to conventional radiography and bone scans in management of Langerhans cell histiocytosis. Pediatr Blood Cancer. 2009;52:97–101.
125. Kaste SC, Rodriguez-Galindo C, McCarville ME, et al. PET-CT in pediatric Langerhans cell histiocytosis. Pediatr Radiol. 2007;37:615–22.
126. Janssen D, Harms D. Juvenile xanthogranuloma in childhood and adolescence: a clinicopathologic study of 129 patients from the kiel pediatric tumor registry. Am J Surg Pathol. 2005;29:21–8.
127. Hoeger PH, Diaz C, Malone M, et al. Juvenile xanthogranuloma as a sequel to Langerhans cell histiocytosis: a report of three cases. Clin Exp Dermatol. 2001;26:391–4.
128. Yu H, Kong J, Gu Y, et al. A child with coexistent juvenile xanthogranuloma and Langerhans cell histiocytosis. J Am Acad Dermatol. 2010;62:329–32.
129. Zvulunov A, Barak Y, Metzker A. Juvenile xanthogranuloma, neurofibromatosis, and juvenile chronic myelogenous leukemia. World statistical analysis. Arch Dermatol. 1995;131:904–8.
130. Aparicio G, Mollet J, Bartralot R, et al. Eruptive juvenile xanthogranuloma associated with relapsing acute lymphoblastic leukemia. Pediatr Dermatol. 2008;25:487–8.
131. Reinhardt D, Creutzig U. Isolated myelosarcoma in children-update and review. Leuk Lymphoma. 2002;43:565–74.
132. Dusenbery KE, Howells WB, Arthur DC, et al. Extramedullary leukemia in children with newly diagnosed acute myeloid leukemia: a report from the Children's Cancer Group. J Pediatr Hematol Oncol. 2003;25:760–8.
133. Guermazi A, Feger C, Rousselot P, et al. Granulocytic sarcoma (chloroma): imaging findings in adults and children. Am J Roentgenol. 2002;178:319–25.
134. Klco JM, Welch JS, Nguyen TT, et al. State of the art in myeloid sarcoma. Int J Lab Hematol. 2011;33:555–65.